Kinome-wide screens to identify novel regulators of DNA double-strand breaks repair

A THESIS SUBMITTED TO THE FACULTY OF THE UNIVERSITY OF MINNESOTA

BY:

Chen Wang

IN PARTIAL FULFILLMENT OF THE REQUIREMENTS FOR THE DEGREE OF DOCTOR OF PHILOSOPHY

Advisor:

Dr. Eric A. Hendrickson

Department of Biochemistry, Molecular Biology, and Biophysics

January 2023

Acknowledgments

First, I would like to thank my advisor, Dr. Eric A. Hendrickson for his outstanding guidance and support over the past years. I always appreciated his patience and willingness to help his students out. During my stay at the Hendrickson laboratory, Eric was always willing to listen to my opinion on my thesis work, which really encouraged me to think in new directions for my project. Also, Eric taught me skills of scientific communication, grant application, and paper preparation. My time at Hendrickson laboratory has made me ready for the future changes in my career and science.

I would also like to thank my committee members Drs. Aaron Goldstrohm, Reuben Harris, and David Largaespada for their advice and support. They have provided me with valuable feedback and help. I feel lucky to have had such an amazing committee.

Many current and former members in Hendrickson laboratory deserve many thanks. Brian Ruis mentored me when I first joined the Hendrickson laboratory. Without his help, I cannot imagine how I could have gotten started up in a new environment. Dr. Mohammad Shameem joined the Hendrickson laboratory after me, but he provided tremendous help on the progress of my project. Dr. Mohammad Shameem kindly helped me with comet and replication combing assays and I cannot say enough thanks to him. I also would like to

thank Colette Rogers for her considerate help in learning the sister-chromatid exchange assay. To Summer (Huiyan) Ma and Yujie Zhao: thank you for your friendship and support over the years. I also have had the pleasure to work with other Hendrickson laboratory members and would like to acknowledge them for all their support, help, and discussion of my work.

Thank you to my many friends who have accompanied me through graduate school, especially Ang Li and Tianpeng Zhang.

Finally, I would like to thank my family, especially my mom, dad, and Shujin for their unwavering support and encouragement.

DEDICATION

To my family — Shujin and Smaellsky

Abstract

Non-homologous end joining (NHEJ) and homologous recombination (HR) are the two main DNA double-strand breaks (DSBs) repair pathways utilized to maintain genome stability in mammalian cells. NHEJ is initiated by binding of the Ku70/86 heterodimer, which subsequently recruits the DNA-dependent protein kinase, catalytic subunit (DNA-PKcs) protein (alternately referred to as PRKDC, protein kinase, DNA-dependent, catalytic subunit) to form the trimeric DNA-PK complex. After limited end processing by Artemis (a nuclease) and DNA polymerases Pol λ and Pol μ, the broken ends are re-ligated by a complex consisting of DNA ligase IV, XRCC4 (X-ray cross complementing 4) and XLF (XRCC4-like factor). The mechanism of NHEJ has been studied for decades, but in spite of that, the role and importance of DNA-PK_{cs} in NHEJ remains unclear. To illuminate the function of DNA-PK_{cs} in NHEJ, our laboratory has generated two human colorectal carcinoma HCT116 cell lines that are DNA-PK_{cs}-deficient: a complete knockout (DNA-$PKcs^{-/-}$) and a version expressing a dominant-negative kinase-dead (KD) protein from one allele (DNA-$PKcs^{KD/-}$). The latter cell line will be featured prominently in this thesis.

In contrast to NHEJ, HR requires the displacement of Ku70/86 heterodimers from the damaged DNA ends to instead facilitate end resection by Meiotic recombination defective 11 (Mre11):Radiation sensitive 50

(Rad50):Nijmegen chromosome breakage syndrome 1 (NBS1) commonly referred to as the MRN complex. MRN is often assisted in this resection process by the C-terminal binding protein 1 (CtBP1) interacting protein (CtIP). This initial resection is then enhanced by additional nucleases, primarily DNA replication helicase/nuclease 2 (DNA2), and Exonuclease 1 (EXO1). Human replication protein A (RPA) and Radiation sensitive 51 (RAD51) then bind to the 3' overhangs generated by end resection to sequentially protect ssDNA and perform the strand invasion process, respectively. Depending on whether a double Holliday junction is formed, HR is divided into two sub-pathways: double-strand break repair (DSBR) and synthesis-dependent strand annealing (SDSA). These pathways can then facilitate essentially error-free repair resulting in products with (DSBR) or without (DSBR and SDSA) crossovers.

In mammals, NHEJ- or HR-mediated repair results in radically different repair products and this fact underscores the importance of a cell making the proper pathway choice decision when a DSB happens. How pathway choice is mechanistically decided, however, is unclear. Parsimoniously, it seems likely that there will be regulators (both positive and negative) for both pathways and that the interplay and or varied expression of these regulators will modulate pathway choice. To this end, after the core repair proteins that are required for the NHEJ and HR pathways had been identified, recent research has focused on the impact of chromatin status on DSB repair pathway choice. In particular, histone acetylation and its "reader" proteins — bromodomain-containing

proteins — have been shown to play central roles in regulating chromatin status and through this to influence both the efficiency and pathway choice of DSB repair.

The goal of this thesis work was to identify and then characterize novel DSB repair regulators. Multiplexed inhibitor beads (MIBs) coupled mass spectrometry (MS) was performed to determine the kinome change in a DNA-$PK_{cs}^{KD/-}$ cell line. MIBs consist of multiple covalently bound ATP analogs. Therefore, proteins with ATP binding pockets will be captured by MIBs and can be subjected to MS analysis. The rationale for this approach was that since NHEJ is ablated in this cell line the cells may need to upregulate HR in order to survive and we postulated that some of these regulators might be ATP-binding or utilizing proteins. Through MIBs-MS, I have identified Bromodomain containing protein 3 (BRD3), a member of bromodomain and extra-terminal domain (BET) family, as a novel DSB repair regulator.

Contents

List of Figures

List of Abbreviations

Ad2	Adenovirus Serotype 2
Alt-NHEJ	Alternative Non-Homologous End Joining
AR	Androgen Receptor
APLF	Aprataxin and PNK-like Factor
ATAD5	ATPase Family AAA Domain Containing 5
ATM	Ataxia Telangiectasia Mutated
ATR	Ataxia Telangiectasia and Rad3-related
ATRIP	ATR-Interacting Protein
BAF	BRG1/BRM-associated Factor
BARD1	BRCA1-associated Ring Domain 1
BAZ1A/B	Bromodomain Adjacent to Zinc Finger Domain 1A/B
BD	Bromodomain
BER	Base Excision Repair
BET	Bromodomain and Extra-Terminal Domain
BLM	Blooms Syndrome
BRCA1	Breast Cancer Allele 1
BRCA2	Breast Cancer Allele 2
BRD2	Bromodomain-containing Protein 2
BRD3	Bromodomain-containing Protein 3
BRD4	Bromodomain-containing Protein 4
BRD7	Bromodomain-containing Protein 7
BRDT	Bromodomain Testis Associated
BRG1	Brahma Protein-like 1
CBP/P300	CREB-binding Protein/E1A Binding Protein p300
CDC25	Cell Division Cycle 25
CDK	Cyclin-dependent Kinase
CDK9	Cyclin-dependent Kinase 9
CHD4	Chromodomain Helicase DNA Binding Protein 4
CHK1	Checkpoint Kinase 1
CHK2	CheckpointKkinase 2
CldU	5-Chloro-2'-deoxyuridine
C-Myc	Cytoplasmic-myelocytomatosis Viral Oncogene Homolog
CRISPR	Clustered Regularly Interspaced Short Palindromic Repeats
CtBP1	C-terminal Binding Protein 1
CtIP	CtBP1 Interacting Protein
CUL3	Cullin 3
DDR	DNA Damage Response
DNA2	DNA Replication Helicase/Nuclease 2
DNA-PK$_{cs}$	DNA-dependent Protein Kinase, Catalytic Subunit
DSB	Double-Strand Break
DSBR	Double-Strand Break Repair

EdU	5-Ethynyl-2'-deoxyuridine
ET	Extra-terminal Domain
ERCC1	Excision Repair Cross Complementing 1
EXO1	Exonuclease 1
FA	Fanconi Anemia
FACS	Fluorescent Activated Cell Sorting
FANCD2	FA Complementation Group D2
FEN1	Flap Endonuclease 1
GFP	Green Fluorescent Protein
GO	Gene Ontology
GRASP	GRP1-associated Scaffolding Protein
γ-H2AX	Phosphorylated H2AX on Ser139
H2	Histone H2
H3	Histone H3
H3K14ac	Acetylated H3 Lysine 14
H4	Histone H4
HAT	Histone Acetyltransferase
HDAC	Histone Deacetylase
HJ	Holliday Junction
HMGN1	High Mobility Group Nucleosome Binding Domain 1
HR	Homologous Recombination
ICL	Inter-strand Crosslink
IdU	5-Iodo-2'-deoxyuridine
IR	Ionizing Radiation
JMJD6	Jumonji Domain Containing 6
KD	Kinase Dead
KEAP1	Kelch-like ECH-associated Protein 1
Ku70/86	Ku Autoantigen, 70/86 kDa
MDC1	Mediator of DNA Damage Checkpoint 1
MIB	Multiplexed Inhibitor Bead
MMC	Mitomycin C
MMR	Mismatch Repair
MMS	Methylmethanesulfonate
MRN	Mre11-Rad50-Nbs1
MS	Mass Spectrometry
NBS1	Nijmegen Chromosome Breakage Syndrome 1
NER	Nucleotide Excision Repair
NHEJ	Non-Homologous End Joining
NMR	Nuclear Magnetic Resonance
N-Myc	Nuclear-myelocytomatosis Viral Oncogene Homolog
NSD3	Nuclear Receptor Binding SET Domain Protein 3
NuRD	Nucleosome Remodeling and Deacetylase Complex
OCT4	Octamer-binding Transcription Factor 4
p53	Tumor Antigen p53

PALB2	Partner and Localizer of BRCA2
PARP	Poly (ADP) Ribose Polymerase
PBAF	Polybromo-associated BAF
PBRM1	Polybromo 1
PCAF	P300/CBP-associated Factor
PCNA	Proliferating Cell Nuclear Antigen
PEM1	Phosphatidylethanolamine methyltransferase 1
PIGA	PhosphatidylInositol Glycan Anchor Biosynthesis Class A
PNK	Polynucleotide Kinase
Pol λ	DNA Polymerase λ
Pol μ	DNA Polymerase μ
PRDM14	PR/SET Domain 14
PRKDC	Protein Kinase, DNA-activated, Catalytic Subunit
PTEF-β	Positive Transcription Elongation Factor β
PTM	Post-translational Modification
RAD21	Radiation Sensitive 21
RAD51	Radiation Sensitive 51
RAD52	Radiation Sensitive 52
RAN	Ras-related Nuclear Protein
RBX1	Ring Box Protein 1
ROS	Reactive Oxygen Species
RPA	Replication Protein A
SCE	Sister Chromatid Exchange
SDSA	Synthesis-dependent Strand Annealing
SIRT6	Silent Mating Type Information Regulation 2, *S. Cerevisiae*, Homolog 6
SMARCA	SWI/SNF-related, Matric-associated, Actin-dependent Regulator of Chromatin, Subfamily A
SSA	Single Strand Annealing
SSB	Single Strand Break
SSBR	Single Strand Break Repair
ssDNA	Single-stranded DNA
SWI/SNF	Switch/Sucrose Non-Fermentable
Tdt	Terminal Transferase
Tgf1	Transforming Growth Factor 1
TOPO1	Topoisomerase 1
TRRAP-TIP60	Transformation/Transcription Domain Associated Protein-tat-interactive Protein, 60 kDa
WT	Wild Type
UV	Ultraviolet
V(D)J	Variable(Diversity) Joining
XLF	XRCC4-like Factor
XPF	Xeroderma Pigmentosum Factor
XRCC1	X-ray Cross Complementing 1
XRCC4	X-ray Cross Complementing 4
ZMYND8	Zinc Finger and MYND (Myeloid, Nervy, and DEAF-1) Domain Containing 8
53BP1	p53 Binding Protein 1

Chapter 1: DNA damage and repair

1.1 DNA and DNA damage response

Nucleic acids, along with proteins, lipids, and polysaccharides are one of the four major macromolecules in all known types of living organisms. DNA was first discovered in 1869 by a Swiss biochemist, Friedrich Miescher[1]. However, the function of DNA was not determined until 1944 when Oswald Avery, with his co-workers Colin MacLeod and Maclyn McCarty, first elucidated that it was DNA that was responsible for the transformation of bacteria instead of protein as most people had thought[2]. The theory that 'DNA is the genetic material' was further confirmed by Erwin Chargaff in 1951 who discovered that different species had different amounts of nucleoside bases (the basic building blocks of DNA), but that the amount of guanine was always equal to cytosine and the amount of adenine was always equal to thymine[3]. The structure of DNA was then identified by James Watson and Francis Crick with the assistance of X-ray diffraction photographs of the DNA taken by Rosalind Franklin[4].

Since the identification of DNA as the carrier of genetic information, the mechanism of maintaining DNA integrity has been extensively studied. The integrity of DNA is being constantly challenged by endogenous and exogenous sources[5]. Endogenous DNA damage can be generated by mismatches that occur during DNA replication, oxidative damage caused by reactive oxygen species (ROS) produced by metabolic processes, natural deamination and

depurination of nucleosides, and Variable(Diversity)Joining V(D)J recombination during lymphocyte development. Exogenous DNA damage is generally divided into two types: physical sources including daily exposure to pollutants, cosmic radiation, and sunshine, and therapeutic sources that might include X-rays generated by medical device, and radioactive and chemotherapeutic compounds including DNA inter-strand crosslinking agents [*e.g.*, mitomycin C (MMC) and cisplatin], topoisomerase I and II inhibitors [*e.g.*, camptothecin (CPT), doxorubicin, and etoposide], and DNA alkylating agents [*e.g.*, methyl methane sulfonate (MMS) and cyclophosphamide].

To maintain the stability of the genome, DNA pathways that are equipped for repairing different DNA lesions have evolved in mammalian cells. Base alterations caused by deamination or depurination are repaired via base excision repair (BER) while pyrimidine dimers [caused primarily by exposure to ultraviolet (UV) light] are excised by nucleotide excision repair (NER). Mismatched bases that erroneously occur during DNA replication are corrected through mismatch repair (MMR). Similarly, DNA single-strand breaks (SSBs) are repaired via single-strand break repair (SSBR), a variation of BER. The most deleterious form of DNA damage, DNA double-stranded breaks (DSBs), is so toxic that virtually all living cells have evolved multiple pathways to repair them: NHEJ, HR, and alternative non-homologous end joining/single strand annealing (Alt-NHEJ/SSA). More complex DNA damage, such as DNA inter-strand crosslinks (ICLs), require collaborations between different DNA damage

repair pathways including NER and HR with the assistance of Fanconi Anemia (FA) proteins. Although DNA repair is complex, perfection is nonetheless required as unrepaired DNA damage, mis-repaired DNA damage and overactive DNA damage repair mechanisms all result in genome instability, cell death, or tumorigenesis. To efficiently recognize the type of DNA damage and regulate the proper repair pathways, a DNA damage response (DDR) pathway has evolved.

The DDR is a signal transduction pathway that detects both DNA damage and replication stress and recruits appropriate DNA damage mediators and effectors to mitigate the impact of that DNA damage/replication stress to the cell. Based on the type and severity of DNA damage (and when it occurs during the cell cycle), the DDR regulates a series of phosphorylation cascades to determine the fate (*e.g.*, apoptosis, senescence, replication fork restart, and DNA repair) of the cell (**Figure 1**). The DDR initiates with the detection of DSBs by the MRN complex[6] or via the accumulation of single-strand DNA coated by RPA and the RAD9-RAD1-HUS1 (9-1-1)[7,8,9] complex. The MRN complex and RPA together with the 9-1-1 complex recruit apical kinases [Ataxia telangiectasia mutated (ATM)[6] and Ataxia telangiectasia and Rad3-related (ATR)] to the damage sites, respectively[8,9]. Thus, ATM predominantly responses to DSBs while ATR is activated under replication stress and responds predominantly to RPA-coated single-stranded DNA (ssDNA). ATM and ATR [the latter via the ATR-interacting protein (ATRIP)] auto-activate

themselves via phosphorylation and, in turn, phosphorylate the histone variant H2AX on Ser139 (γH2AX) at the proximal region of the DNA lesion[10,11]. When a frank DSB occurs, γH2AX recruits the mediator of DNA damage checkpoint 1 (MDC1), which is also phosphorylated by ATM, to amplify the DDR signaling by recruiting more MRN complex and ATM to the DNA lesion[12].

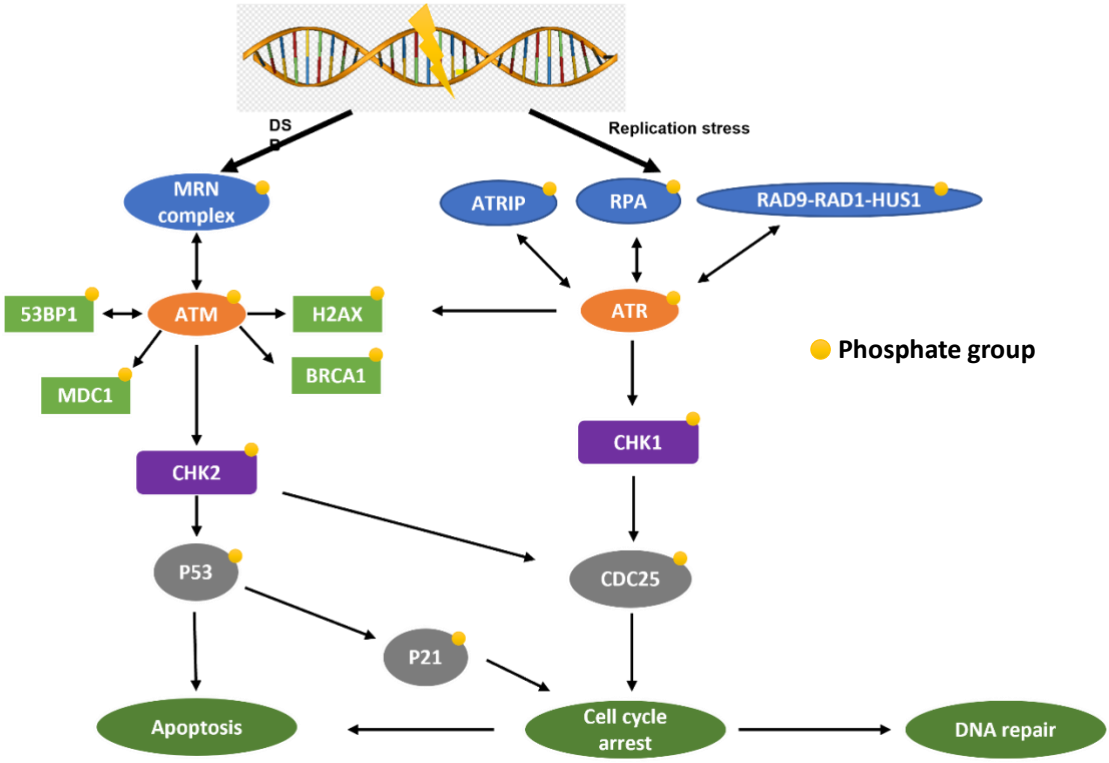

Figure 1. The DNA damage response

MRN and the RPA:9-1-1 complex recognize DSBs and replication stress, respectively, and in turn, this recruits and activates members of phosphatidylinositol 3-kinase-related kinases (PIKKs) family ATM and ATR by auto-phosphorylation, respectively. Phosphorylated ATM and ATR then phosphorylate the downstream kinases CHK2 and CHK1, respectively, which activates the effector proteins including p53 and CDC25 to induce cell apoptosis, senescence, and cell cycle arrest for DNA repair. ATM and ATR also recruit and phosphorylate other DNA repair factors including H2AX, 53BP1, BRCA1, MDC1, and TOPBP1.

Adapted from [183]

[13,14]. Ultimately, the downstream kinases, checkpoint kinase 1 (CHK1) and checkpoint kinase 2 (CHK2), are phosphorylated by ATR and ATM, respectively [15,16], and they, in turn, phosphorylate effectors such as cell division cycle 25 (CDC25) and tumor antigen p53 (p53) to induce apoptosis or cell cycle arrest for DNA repair[17–19].

1.2 DNA double-stranded break (DSB) repair

Although programmed DSBs are essential for the development of lymphocytes during the early stages of T and B cell maturation, unwanted DSBs are one of the most detrimental DNA lesions because they (or their repair) almost always cause insertions, deletions, translocations, and chromosome fusions, which, in turn, result in apoptosis, senescence, or tumorigenesis[20]. To cope with DSBs, mammalian cells have evolved four DSBs repair pathways: NHEJ, HR, Alt-NHEJ, and SSA (**Figure 2**).

The NHEJ pathway initiates with the recognition and binding of Ku70/86 heterodimers (Ku70/80 in yeast) to damaged sites, which, in turn, recruits DNA-PKcs to the broken ends[21,22]. After the loading of DNA-PKcs, depending on whether the damaged ends contain non-ligatable nucleotides or gaps that need to be filled, DNA end processing factors like Artemis, the Aprataxin and PNK-like factor (APLF) nuclease, polynucleotide kinase (PNK) kinase/phosphatase, terminal transferase (Tdt) and DNA polymerases λ and μ (pol λ and pol μ) are

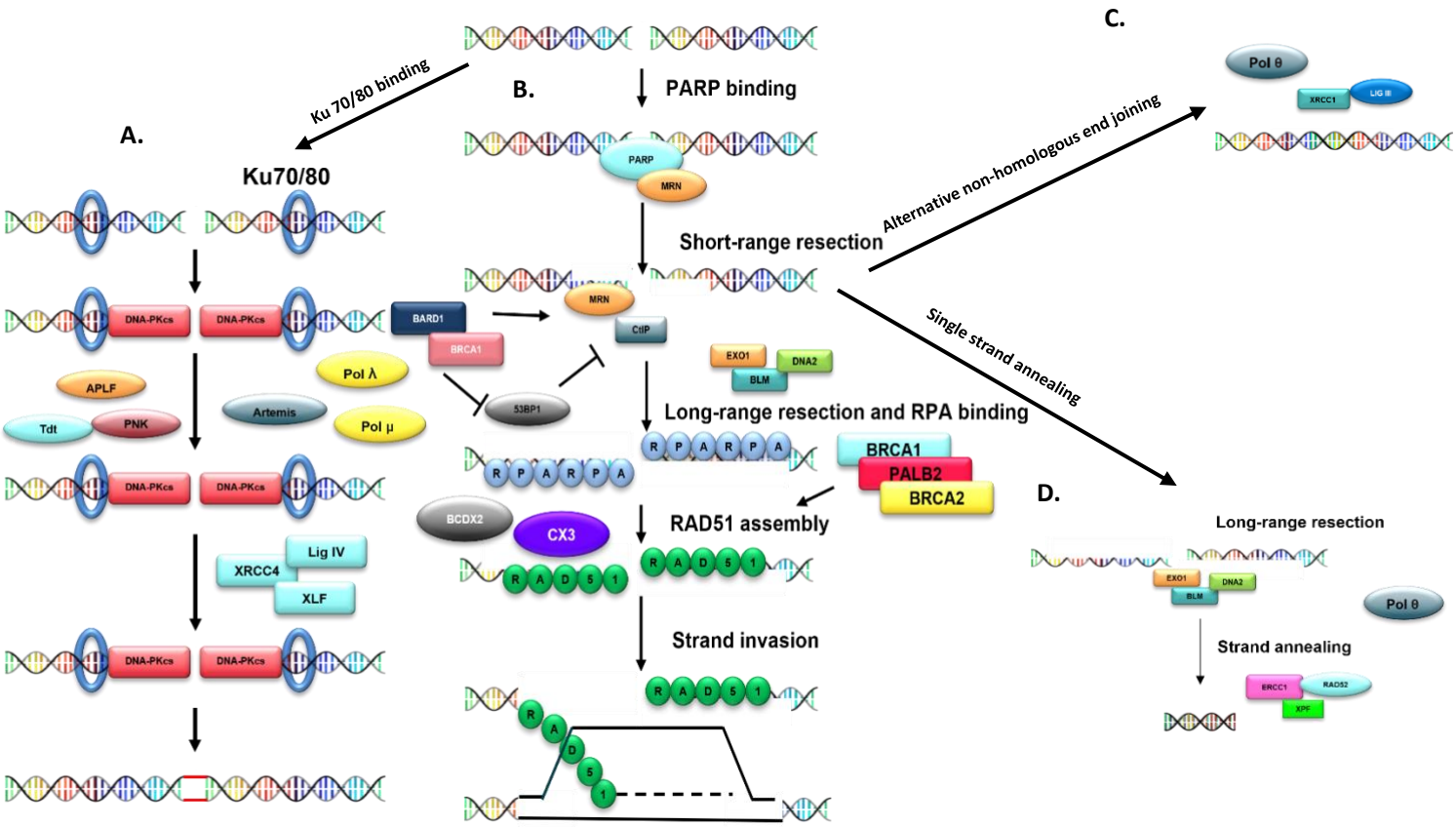

Figure 2. The double-strand break (DSB) repair pathways in mammalian cell.

- ***A. Non-homologous end joining (NHEJ) pathway.*** *NHEJ can be both error-prone and error-free. When damaged ends are compatible and only harbor undamaged nucleotides, NHEJ can repair DSBs precisely by direct re-ligation. However, when nucleotides are damaged or the break ends are incompatible, additional end processing proteins, including Artemis, APLF, PNK, pol λ and pol μ, are required to enable NHEJ.*
- ***B. Homologous recombination (HR) pathway.*** *The MRN complex competes with Ku heterodimers to perform end resection. This step is also facilitated by Poly (ADP-ribose) Polymerase (PARP), CtIP, BARD1, and BRCA1.*
- ***C. Alternative non-homologous end joining (Alt-NHEJ) pathway. The*** *Alt-NHEJ pathway is active when the DSBs end resection occurs in G_1 phase, which is a time when a homologous DNA sequence is unavailable for HR-mediated repair.*
- ***D. Single-strand annealing (SSA) pathway.*** *After the generation of long 3'-overhangs, RAD52 can direct the annealing of homologous sequences.*

relocated to process DNA ends[23–26]. The ligation factors DNA ligase IV, XRCC4, and XLF are then recruited to DNA ends to promote the ligation process[27,28] (Figure 2A). The majority (~80%) of ionizing radiation (IR)-induced DSBs are repaired by NHEJ, which makes it the predominant DSBs repair pathway in mammalian cells. Although NHEJ is active throughout the cell cycle, it occurs more frequently in G1 phase[29].

Unlike the NHEJ pathway, in which DNA ends are protected from resection by Ku70/86 heterodimers and DNA-PKcs, the HR pathway requires DNA end resection which is initiated by the MRN complex and CtIP[30,31](**Figure 2B**). The end resection mediated by the MRN+CtIP complex is limited (usually only 2 to 20 bp). To generate the long 3' ssDNA overhangs required for HR, EXO1, Blooms Syndrome (BLM), and DNA2 are recruited to the partially resected DNA ends to perform longer resection[32–34]. After the generation of long 3' overhangs, RPA is bound to 3' overhangs to protect ssDNA. RPA is rapidly replaced by recombinase, RAD51 with the assistance of BRCA1, Breast cancer allele 2 (BRCA2), and Partner and localizer of BRCA2 (PALB2) to form RAD51:DNA nucleofilaments[35,36]. In addition to RAD51, six RAD51 paralogs (RAD51B, C, D, XRCC2, XRCC3, and DMC1) have also been identified to be involved in HR. Those six RAD51 paralogs form two major complexes - BCDX2 (RAD51B, C, D, XRCC2) and CX3 (RAD51C and XRCC3). Both BCDX2 and CX3 complexes are involved in facilitating RAD51 loading and ssDNA remodeling. RAD51:DNA nucleofilaments then search the genome via strand invasion to find a

homologous DNA sequence (*e.g.*, sister-chromatid) with which to enact HR repair. DNA polymerases then fill in the gaps using the homologous DNA sequence as the template. Based on the formation of a HJ or not, there are two subtypes of HR: DSBR (with the formation of HJ) and SDSA (without the formation of HJ). In contrast to NHEJ, HR is only active during S/G2 phase, when a homologous DNA sequence is present[37]. Since HR repairs DSBs utilizing homologous DNA as a template, HR-mediated repair is considered accurate.

Although both NHEJ and HR are DSBs repair pathways, HR is distinct from NHEJ especially at the beginning of the repair process. To achieve this distinction, the activity of the MRN complex is tightly regulated by the cell cycle. However, there are still small amount of DSB ends resected by MRN and CtIP during G1 phase when the other HR repair proteins are unavailable[38]. Those DSBs are repaired by Alt-NHEJ (**Figure 2C**). The Alt-NHEJ pathway can therefore be considered as a contingency plan for DSBs repair when HR is inactive, but the DSB ends nonetheless have been resected. Alt-NHEJ is initiated with DSB end resection by MRN and CtIP to generate homologous arms with short resections. The damaged or incompatible nucleotides are then removed by Flap endonuclease 1 (FEN1)[39]. DNA Ligase III and X-ray cross complementing 1 (XRCC1) then ligate the compatible ends. Like Alt-NHEJ, SSA is also highly error-prone and requires both the short range and long range of end resection mediated by MRN, CtIP, EXO1, DNA2, and BLM. In contrast

to HR, however, in which long 3'-overhangs are coated by RPA, SSA requires the recruitment of Radiation sensitive 52 (RAD52) to the 3' overhangs to direct the annealing of the homologous strands and the incompatible nucleotides are removed by the Excision repair cross complementing 1 (ERCC1)-Xeroderma pigmentosum factor (XPF) endonuclease[40,41]. Due to the nature of Alt-NHEJ/SSA, which uses microhomologous sequences to pair two broken ends along with damaged or incompatible nucleotides, Alt-NHEJ/SSA is considered highly error-prone.

1.3 DSBs repair pathway choice in mammalian cells

NHEJ pathway is the most active of the DSBs repair pathways, but it can be both error-prone and error-free depending on the status of DSB ends. In contrast, HR is almost always conservative, but it requires a much longer time than NHEJ and is only active during the S/G2 phase when a homologous DNA sequence is present. Alt-NHEJ/SSA pathways are highly error-prone but recent studies have somewhat paradoxically identified Alt-NHEJ as the dominant DSB repair pathway in S phase and in mitochondria[42–45]. The existence of multiple DSBs repair pathways enables mammalian cells to handle all types of DSBs, generated during all phases of the cell cycle, in a quick and efficient manner. On the other hand, the existence of multiple DSBs repair pathways implies that once a DSB occurs, mammalian cells must make a series of decisions to

determine which pathway to use. Thus, the DSB repair system can be thought of as a decision tree (**Figure 3**).

The first DSB repair decision factor is the DNA lesion itself. The presence of long ssDNA tails on a DSB end affects the repair pathway choice since the DNA binding ability of Ku70/86 heterodimers are restricted to DNA ends with no or very short ssDNA tails[46].

The second DSB decision factor is timing. In mammalian cells, IR induces bulk DSBs across the whole genome, which requires rapid repair to keep mammalian cells alive. The kinetics of the NHEJ (in which the repair of DSBs

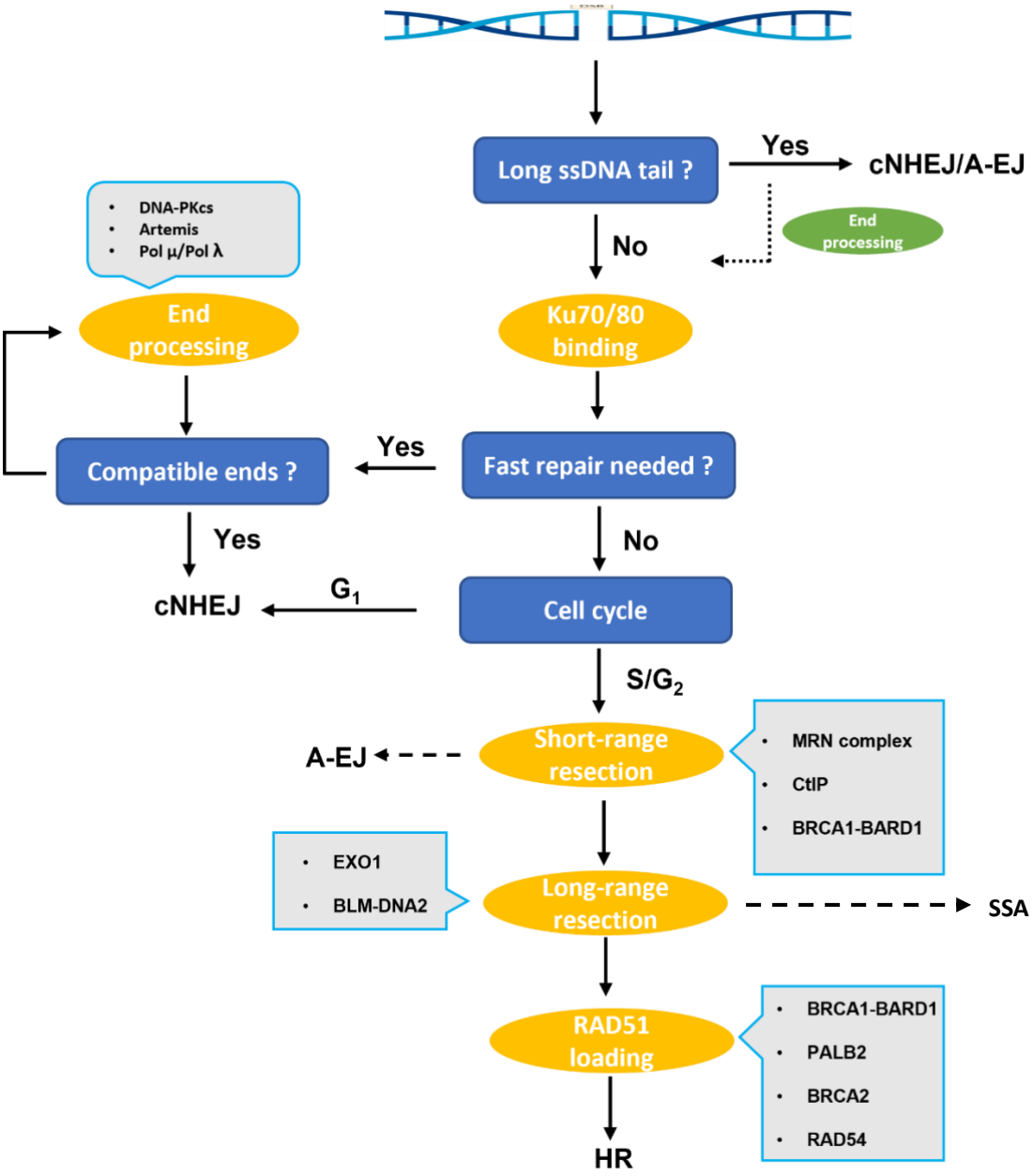
Long ssDNA tail ?
Yes
cNHEJ/A-EJ
End processing
No
Ku70/80 binding
Fast repair needed ?
Yes
Compatible ends ?
Yes
End processing
DNA-PKcs
Artemis
Pol μ/Pol λ
No
Cell cycle
G1
cNHEJ
S/G2
Short-range resection
A-EJ
MRN complex
CtIP
BRCA1-BARD1
Long-range resection
SSA
EXO1
BLM-DNA2
RAD51 loading
BRCA1-BARD1
PALB2
BRCA2
RAD54
HR

Figure 3. A decision tree for DSB repair pathway choice

There are three decision points that can affect DSB pathway choice in mammalian cells. The first one is the structure of the DSB lesion. The DNA binding capacity of Ku70/86 heterodimers are limited when the broken ends contain long ssDNA tails. Without end processing, mammalian cells cannot repair a DSB possessing a long ssDNA tail via NHEJ. Depending on the availability of RAD51, DSBs with long ssDNA tails can be repaired by HR or Alt-NHEJ. The second decision point is the resection environment, which includes the parameters of cell cycle phase and the presence of homologous DNA sequence. If the resection environment is not permissive, mammalian cells can only repair DSBs via the NHEJ pathway, which can be both error-free and error-prone depending on whether the DSB ends require end processing. However, if the resection environment is permissive (as when the cell is in S/G_2 phase), the DSB ends can be resected by MRN, CtIP, and BRCA1-BARD1, which results in the displacement of Ku70/86 heterodimers. Mammalian cells then have a final decision point — the availability of RAD51. If RAD51 is available, DSBs will be repaired by HR. If not, DSBs will be repaired by Alt-NHEJ/SSA.

occurs in a few minutes) and the HR (which requires a half-hour to several hours to repair DSBs), explain why NHEJ is the default and predominant DSB repair pathway in mammalian cells[47].

The third DSB repair decision factor is the phase of the cell cycle in which DSBs occur and/or are repaired. NHEJ is active throughout the cell cycle but dominant in G1, while HR is only active in S/G2 phase and Alt-NHEJ/SSA is more active during S phase. Given that resection is also a key to pathway choice, mammalian cells regulate this choice by using the cell cycle to activate or inactive relevant resection activities. For example, in order to be active for end resection, CtIP needs to be phosphorylated at Thr847 by a cell cycle-dependent kinase (CDK), which itself increases in activity when cells enter S phase[48,49]. Also, the phosphorylation of CtIP at Ser327 in G2 phase is important for enhancing the interaction between CtIP and BRCA1[50], which promotes DSB end resection during S/G2 phase. Besides the post-translational modification-mediated end resection regulation, pathway choice is also influenced by the activity of HR inhibitors like DNA helicase B whose activity is inhibited during S/G2 phase[51]. In addition to regulating DSB end resection via cell cycle dependent phosphorylations, the formation of the BRCA1-PALB2-BRCA2-RAD51 recombinase complex is inhibited in G1 via Cullin 3 (CUL3)-(Ring box protein 1) RBX1-Kelch-like ECH-associated protein 1 (KEAP1), which

constitutes an ubiquitin ligase complex that mediates the degradation of PALB2[37].

Chapter 2: The bromodomain and extra-terminal domain (BET) family

2.1 The bromodomain

In addition to transcription and translation, post-translational modification (PTM) including phosphorylation, acetylation, ubiquitination, methylation, and SUMOylation are other mechanisms by which mammalian cells regulate the expression level, function, and activity of proteins. Among PTMs, the acetylation of Lys residues is one of the most important and widespread PTMs and one which influences transcription, cell signaling, and metabolism[52]. Acetylation neutralizes the positive charge of Lys residues, which results in changes in the modified proteins' interaction with other proteins and/or with DNA[53]. Since histone:DNA interactions rely on the negative charge of the DNA molecule and the positive charge of Lys residues on the histone, the acetylation of histones results in weakened histone:DNA interactions and this is why it is considered a hallmark of euchromatin. Acetylated proteins - including acetylated histones - are specifically recognized by proteins possessing bromodomains (BDs), which form a structural binding cleft that is conserved throughout the evolution[54]. BDs were first discovered by John W. Tamkun with his colleagues in 1992 during their study of the *Drosophila* gene Braham/brm55 However, the structure of a BD wasn't elucidated until 1999 by Christophe Dhalluin with co-workers using nuclear magnetic resonance (NMR). Their work has demonstrated that a BD always contains approximately 110 amino acids.

Even though the amino acid sequence is not conserved among different proteins, the three-dimensional structures of BDs are highly conserved. More specifically, the tertiary structure of a BD contains an all-α protein fold, a bundle of four α helices (αA, αB, αC, αZ) separated by two intervening loops: the ZA and BC loops. The sequence and structural differences in the ZA and BC loops result in different binding affinities of the BDs.

2.2 The BET family

The acetylation of Lys residues regulates a large variety of cellular processes including RNA splicing, DNA damage repair, cell cycle, nuclear transport, actin cytoskeleton remodeling, chaperone activity, ribosome activity, chromosome remodeling, and transcription[56]. BD-containing proteins, which are the primary acetylation readers, thus play key roles in interpreting the acetylation signal in different cellular conditions. There are 46 known BD-containing proteins in mammalian cells[57]. Based on the similarity of their structure and function, these proteins are divided into eight families (from I to VIII).

There are four members in the BET family [bromodomain containing protein 2, 3, 4, (BRD2, 3, 4) and bromodomain testis associated (BRDT)]. Except for BRDT, which is a protein expressed exclusively in testis/ovary[58], BRD2, 3, 4 are ubiquitously expressed. The BET family members share a similar domain structure (**Figure 4Error! Reference source not found.**) with two tandem BDs (BD1 and BD2) and one extra-terminal (ET) domain. BD1 and BD2 are responsible for the interaction of these proteins with acetylated chromatin while the ET domain is responsible for the interaction with other proteins[59–61].

The function of BET family members relies on the interaction between acetylated histone tails and their two tandem BDs. As mentioned above, acetylated histone is a hallmark of euchromatin. As a result, the physiological

role of BET family members is related to RNA transcription and with the heritage of epigenetic marks[62–64]. The individual roles of BET members in mammalian cells are discussed in the following sections.

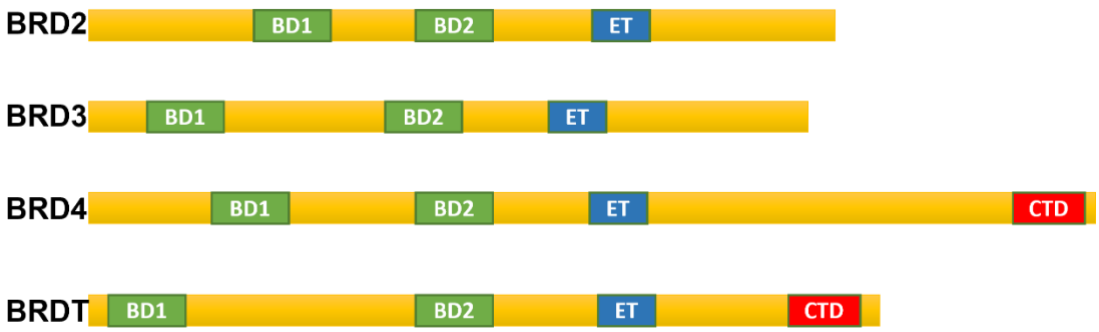

Figure 4 The schematic of BET family members

All BET family members share a similar structure: two tandem BDs and one ET domain. BRD4 and BRDT also contain homologous C-terminal domains (CTD).

2.3 BRD4

BRD4 is the most well-studied protein in the BET family because of its essential role in embryogenesis, oncogenesis, and transcriptional regulation[65]. BRD4 was first identified as a cell cycle regulating protein that promoted cell cycle progress via its regulation of Ras-related nuclear Protein (Ran), Topoisomerase 1 (Topo1), Radiation sensitive 21 (Rad21), and Transformation growth factor 1 (Tgf1)[66–69]. Subsequent studies on BRD4 then demonstrated that BRD4 is essential for maintaining pluripotency via its regulation of the transcription and activity of core stem cell genes like Octamer-binding transcription factor 4 (OCT4), PR/SET domain 14 (PRDM14), and Nanog[70–72].

Consistent with that description, BRD4 depletion results in the lethality of mouse embryos[73]. BRD4 is also involved in oncogenesis as it has been demonstrated in multiple types of cancer to regulate the expression of Cytoplasmic-myelocytomatosis viral oncogene homolog (c-Myc), the androgen receptor (AR), and Nuclear-Myc (N-Myc)[74–78].

The underlying mechanism of BRD4-mediated cell cycle progression, oncogenesis, and embryogenesis is its transcriptional regulation (**Figure 5**). BRD4 utilize its two tandem BDs to recognize and bind to the acetylated histone regions and then interacts with transcriptional activators like Nuclear receptor binding SET domain protein 3 (NSD3; a histone methyltransferase), Jumonji domain containing 6 (JMJD6; a histone arginine demethylase), Chromodomain helicase DNA binding protein 4 [CHD4; the catalytic subunit of the nucleosome remodeling and

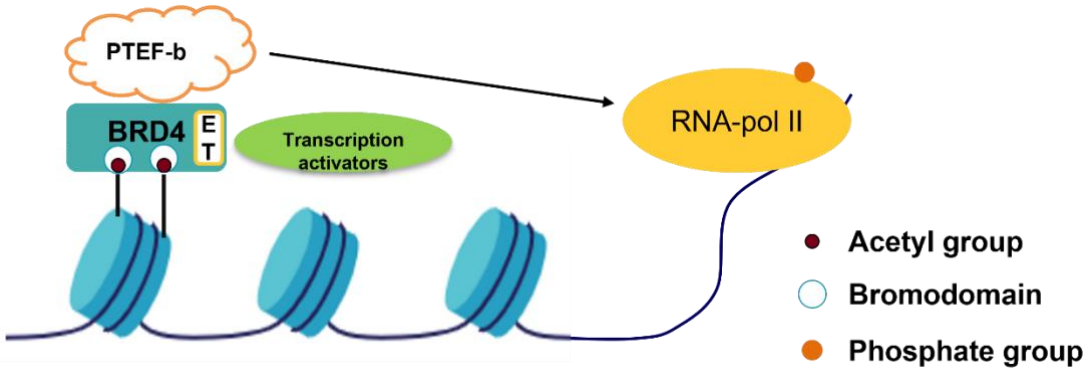

Figure 5. BRD4 regulates transcription via both transcription initiation and elongation

Simplified model of the role of BRD4 in transcription. *The two BDs of BRD4 can specifically recognize and bind to acetylated histone. The positive transcription elongation factor b (PTEF-b) is then recruited by BRD4 and phosphorylate RNA-pol II to initiate the transcription. In the meanwhile, BRD4 can interact with other transcriptional activators via its ET domain.*
Adapted from [187]

deacetylase (NuRD) complex] to facilitate the transcriptional initiation[59,79] through its ET domain. On the other hand, BRD4 also recruits positive transcription elongation factor β (PTEF-b) complex and activates its kinase subunit CDK9 via its C-terminal domain to phosphorylate RNA polymerase II to assist transcription elongation[80,81].

Several recent studies have also implicated BRD4 in the DDR pathway and DSBs repair. In 2013, Floyd et al., first reported that one isoform of BRD4 (isoform B, with a unique C-terminal coding exon), is able to attenuate a DDR signal (the formation of γH2AX) and that the loss of this unique isoform of BRD4 results in a relaxed chromatin structure, rapid cell-cycle checkpoint recovery and increased survival after IR[82]. Later, the same group reported that BRD4 prevents the formation of R-loops and transcription:replication collisions to protect the integrity of genome[83,84]. Perhaps most surprisingly, in 2014 and 2017, two independent groups demonstrated that BRD4 is critical for the NHEJ activity[85,86]. Both groups reported that after DSBs occur, histone H4 (H4) at the proximal region is highly acetylated and that H2AX is phosphorylated by ATM to form γH2AX. BRD4 is then recruited to these damaged sites and apparently serves as a scaffold for other NHEJ factors. More interestingly, another group demonstrated that in a cell-free system (*Xenopus* egg extracts), that BRD4 promotes DNA end resection and HR via an interaction between BRD4, Brahma protein-like 1, (BRG1, one subunit of SWI/SNF complex) and CtIP[87]. The pervasive involvement of BRD4 in transcription, the DDR, and NHEJ,

emphasizes its importance while simultaneously making it experimentally difficult to elucidate all of its roles/activities.

2.4 BRD2 & BRD3

Unlike BRD4, which is its own cottage research industry, the scientific literature on BRD2 and BRD3 is extremely scant. Compared to BRD4, BRD2 and BRD3 lack the C-terminal domain. As a result, even though BRD2 and BRD3 are also implicated in facilitating transcription[88], they seem to serve more as scaffold proteins for transcriptional activators[89,90]. Unlike BRD4, which is implicated in embryogenesis, osteogenesis, adipogenesis, myogenesis, cardiovascular homeostasis, immune system development, DNA repair, and oncogenesis[65], the function of BRD2 appears to be restricted to neuronal differentiation and central nervous system development[91]. Because of its important role in the brain, BRD2 is also essential for mouse embryonic development[93]. BRD3 is the least researched BET family member and it has been mostly implicated in the regulation of erythroid and megakaryocyte-specific genes[92]. There are to date still no reports on the viability of BRD3-deficient mice.

2.5 BRDT

As mentioned above, BRDT is only expressed in the testis and ovary.

Unsurprisingly, BRDT is required for spermatogenesis and BRDT is considered a potential target for male contraceptives[94]. On a mechanistic level, BRDT is also required for chromatin remodeling and the maintenance of chromatin integrity[95]. In addition, BRDT becomes activated at the onset of meiosis, and it ensures the timely expression of testis-specific genes to ensure the meiotic process[96]. Due to the highly conserved C-terminal domain also found in BRD4[97], BRDT appears to work like a tissue-specific BRD4 to regulate gene expression via the recruiting and activation of PTEF-β[96]. Although BRDT is also expressed in the ovary, especially in oocytes, there are no reports to date on the role of BRDT in ovarian or oocyte maturation. On the other hand, BRDT has been implicated in ovarian carcinoma and (somewhat surprisingly given its low expression in these tissues) lung carcinoma and renal carcinoma as well[98–100].

Chapter 3: The role of histone acetylation and BD-containing proteins in DNA DSB repair

3.1 The role of histone acetylation in DNA DSB repair

The efficient and accurate repair of DNA damage is fundamental for the survival and well-being of all organisms. In eukaryotes, DNA is wrapped by histones (H2A, H2B, H3, and H4) to form a highly condensed structure (chromatin) that is required for all mitotic and meiotic transactions[98]. The status of the chromatin determines the accessibility of the underlying DNA, and this, in turn, regulates both gene transcription and the DNA repair process. Chromatin structure is mainly determined by PTMs on histone tails, of which, histone acetylation is by far the most important. Upon DNA damage, over one-half of the histone acetyltransferases (HATs) and histone deacetylases (HDACs) are recruited to the damaged sites[101], underscoring the importance of histone acetylation on DNA damage repair.

In response to DSBs, histone acetylation and deacetylation processes occur on multiple sites. For histone 2 (H2, including H2A, H2AX, and H2B), H2AK15 and H2AXK5 are acetylated by transformation/transcription domain associated protein-tat-interactive protein, 60KD (TRRAP-TIP60)[102–104], which regulates the binding of 53BP1 and NBS1, respectively. The acetylation of H2AXK36 by CREB-binding protein/E1A binding protein p300 (CBP/P300) also promotes DSB repair, albeit the underlying mechanism is still unknown[105].

For histone 3 (H3), the acetylation on H3K14 (H3K14ac) is involved in the DDR by facilitating ATM activation although the global increase of H3K14ac is dependent on high mobility group nucleosome binding domain 1 (HMGN1)[106]. Interestingly, the acetylation status of H3K56 is dynamic and both the acetylation of H3K56 by CBP/P300 and the deacetylation of H3K56ac by HDAC1 and HDAC2 play a vital role in DNA repair (**Figure 6**)[107–109]. The deacetylation of H3K56ac at DSBs can also be performed by silent mating type information regulation 2, *S. Cerevisiae*, homolog 6 (Sirtuin 6, SIRT6)[110].

As for histone 4 (H4), multiple acetylation sites on H4 including H4K5, H4K8, H4K12, and H4K16 were reported in two independent studies after DSBs were induced[111,112]. Interestingly (or perhaps confusingly), the two groups identified the same acetylation sites on H4, but proposed that the acetylation process was carried out by CBP/P300 or TRRAP/TIP60 respectively[111,112]. Given that both CBP/P300 and TRRAP/TIP60 can facilitate NHEJ pathway TRRAP/TIP60 is also reported to assist the HR pathway[111,112] it is not unreasonable to predict that these complexes are at least partially redundant. Of the H4 acetylation sites, H4K16 seems to be vital for regulating DSB repair. Immediately after the introduction of DSBs, H4K16ac accumulates at DSBs, but is then rapidly deacetylated by HDAC1 and HDAC2[113]. Thus, H4K16 appears to act as a switch. When H4K16 is acetylated it inhibits the binding of 53BP1 to damaged sites, which promotes resection and enhances HR. The observation that HDAC1 and HDAC2 deficiency (which increases H4K16 acetylation) favors

reduced NHEJ

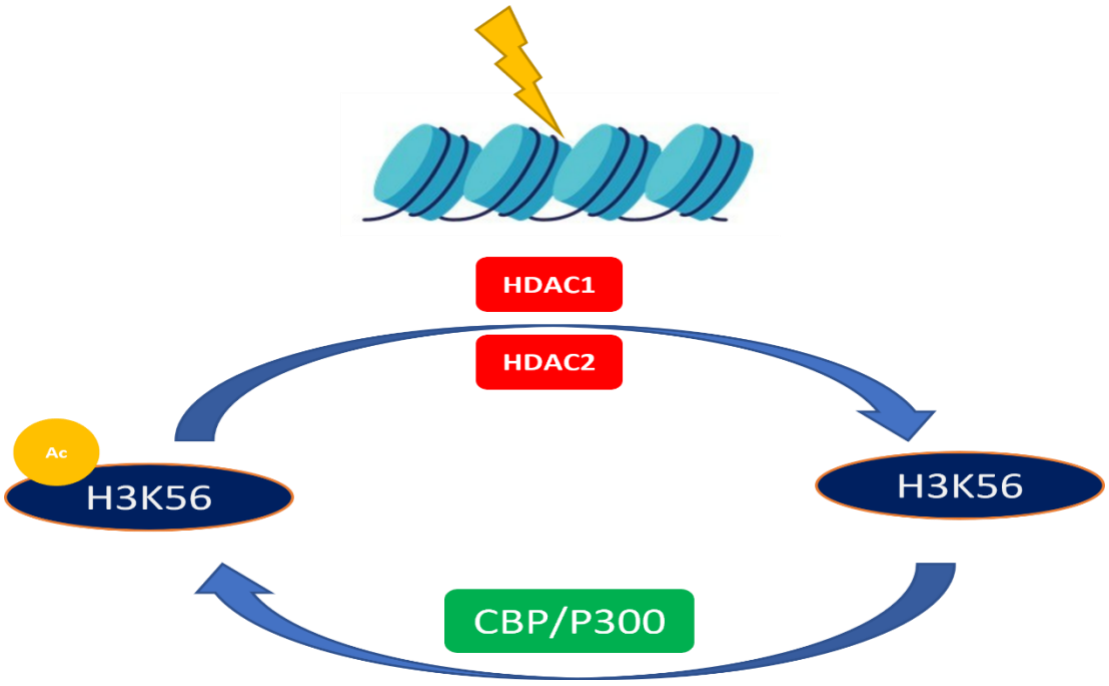

Figure 6. The controversial role of H3K56ac upon DSB induction

The deacetylation of H3K56ac by HDAC1 and HDAC2 and the acetylation of H3K56 by CBP/P300 occur after DSBs, but their importance is debated.

Adapted from[183]

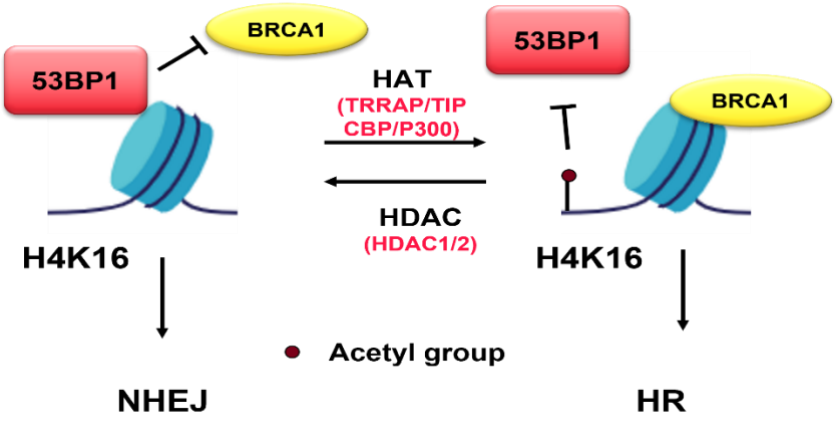

Figure 7. The dual role of H4K16ac in DSB repair

The deacetylation of H4K16ac by HDAC1 and HDAC2 occurs immediately after DSBs to promote NHEJ while H4K16 is acetylated by both CBP/P300 and TRRAP/TIP60 to promote HR.

Adapted from[114]

HR is consistent with this[113,114]. Thus, the deacetylation and re-acetylation cycle of H4K16 regulates the timing of the NHEJ and HR pathways and underscores its importance in regulating DSB repair (**Figure 7**).

3.2 The role of BD-containing proteins in DSB repair

As elaborated above, acetylation signals are mainly translated into meaningful biology by proteins containing BDs. In mammals, there are 42 known BD-containing proteins. In 2015, Gong *et al*., performed a BD-containing protein screen utilizing laser micro-irradiation in GFP-tagged BD-containing protein cell lines and they demonstrated that over one-third of all BD-containing proteins are relocalized upon DNA damage induction to DSBs[115]. Although circumstantial, this observation certainly supports the hypothesis that BD-containing proteins are likely important for DSB repair.

BD-containing proteins are divided into eight functional categories. The BD-containing proteins implicated in DNA DSB repair are focused on the BD-containing HAT group, the BD-containing chromatin remodeling group, and the BET family (**Figure 8**)[118]. Specifically, the BD adjacent to zinc finger domain 1A and 1B (BAZ1A and BAZ1B) proteins are reported to be involved in DSB repair through SWI/SNF-related, matrix-associated, actin-dependent regulator of chromatin, subfamily A, member 5 (SMARCA5)[119,120]. The BRG1/BRM-associated factor (BAF) and Polybromo-associated BAF (PBAF) complex,

which belong to the Switch/sucrose non-fermentable (SWI/SNF) family, also mediate DSB repair. Polybromo 1 (PBRM1), a subunit of PBAF, contributes to the NHEJ pathway immediately after DSBs occur[121]. Another subunit of PBAF, Bromodomain containing 7 (BRD7) is recruited to DSB sites near transcriptionally active regions to coordinate DNA repair and transcription[122]. The PBAF and BAF complex common subunit, SMARCA4 (or BRG1), works with multiple proteins including BRCA1, Fanconi Anemia complementation group D2 (FANCD2), PARP1, CtIP, and SIRT1 to facilitate HR by modulating nucleosome density at a DSBs site, by facilitating DNA end resection and the loading of RAD51[123–127]. More recently, zinc finger and MYND [Myeloid, Nervy, and DEAF-1] domain containing 8 (ZMYND8) was implicated in the regulation of HR[115]. Another BD-containing chromatin remodeler, BRD9, also regulates HR by facilitating RAD51:RAD54 complex formation[128]. Lastly, as mentioned before, BRD4 is involved in the DNA damage response signaling and DNA repair.

The ability of BRD-containing proteins to relocate either to or from DSB

sites demonstrate their likely involvement in either DDR signaling or DNA repair or both. A further investigation of the role of BD-containing proteins in DNA repair will allow us to have a better understanding of the mechanism of both

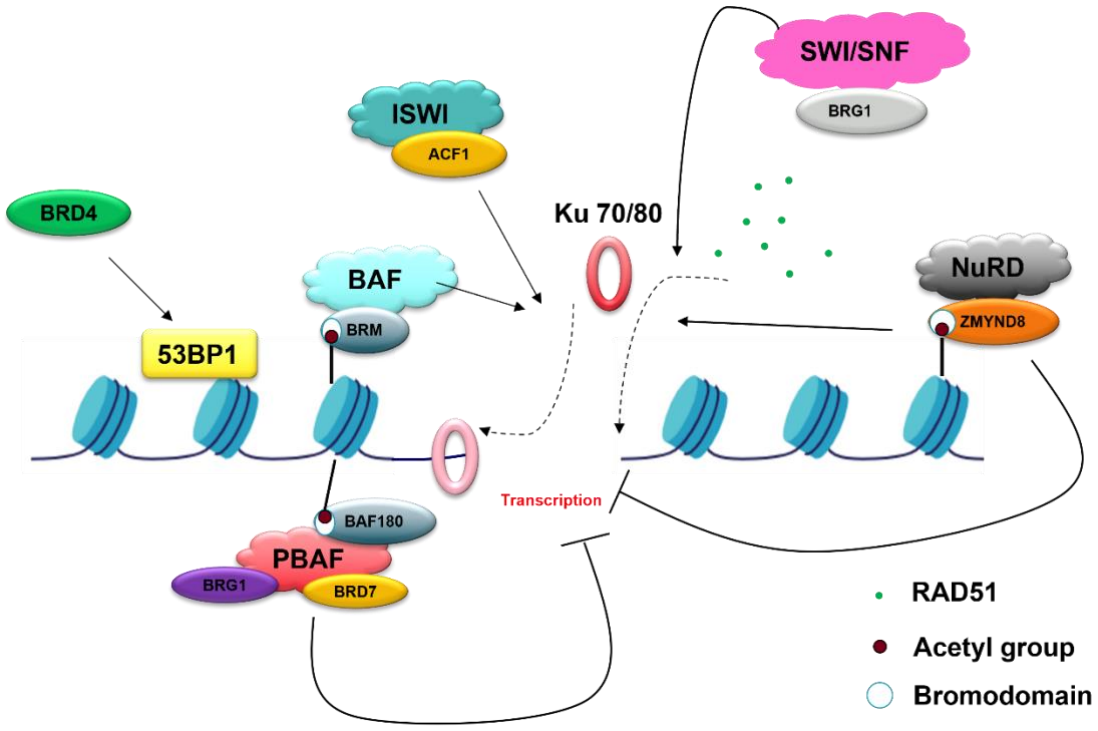

Figure 8. The role of BD-containing proteins in DSB repair pathways

Simplified model for the function of different BD-containing proteins in DSB repair pathways. *ISWI and BAF complex can facilitate the loading of Ku heterodimers on to damage sites through their ACF1 and BRM subunit, respectively. BRD4, one of the BET family members, can promote the recruitment of 53BP1 to damage sites. Both PBAF and NuRD complex coordinate the DNA repair and transcription upon DNA DSBs. ZMYND8 and BRG1 also facilitate the loading of RAD51 to promote HR.*

Adapted from[118]

epigenetics and DNA repair.

Chapter 4: Kinome-wide screening uncovers a role for bromodomain protein 3 in DNA double-stranded break repair

Chen Wang[1], Doug Chan[2], and Eric A. Hendrickson[1]

[1]Department of Biochemistry, Molecular Biology and Biophysics, University of Minnesota Medical School, Minneapolis, MN, 55455.

[2]Lester and Sue Smith Breast Cancer Center, Baylor College of Medicine, Houston, TX, 77030.

Author contribution

C.W. and E.A.H. designed the research. D.C. performed mass spectrometry for kinome analysis. C.W. and E.A.H. prepared and edited the manuscript.

4.1 Outline

Double-stranded breaks (DSBs) are toxic DNA damage and a serious threat to genomic integrity. Thus, all living organisms have evolved multiple mechanisms of DNA DSB repair, the two principal ones being classical-non homologous end joining (C-NHEJ), and homology dependent recombination (HDR). In mammals, C-NHEJ is the predominate DSB repair pathway, but how a cell chooses to repair a particular DSB by a certain pathway is still not mechanistically clear. To uncover novel regulators of DSB repair pathway choice, we performed a kinome-wide screen in a human cell line engineered to express a dominant-negative C-NHEJ factor. The intellectual basis for such a screen was our hypothesis that a C-NHEJ-crippled cell line might need to upregulate other DSB repair pathways, including HDR, in order to survive. This screen identified Bromodomain Containing Protein 3 (BRD3) as a protein whose expression was almost completely ablated specifically in a C-NHEJ-defective cell line. Subsequent experimentation demonstrated that BRD3 is a negative regulator of HDR as BRD3-null cell lines proved to be hyper-recombinogenic for gene conversion, sister chromatid exchanges and gene targeting. Mechanistically, BRD3 appears to be working at the level of Radiation Sensitive 51 (RAD51) recruitment. Overall, our results demonstrate that BRD3 is a novel regulator of human DSB repair pathway choice.

4.2 Introduction

Most living organisms have evolved at least two discrete mechanisms to repair DNA double-stranded breaks (DSBs): homology dependent recombination (HDR) and classical non-homologous end joining (C-NHEJ). In HDR, a DSB is repaired using an undamaged homologue or sister chromatid in a process that generally requires extensive regions of homology between the damaged chromosome and the undamaged donor[129,130]. Most mitotic and meiotic recombination and the repair of DSBs in late S and G_2 phases of the cell cycle (*e.g.*, stalled replication forks[131]) are carried out by HDR. Thus, HDR accounts for an important portion of the DNA DSB activity in a wild-type human cell. Not surprisingly therefore, mutations of many HDR genes are associated with cancer predisposition in humans[132,133]. One of the most critical HDR genes is Radiation Sensitive 51 (RAD51), which is responsible for the homology searches and strand exchanges required during HDR[134].

The bulk of DSB repair in higher eukaryotes proceeds, however, more frequently by a process that does not require large regions of homology. Specifically, mammalian cells have evolved an efficient ability to join nonhomologous DNA molecules together[135] using the C-NHEJ pathway[136]. C-NHEJ is critically required for the proper development of the immune system and it is especially clinically relevant because it is the preferred pathway that

cells utilize to repair ionizing radiation (IR)-induced DSBs[137,138]. Three important C-NHEJ genes are the protein kinase, DNA-activated, catalytic subunit (PRKDC or DNA-PK_{cs}), and its DNA binding heterodimeric subunit, Ku70:Ku86[139,140]. Relevantly, mutations in PRKDC have been associated with IR^s (IR sensitivity), immune deficiency and/or cancer predisposition in humans[141–143].

Although much work has been carried out and great progress has been made over the last decade[144,145], a complete mechanistic understanding of how a cell decides to repair a DSB via HDR or C-NHEJ is still lacking. The mammalian DNA damage response (DDR) is regulated by PRKDC and the related kinases ataxia telangiectasia mutated (ATM), and ataxia telangiectasia and RAD3 related (ATR)[146,147]. Some of the relevant substrates for these kinases have been identified, but their pathways are also still not completely defined. In the past, this problem has been addressed by knocking down the expression of ATM, ATR, and/or PRKDC in a favorite model system and then identifying those proteins phosphorylated in the control, but not the treated, cells following IR exposure[148]. Alternatively, mutations were made in one of these kinases and then mRNA was quantitated to identify genes that were either up or down regulated plus or minus IR exposure[149–151]. We have taken a unique approach to this problem. First, we generated human cell models for PRKDC including a knockout[152] and a kinase-dead knock-in[153]. We then used the kinase-dead and the parental cell line to perform "kinome" analyses[154]

following IR exposure. In this approach, cellular extracts are incubated with beads onto which a dozen ATP-analog inhibitors have been immobilized. Since every kinase has an ATP-binding domain, these beads bind mostly kinases and other proteins containing ATP-binding domains (*e.g.*, ATPases, chromatin remodelers, *etc.*). The beads are then centrifuged down, washed and subjected to quantitative proteomics. In this fashion, ~70% of all human kinases and a multitude of additional ATP-binding proteins can be queried[154]. These analyses identified BRD3 (bromodomain containing protein 3) as a protein whose expression was almost completely downregulated in the PRKDC kinase-dead cell line. Importantly, although BRD3 is not a kinase, it is an ATP-dependent chromatin remodeler[155] and we believe its ATP-binding domain allowed it to be identified by this screen.

There are 46 bromodomain-containing proteins (BRDs) encoded in the human genome. A BRD subfamily, called the bromodomain (BD) and extra terminal (ET) domain (BET) family, consists of 4 members [BRD2, BRD3, BRD4, and BRDT (T = testis/ovary specific)] each of which contains two N-terminal BD domains and an "extra" C-terminal domain[156,157]. BDs are modules that facilitate a protein's ability to bind to acetylated lysines[158]. Since acetylation is often associated with histone modification it is not surprising that the majority of BRDs (including the BET family members) are involved in chromatin regulation and transcription[155]. The most intensely researched BET family member is BRD4, an important transcription factor[159] and a protein that has

been implicated in the DDR[82] potentially by preventing the accumulation of R-loops[83,84].

In stark contrast, there is little known about BRD3 and there are no reports of BRD3's involvement in HDR. To date, the best function for BRD3 was inferred from an isolation of proteins on nascent DNA analysis where it was determined that BRD3 can bind to and regulate a protein called ATPase Family AAA domain containing 5 (ATAD5)[160]. ATAD5, in turn, is the main component of a complex that unloads proliferating nuclear cell antigen (PCNA) from replicating DNA. Thus, BRD3, through its interaction with ATAD5, positively regulates the amount of PCNA on a replication fork via ATAD5's PCNA unloading activity[160]. Other than this one report, however, there is little biochemical information available about BRD3.

Here we demonstrate that BRD3-null human cells are hyper-recombinogenic. Thus, human cells that have been genetically engineered to lack BRD3 expression show elevated levels of gene conversion, sister chromatid exchanges and gene targeting. Biochemically, this increase in HDR activity appears to be related to the altered kinetics of RAD51 recruitment at DSBs. Thus, we have identified BRD3 as a potent negative regulator of human HDR and this function may explain why BRD3 expression was specifically ablated in PRKDC/DNA-PK_{cs} kinase-dead cells, which are incapable of performing C-NHEJ.

4.3 Materials and methods

4.3.1 Cell lines and cell culture

Human hTERT-RPE1 (ATCC® CRL-4000™) cells were cultured in Dulbecco's modified Eagle's medium F12 (DMEM-F12) supplemented with 10% fetal bovine serum and 100 U/ml penicillin and 100 µg/ml streptomycin. HCT116 (ATCC® CCL-247™) cells and U-2 OS (ATCC® HTB-96™) cells were cultured in McCoy's 5A medium supplemented with 10% fetal bovine serum and 100 U/ml penicillin and 100 µg/ml streptomycin.

BRD3-null cell lines were constructed using Clustered Regularly Interspaced Short Palindromic Repeats (CRISPR):CRISPR-associated 9 (Cas9)-mediated gene editing technology[161–163]. Human hTERT-RPE1 cells were electroporated with a pSpCas9(BB)-2A-GFP (px458) plasmid containing a single-guide RNA targeting exon 7 of BRD3. These cells were then flow sorted to select for GFP-positive cells, which were then subsequently subjected to single cell subcloning. Candidates were screened by PCR and confirmed by DNA sequencing to obtain clones containing indels resulting in frameshift mutations.

To complement BRD3$^{-/-}$ cell lines, wild type (WT) and mutant BRD3 cDNAs were cloned into a PiggyBac transposon vector that co-expresses a neomycin

resistance selection cassette[164]. Candidate clones were selected by resistance to G418 and then the expression of WT and/or mutant BRD3 proteins were identified/quantitated by western blot analysis.

4.3.2 Antibodies

The following antibodies were used in this study: anti-BRD3 (A302-367A, A302-368A, Bethyl Laboratories), anti-53bp1 (Ab133534, Abcam), anti-RAD51 (PC-130, EMD Millipore Corp), anti-ATAD5 (Ab72111, Abcam), anti-actin (NB600-501, NOVUS Bio), anti-gamma H2A.X (phosphoS139; Ab81299, Abcam), anti-Flag (F31165-1MG, Sigma), anti-mouse IgG:HRP (170-6516, Biorad), anti-rabbit IgG:HRP (5213-2504, Biorad).

4.3.3 Muleiplexed inhibitor beads (MIBs) affinity chromatography

MIBs chromatography was performed essentially as described[154]. Briefly, cells were lysed on ice for 20 min in buffer containing 50 mM HEPES (pH 7.5), 0.5% Triton X-100, 150 mM NaCl, 1 mM EDTA, 1 mM EGTA, 10 mM sodium fluoride, 2.5 mM sodium orthovanadate, 1X protease inhibitor cocktail from Roche, and 1% each of phosphatase inhibitor cocktails 2 and 3 from Sigma. The cell lysate was sonicated (3 X 10s) on ice, centrifuged for 15 min (13,000 rpm) at 4°C and then the supernatant was collected and filtered through a 0.2 mM membrane. The filtered lysate was brought to 1 M NaCl and pre-

cleared by flowing over 500 µl of blocked and washed NHS-activated Sepharose 4 Fast Flow beads. The flow-through was collected and passed through a column of layered inhibitor-conjugated beads [Bisindoylmaleimide-X (50 µl), SB203580 (50 µl), Lapatinib (100 µl), Dasatinib (100 µl), Purvalanol B (100 µl), VI16832 (100 µl), PP58 (100 µl)] to isolate protein kinases from the lysates. Kinase-bound inhibitor beads were washed with 20 ml of high-salt buffer and 10 ml of low-salt buffer, each containing 50 mM HEPES (pH 7.5), 0.5% Triton X-100, 1 mM EDTA, 1 mM EGTA, and 10 mM sodium fluoride, and 1 M NaCl or 150 mM NaCl, respectively. A final wash of 1 ml 0.1% SDS was applied to the columns before elution in 1 ml of a 0.5% SDS solution in high heat. Elutions from all columns were combined and cysteines were alkylated by sequential incubations with DTT for 20 min at 60°C and iodoacetamide for 30 min at room temperature in the dark. The elution was spin-concentrated to 100 ml and detergents were removed by a chloroform/methanol extraction. After a final mixing, the sample was centrifuged for 5 min to pellet the protein at the interface and the upper phase was removed with care to leave the protein pellet intact. The protein pellet and lower phase were resuspended in 300 ml of methanol, and the sample was again vortexed and centrifuged for 5 min to pellet the protein at the bottom of the tube. The supernatant was removed and one or more methanol washes were performed to ensure the removal of detergents.

4.3.4 Immunoblotting

For whole cell lysates, cells were collected and resuspended in radioimmunoprecipitation assay (RIPA) buffer with protease inhibitors. The cells were incubated in RIPA for 30 min at 4 ^{o}C and then centrifuged at 4 ^{o}C for 15 min.

For chromatin fraction lysates, cells were collected and resuspended in Buffer A (10 mM Hepes, pH = 7.9, 10 mM KCl, 1.5 mM $MgCl_2$, 0.34 M sucrose, 10% glycerol, 0.1% Triton X-100, 1 mM phenylmethylsulfonyl fluoride (PMSF), and 1 µg/ml leupeptin). The cells were incubated in Buffer A for 5 min at 4 ^{o}C and then centrifuged for 5 min at 4 ^{o}C. The pellets were then resuspended in TSE 500 buffer (20 mM Tris, pH = 8.0, 2 mM EDTA, 500 mM NaCl, 0.1% SDS, 1% Triton X-100, 1mM PMSF, and 1 µg/ml leupeptin), followed by sonication and centrifugation at 4 ^{o}C. The resulting protein concentrations were determined using a Bradford protein assay and appropriate samples were then subjected to sodium dodecyl sulfate-polyacrylamide gel electrophoresis (SDS-PAGE) and then transferred to nitrocellulose membranes. The membranes were blocked with 5% milk in Tris-buffered saline:0.1% Tween (TBST) for 1 hr at room temperature followed by overnight incubation with the primary antibody (diluted in 5% milk in TBST). Proteins were detected by incubating membranes with horseradish peroxidase-conjugated secondary antibodies for 1 hr at room temperature and an enhanced chemiluminescence kit.

4.3.5 Immunofluorescence staining

Cells were grown in chamber slides to 70% confluency. Cells were washed with phosphate-buffed saline (PBS) and then fixed with 4% formaldehyde at room temperature for 10 min. After fixing, cells were treated with 0.5% NP-40 at room temperature for 10 min. Cells were blocked with 1% bovine serum albumin (BSA) in PBS for 30 min. Slides were incubated with primary antibodies overnight at 4℃ followed by application of fluorescent secondary antibodies. Slides were mounted with ProLong™ Gold and Diamond Antifade Mountant with DAPI. Images were obtained with a Nikon inverted TI-E deconvolution microscope and analyzed with Image J.

4.3.6 Flow cytometry

Cells were collected in PBS and fixed in 4% formaldehyde. After fixing, the cells were treated with FLAER (Alexa 488 proaerolysin variant) in a liquid format for *in vitro* detection. Cells were then processed on a Becton Dickson Fortessa X-20 machine and profiles were analyzed with Flowjo.

4.3.7 Sister-chromatid exchange (SCE) assay

Cells were seeded in 6-well plates and treated with thymidine for 18 hr.

Cells were then washed with PBS and grown in fresh media for 9 hr. After first-round release, the cells were treated with thymidine and 5-ethynyl-2'-deoxyuridine (EdU) for 15 hr. Then, cells were washed with PBS and grown in fresh media with EdU for 9 hr. After the second-round release, cells were washed with PBS and grown in fresh media for 33 hr. At this juncture, many cells were in metaphase.

The cells were then treated with 0.25 μg/ml colcemid for 1.5 hr. Cells were collected in PBS followed by 0.075M KCl treatment at 37℃. After KCl treatment, cells were slowly fixed by the addition of fixative (1:3 acetic acid to methanol) while vortexing. The cells were then dropped onto pre-warm slides in a 37℃ water bath. Slides were then incubated in a 37℃ water bath for 5 min and air-dried overnight.

The slides were rehydrated in PBS for 5 min and fixed with fresh 3.7% formaldehyde/PBS. After washing with PBS, slides were incubated with click reaction buffer (10 μM biotin-azide, 10 mM sodium ascorbate, and 2 mM CuSO4 in PBS) for 1 hr. After washing with PBS, slides were blocked in ABDIL buffer (20 mM Tris, pH 7.5, 2% BSA, 0.2% fish gelatin, 150 mM NaCl, 0.1% sodium azide) for 1 hr at room temperature followed by anti-streptavidin Alexa Flour 488 conjugate incubation for 1 hr at room temperature. After washing with PBS, slides were mounted with ProLong™ Gold and Diamond Antifade Mountant with DAPI.

4.3.8 Gene targeting assay

The gene-targeting assay was performed essentially as described (46) by first knocking out the expression of the Phosphatidylinositol Glycan Anchor Biosynthesis Class A (PIGA) gene and then restoring its expression via gene targeting using a donor plasmid. To first inactivate PIGA expression in RPE1-hTERT WT, BRD3-/-, and BRD3-/-:+BRD3cDNA [1-8] cell lines, a TGATCGGGTATCAGTGGAAG sgRNA was used with a CRISPR/Cas9 methodology. To reconstitute the expression of PIGA and minimize the effect of the NHEJ pathway, we used a sgRNA (TGGGTGAAAGTGCTCACACT) targeting a distal intronic region. To perform the gene targeting assay, the following nucleic acids were transfected into RPE1-hTERT cells (1 x 106) using a Neon Transfection System: 1 µg CleanCap® Cas9 mRNA; 1 µg donor plasmid; 1 µg mCherry expression plasmid (from Clontech); 50 pmol PIGA intron 5 sgRNA from Synthego Corporation. The cultures were grown for a subsequent ~14 days. All cells were then fixed with 4% formaldehyde for 15 min. The fixed cells were then resuspended in phosphate buffered saline (PBS) at a low density and stained with 5 X 10-9 M fluorescent Alexa aerolysin (FLAER) 488 (Pinewood Scientific Services) for 15 min. Eventually, the percentage of FLAER-negative and FLAER-positive cells was quantitated by flow cytometry (FACSCanto II, BD Biosciences).

4.3.9 DNA repair assay

The pEGFP-Pem1-Ad2 plasmid based NHEJ assay was performed essentially as described[165]. Prior to transfection, the pEGFP-Pem1-Ad2 plasmid was digested by either the I-*Sce*I or HindIII restriction enzymes (NEB) for 1 hr. After gel purification, 0.4 μg of digested plasmids and 0.1 μg of an mCherry transfection control expression plasmid (Clontech) were co-transfected into 24-well plates using Lipofectamine 3000 Reagent. Cells were collected 48 hr post transfection and analyzed by flow cytometry for GFP expression as described[165].

For the DR-GFP assay, 0.2 μg DR-GFP plasmid, 0.2 μg I-*Sce*I expression plasmid (from Clontech), and 0.1 μg mCherry expression plasmid (from Clontech) were co-transfected into 24-well plates. Cells were collected 48 hr post transfection and analyzed by flow cytometry for GFP expression as described[165].

4.3.10 Imaging and analysis

Images were captured on a Nikon inverted TI-E deconvolution microscope and analyzed with Image J.

4.3.11 Clonogenic survival assay

Cells were seeded in 6-well plates (300 to 500 cells/well based upon the doubling time of a specific cell line) and incubated at 37 °C with 5% CO_2 overnight. The cells were then treated with different doses of IR or etoposide and incubated at 37 °C with 5% CO_2. After approximately one week of incubation, the media was removed from each well by aspiration. The cells were then rinsed with PBS, fixed with 10% methanol:10% acetic acid at room temperature for 15 min. The cells were then stained with 0.5% crystal violet staining buffer at room temperature for 30 min. After rinsing thoroughly with PBS, colonies (defined as > 50 cells) were ready to be counted.

4.3.12 siRNA transfection

SMARTPool ATAD5 siRNA were ordered from Horizon Discovery Ltd., (Catalog ID: L-004738-00-0005) and transfected into RPE1-hTERT cell line using the DharmaFECT™ Transfection Reagents - siRNA transfection protocol. In brief, siRNA was resuspended into DNase/RNase-free water at a final concentration or 5 μM. To transfect siRNA into cells growing on 24-well plates, two tubes were prepared to dilute the siRNA and DharmaFECT 1 transfection reagent separately: tube 1 — A 50 μl volume of the siRNA in serum-free medium was made by adding 2.5 μl of the siRNA to 47.5 μl of serum-free medium; tube 2 — A 50 μl volume of diluted DharmaFECT 1 transfection reagent in serum-free medium was generated by adding 1.25 μl of DharmaFECT 1 transfection

reagent to 48.75 µl of serum free-medium. The contents of tube 1 and tube 2 were then mixed by carefully pipetting them together and then incubating them for 20 min at room temperature. 400 µl of antibiotic-free complete medium was then added for a total volume of 500 µl transfection medium. This transfection medium was then added into each well of a 24-well plate.

4.3.13 Structure/function analysis

To complement BRD3$^{-/-}$ cell line, wild type BRD3 and structure mutant BRD3 cDNA were cloned into a PiggyBac transposase vector with neomycin selection cassette. The expression of WT and mutant BRD3 were identified by western blot.

4.3.14 Statistics and reproducibility

For the statistics of all experiments, p-values were calculated using the student test (t-distribution).

For reproducibility: 1) the DR-GFP assay was repeated up to five times except for the ATAD5-knock down samples, which were repeated only twice). 2) The SCE assay was repeated three times except for the samples using a mutant BRD3, which were repeated only twice. A double-blind method was used for quantification. 3) The gene targeting assay was repeated three times. 4) The focus formation assay was repeated twice.

4.3.15 Nucleic acid sequences

All nucleic acid sequences can be found in ***Table 2***

4.4 results

4.4.1 Identification of BRD3 as a gene differentially regulated in PRKDC-KD cells

PRKDC is essential for C-NHEJ[139,148,166]. In the course of investigating the roles of PRKDC in C-NHEJ, we utilized gene editing methodologies to generate two PRKDC deficient cell lines: DNA-$PK_{cs}^{-/-}$ [152] and DNA-$PK_{cs}^{KD/-}$ (KD = kinase dead; hereafter PRKDC-KD cells)[153] in the human colorectal carcinoma HCT116 cell background. In particular, the dominant negative activity of the KD version of PRKDC makes these cells exquisitely sensitive to IR and essentially ablates C-NHEJ in comparison to wild-type cells[153]. Despite this severe phenotype, PRKDC-KD cells are nonetheless viable[153]. We hypothesized that one explanation for this viability might be due to a compensatory upregulation of other DSB repair pathways, including HDR. On a simplistic level, this could be accomplished by up-regulating activators or inactivating inhibitors of other DSB pathways. Thus, we were interested in identifying proteins whose expression was either enhanced (potential activators) or decreased (potential inhibitors) in a PRKDC-KD cell line.

To identify such putative novel DSB repair factors, we performed a kinome-wide screen using multiplexed inhibitor beads (MIBs) and mass spectrometry (MS)[154]. MIBs are composed of a combination of Sepharose beads with

covalently immobilized kinase inhibitors of selected kinases or pan-kinases. Using this methodology, approximately ~70% of all human kinases can be queried[154]. Thus, this technology reveals the impact of a mutation NOT on downstream substrates *per se*, but on the other kinase signaling pathways in the cell. The rationale for utilizing this approach was the hope for identifying regulatory kinases/factors (activators or inhibitors) whose activity might be altered in the mutant cell lines.

Accordingly, proteins were pulled-down by MIBs and then processed by MS using extracts prepared from HCT116 wild-type (WT) and PRKDC-KD cells. WT cells were used as a baseline and proteins whose expression level changed in the PRKDC-KD cells were identified (**Figure 9**). As a control and as expected, the level of PRKDC was only slightly reduced in the PRKDC-KD cells compared to the WT parental cell line (**Figure 9A**). In total, 3,088 proteins were identified whose expression was either unchanged, enhanced or reduced (data not shown). Of these, 51 proteins in the PRKDC-KD cells exhibited expression changes (either enhanced or reduced) greater than five-fold (**Table 1**). A Gene Ontology (GO) analysis (data not shown) was not particularly informative, but one protein, the BET family member, BRD3, whose relative abundance was altered the most (**Table 1**) in the PRKDC-KD cell line (**Figure 9A**), caught our attention. This protein, which is not a kinase, is a putative chromatin remodeling protein and moreover the BET family of proteins have been implicated in DNA DSB repair[87]. A Western blot

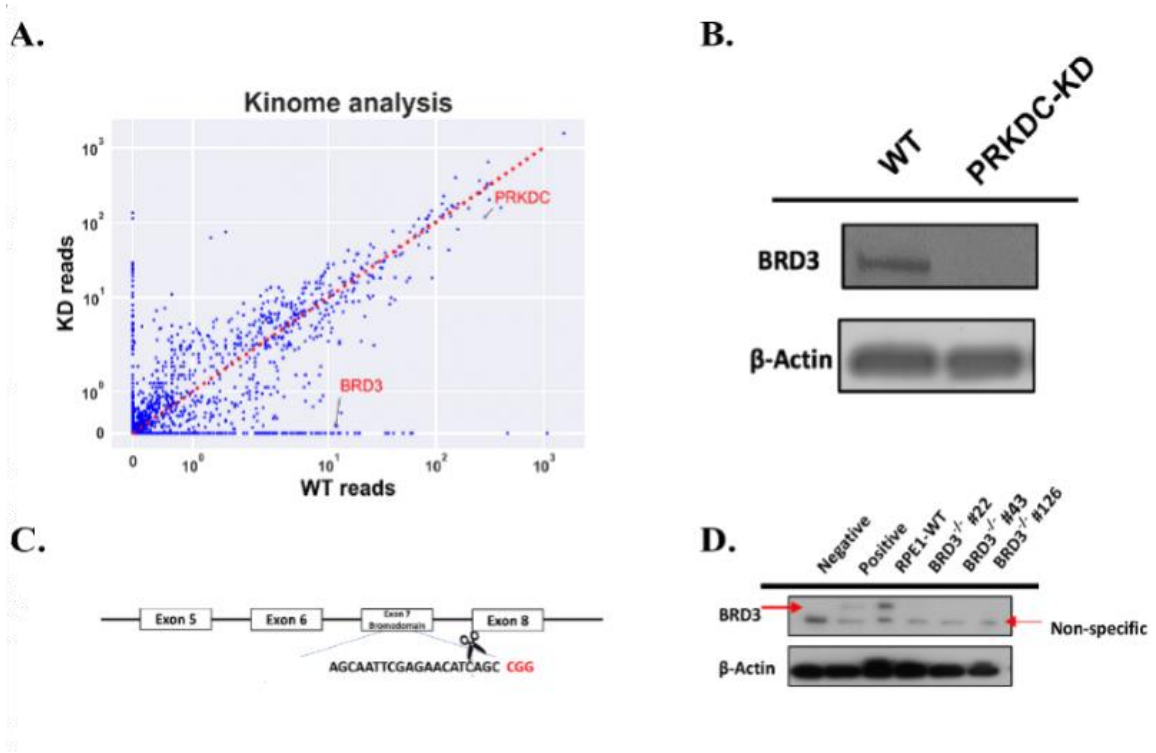

Figure 9. Kinome analysis identifies BRD3 as a protein whose expression is greatly reduced in PRKDC-KD cells

A. The number of peptides that could be unequivocally identified as belonging to a particular protein are shown along the X and Y axes for the parental HCT116 and the PRKDC-KD cell lines, respectively. The red dashed line corresponds to the theoretical equal expression in both cell lines for any given protein and the points above and below the line correspond to proteins whose expression was enhanced or decreased, respectively, in the PRKDC-KD cells. The data points corresponding to PRKDC and BRD3 are shown.

B. Western blot analysis confirms that BRD3 expression is greatly reduced in PRKDC-KD cells. Whole cell extracts were prepared from the indicated cell lines and subjected to a immunoblot analysis using either an antibody to BRD3 or, as a loading control β-actin.

C. Schematic of gene targeting approach for generation of BRD3 KO cell lines. Exon 7, which encodes one of the bromodomains of BRD3 was targeted using a CRISPR sgRNA. The sequence of the sgRNA is shown and the scissors indicate the predicted site of cleavage. The adjacent PAM site is shown in red.

D. Western blot analysis of RPE1 BRD3-KO cell lines. Whole cell extracts were prepared from the indicated cell lines (negative = PRKDC-KD and positive = HCT116 WT) and subjected to an immunoblot analysis using either an antibody to BRD3 or, as a loading control, β-actin.

Table 1. Proteins whose expression was either increased or decreased > 5X-fold when the parental cells were compared to the PRKDC-KD cells

Gene	Fold change	Gene	Fold change	Gene	Fold change
SFN	5.66	IQGAP1	-14.29	PCNA	-15.35
NAP1L4	7.65	ITPR3	-5.52	MTA2	-7.43
AP3S1	14.25	KRT77	-5.80	TIMM17A	-12.68
S100A9	12.79	FAR1	-7.64	EHMT2	-33.00
MRPL28	6.56	CHCHD6	-5.25	NDC1	-10.00
KRT23	14.12	SCD	-14.45	MAK16	-7.65
HMGA1	6.50	CCNT2	-11.09	PIK3R4	-7.31
KIAA0020	6.05	AFF4	-6.57	BMS1	-11.00
ITGB4	6.00	TMEM161A	-15.00	PXMP2	-12.86
SLC25A24	5.79	UNC50	-5.00	PRKAR1A	-14.49
RAB35	8.59	FAM83H	-32.00	KRT76	-5.22
USO1	16.33	UBAC2	-5.56	MAGOH	-9.29
PRKAA2	12.59	COX15	-7.64	TM9SF4	-8.00
KRT7	29.66	COG8	-7.14	DCXR	-11.58
KRT71	8.35	SEC24B	-12.86	TOMM5	-10.91
MELK	15.00	GPD2	-13.57	NQO1	-5.53
ABCF1	5.27	THEM6	-6.55	CCND3	-5.42
IKBKB	8.00	FBXO47	-10.30	ANAPC1	-24.00
S100A4	8.38	BRD3	-52.78	MRPL30	-8.20
PTMA	8.38	ERN1	-9.41	TUBB3	-5.39
SERPINB3	13.33	PDS5A	-6.00	U2AF1	-13.97
IGF2BP3	10.83	FAM83B	-5.59	GNB2	-5.43
SYNJ2BP	39.47	PTGES2	-5.45	GNB4	-5.45
SYNJ2BP-COX16	38.81	GRK6	-6.05	STAU2	-6.52
SET	5.58	SPTBN1	-19.60		
SERPINB4	13.23	HNRNPA3	-11.67		
STK35	6.50	CHP1	-14.22		

analysis of the parental WT HCT116 and the PRKDC-KD cells confirmed that BRD3 expression was reduced in the latter cell line (**Figure 9B**). To further confirm the decrease in BRD3 expression is at protein level instead of mRNA, the mRNA level of BRD3 has been tested in the parental WT HCT116 and the PRKDC-KD cells via RNA-seq (**Figure 10**).

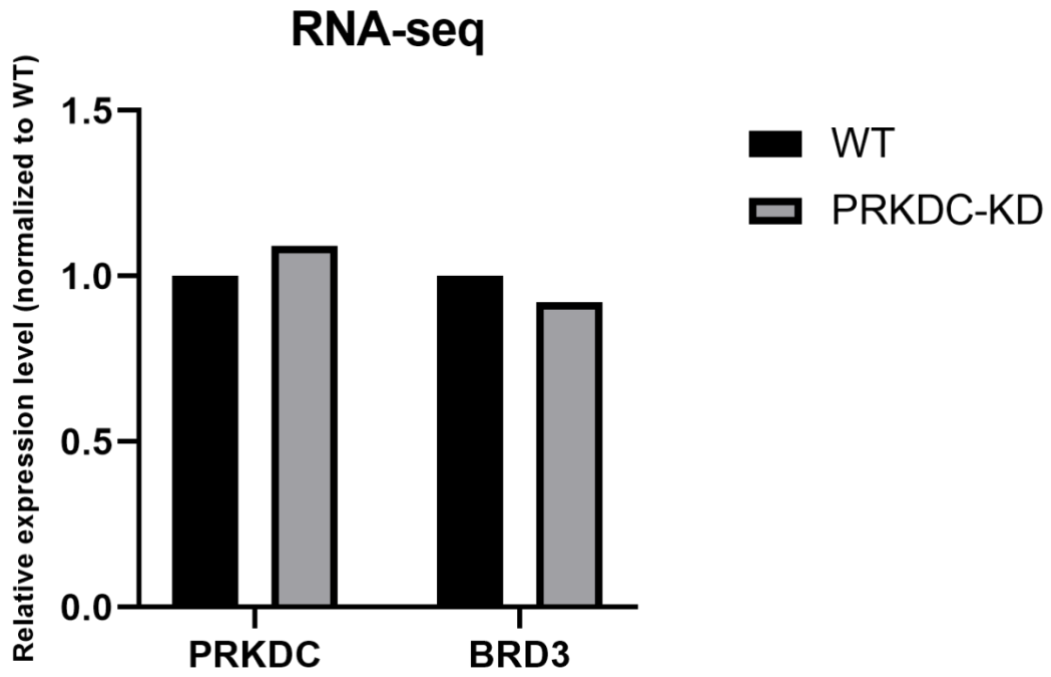

Figure 10. The mRNA level of BRD3 in the parental WT HCT116 and PRKDC-KD cells

The figure shows the mRNA level of BRD3 in both WT and PRKDC-KD cells. There is no significant difference in terms of BRD3 expression at RNA level. This data is produced via RNA-seq.

4.4.2 Derivation of BRD3 knockout (KO) cell lines

To pursue BRD3 in more detail, we next generated human BRD3-KO cell

lines. For these experiments, the parental cell line was the retinal pigment epithelial 1 cell line immortalized by the expression of human telomerase (hTERT-RPE1 or simply RPE1 cells). We chose this cell line, because it has a stable, diploid karyotype and although it is immortalized (allowing for easy propagation in tissue culture), it is not transformed (unlike the HCT116 cell line) and thus conforms to a more "normal" human cell model. The KO cell lines were generated using CRISPR/Cas9 via the strategy of allowing a CRISPR-induced DSB to be mutagenically repaired by the endogenous C-NHEJ pathway. A sgRNA was designed that targeted exon 7, which encodes one of the bromodomains of BRD3 (**Figure 9C**). Single cell clones were isolated, expanded and subjected to DNA sequence analysis. Three independent BRD3 KO ($BRD3^{-/-}$) clones were obtained containing out-of-frame indels of -1 and -2 (#22), +1 and +1 (#43) and -2 and +1 (#126). These cell lines were subsequently subjected to a Western blot analysis to confirm the absence of BRD3 protein expression (**Figure 9D**). Since the three KO clones showed no differences in growth properties (data not shown) we used them interchangeably in subsequent experiments.

4.4.3 BRD3-KO cell lines have aberrant DNA damage response

We treated RPE1 WT and $BRD3^{-/-}$ cells with IR. $BRD3^{-/-}$ cells were more sensitive to IR (**Figure 11**) but the sensitivity was mild (D_{37} for WT = 1.2 Gy; D_{37}

for BRD3-KO cells = 0.8 Gy). Consistent with this observation, the disappearance of g-H2AX foci (**Figure 12A**) following IR exposure (2 Gy) was slightly, but significantly, retarded in BRD3-KO cells (**Figure 12B**). To assess if there was a frank defect in DSB repair, we utilized the pEGFP-Pem1-Ad2 extrachromosomal reporter assay that has been vetted extensively[152,165,167]. This reporter permits the analysis of the relative repair frequency for C-NHEJ. The plasmid contains an EGFP gene interrupted by a 2.4 kb intron derived from the rat phosphatidylethanolamine methyltransferase 1 (PEM1) gene that is itself interrupted by an adenoviral (Ad2) exon. The Ad2 exon, in turn, is flanked on both sides with *HindIII* and *I-SceI* restriction enzyme recognition sites (**Figure 13A**). In its unmodified form, the presence of an adenoviral (Ad2) exon within the PEM1 intron prevents the expression of EGFP due to the Ad2 exon being incorporated into the GFP mRNA (**Figure 13C**). Upon digestion with either a *HindIII* or *I-SceI* restriction enzyme, linearized plasmids lacking the Ad2 exon with either compatible cohesive ends (*HindIII*) or incompatible ends (*I-SceI*) are generated. While the digestion of the *HindIII* recognition sites results in cohesive 4-bp overlapping ends, the fact that the *I-SceI* sites have been arranged in an inverted orientation requires the processing of the DNA ends before they can be rejoined (**Figure 13B**). Importantly, both undigested and partially digested plasmids will not contribute to the GFP positive readout for this assay as any inclusion of the Ad2 exon will create mRNAs with an interrupted EGFP coding region (**Figure 13C**). In addition, the introns spanning

the Ad2 exon provide a substrate that can undergo long-range resection events before losing the capability of expressing EGFP. Therefore, the impact of the loss of BRD3 expression on end joining could be assessed by FACS (fluorescent activated cell sorting) analysis. In order to determine the repair efficiency, cells are co-transfected with a pCherry expression vector that acts as a transfection control. The repair efficiency is reported as a percentage of cherry-positive cells that are also green (*i.e.*, repaired). Using this assay, BRD3 KO cells appeared to have no quantifiable defect in C-NHEJ; neither with HindIII- nor with I-SceI-generated ends (**Figure 13D**).

In summary, BRD3 KO cells were mildly IR-sensitive and appeared to have difficultly completing repair in a timely fashion as indicated by the slower disappearance of g-H2AX foci, but they did not appear to be defective in C-NHEJ.

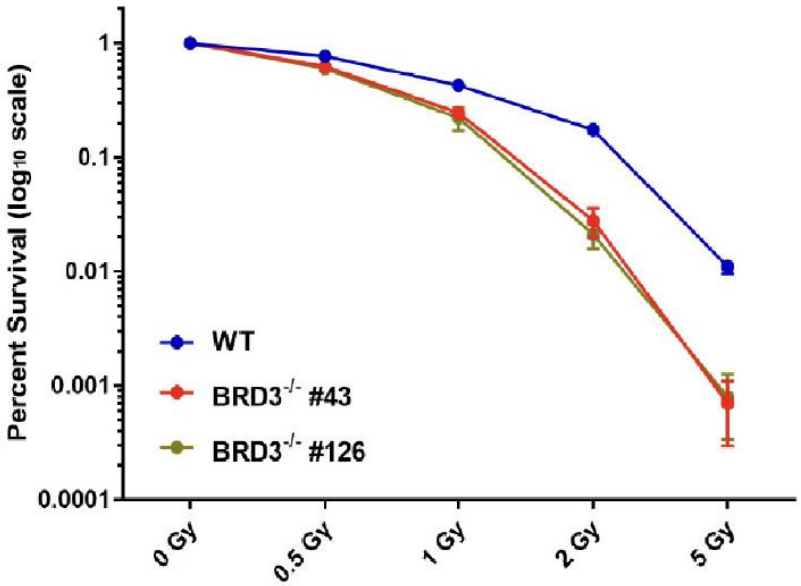

Figure 11. BRD3-KO cells are slightly IR-sensitive

Cells from the indicated cell lines were plated onto tissue culture dishes and grown overnight. The following day, the plates of cells were exposed to the indicated doses of IR. Approximately 10 to 14 days later, the plates were washed, fixed and then stained with crystal violet. The number of cells surviving to form colonies of 50^{+} cells was then quantitated. The data represent the experiment performed independently twice, in triplicate.

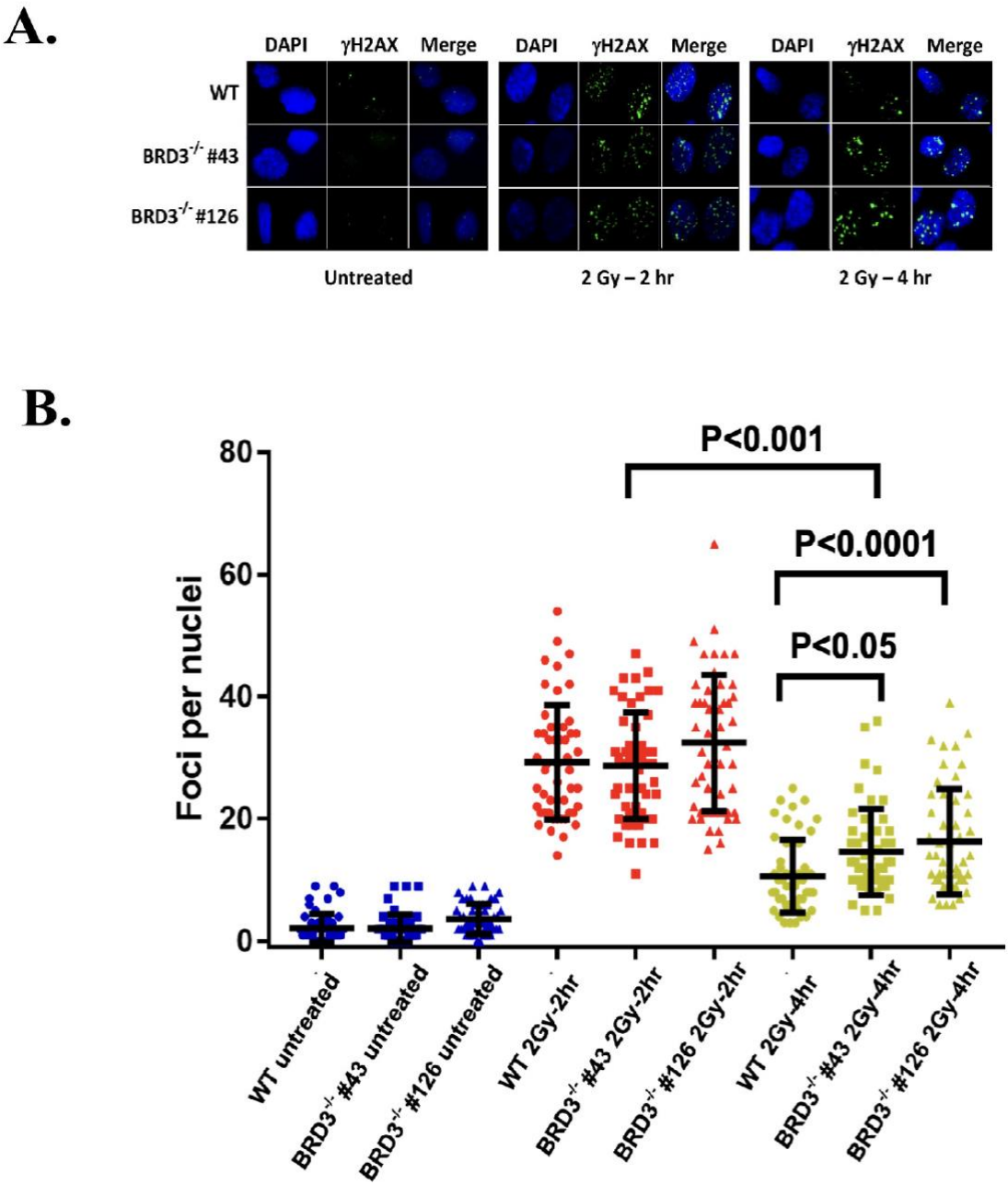

Figure 12. BRD3-KO cells show a deficit in rejoining of IR-induced DSBs as evidenced by residual γH2AX foci

A. Cells from the indicated cell lines were either left untreated or treated with 2 Gy of IR. At the indicated time points the cells were then fixed and scored for the presence of gH2AX foci. The following day, the plates of cells were exposed to the indicated doses of IR. At either 2 or 4 hr post irradiation, the cells were fixed, stained and subsequently quantitated for gH2AX foci.

B. Quantification of (A.) n=50, student test was performed to test significancy.

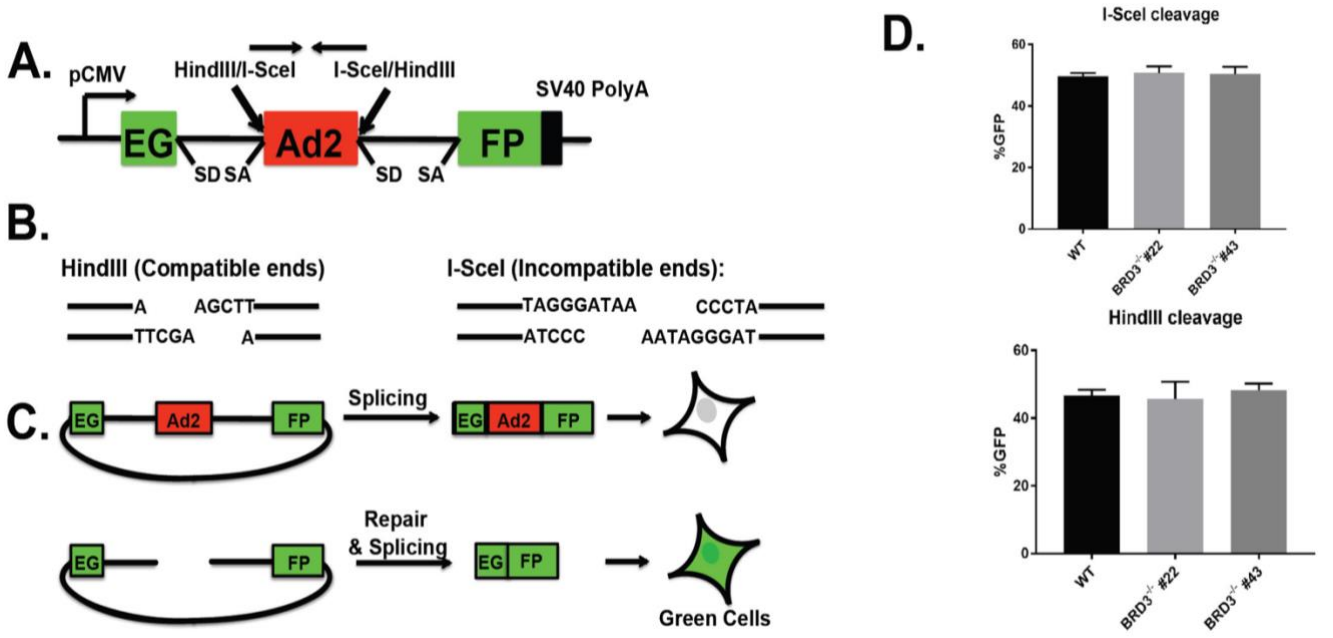

Figure 13. BRD3-KO cells are not defective in C-NHEJ

A. A schematic of the C-NHEJ reporter (pEGFP-Pem1-Ad2) is shown. The construct contains a GFP cassette whose expression is driven by a CMV promoter and terminated by the SV40 polyA sequence. "G" is separated" from "FP" by a 2.4 kb intron containing an exon (Ad2) from adenovirus that is flanked by HindIII and I-SceI restriction enzyme recognition sites. Splice donor (SD) and splice acceptor (SA) sites are also shown.

B. Restriction sites used to introduce DSBs. Digestion with HindIII (left) generates compatible cohesive ends. By contrast, cleavage by I-SceI (right) generates incompatible ends.

C. Due to the presence of the Ad-exon in the middle of the Pem1 intron, the Ad exon is efficiently spliced into the middle of the GFP ORF, inactivating the GFP activity and thus making the starting substrate GFP negative. Both sides of the Ad exon have HindIII/I-SceI restriction sites. Cleavage with either of these endonucleases removes the Ad exon and upon successful intracellular plasmid circularization (generally mediated by C-NHEJ) GFP expression is restored and can be quantitated by flow cytometry.

D. BRD3-null cells are not defective for C-NHEJ. The data using the pEGFP-Pem1-Ad2 reporter cleaved with either I-SceI (top) or HindIII (bottom) are shown.

4.4.4 BRD3-KO cell lines are hyper-recombinogenic

To interrogate the phenotype of BRD3 KO cells in more detail we next assessed their ability to perform HDR using a plasmid reporter. The DR-GFP reporter[168] (**Figure 14A**) contains two inactive green fluorescent protein (GFP) genes along with a recognition site for the *I-SceI* meganuclease. Expression of *I-SceI*, can cleave one of the inactive GFP genes and if HDR occurs it can restore GFP expression resulting in easily-quantitated green fluorescing cells. This reporter measures non-crossover products generated by the HDR sub-pathway of gene conversion[130]. Two independent BRD3 KO clones showed ~2-fold and 2.5-fold, respectively, greater HDR activity relative to the parental cell line (**Figure 14B**). A HCT116 parental cell line and a RAD52 KO cloned derived from it, the latter of which is known to be reduced for HDR activity[169], were used as controls and the RAD52$^{-/-}$ cell line showed an expected ~2-fold reduction in HDR activity. Thus, BRD3 KO cell lines appeared to be hyper-recombinogenic.

To confirm the hyper-recombination phenotype of BRD3$^{-/-}$ cells using endogenous chromosomes, we next conducted a sister chromatid exchange (SCE) assay. In this assay, chromosomes are labeled for 1 cell cycle with the nucleoside analog, EdU. After a 2nd round of replication in the absence of EdU, only one strand of one sister chromatid will contain the EdU label (**Figure 15A**). If exchanges between the sister chromatids subsequently occurs before mitosis,

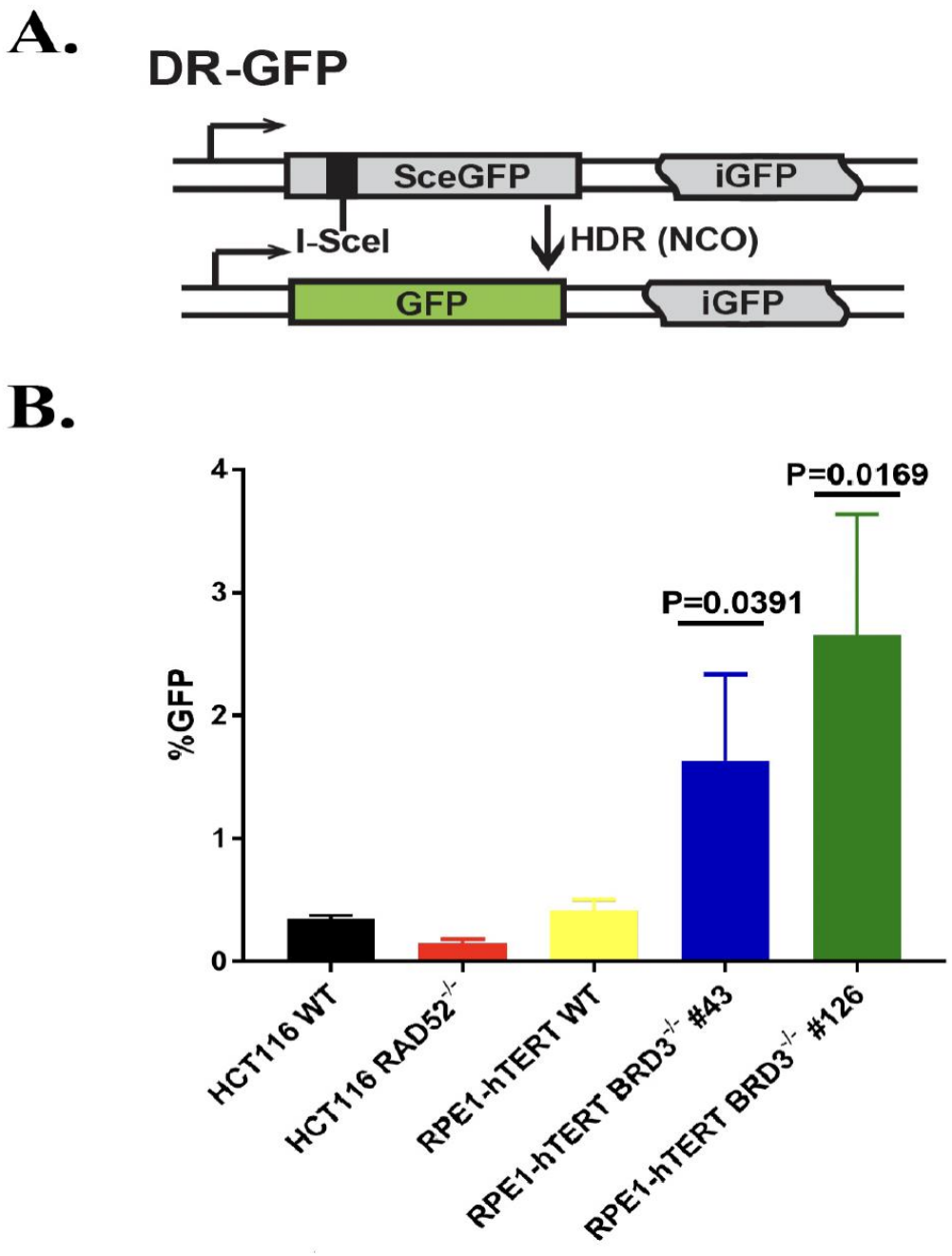

Figure 14. BRD3-null cells are hyper-recombinogenic for gene conversion

A. A schematic of the DR-GFP extrachromosomal reporter is shown. The reporter contains two inactive copies of the GFP open reading frame (ORF). One of the copies, however, contains the recognition site for the I-SceI restriction enzyme. Following cleavage by I-SceI, a non-crossover (NCO) HDR event will restore one of GFP copies into a functional ORF, which can be quantitated by scoring for green fluorescence using FACS.

B. BRD3-KO cells are hyper-recombinogenic. The amount of green fluorescence was quantitated in the respective cell lines. The data represent 2 independent experiments, performed in duplicate.

this can be visualized with a fluorescent dye using click chemistry (**Figure 15A**). Thus, SCEs were quantitated in both the parental RPE1+hTERT cell line as well as in the BRD3 KO clone #126 (**Figure 15B**). The BRD3-null cells had a highly significant ~2-fold greater incidence of SCEs than the parental cells (**Figure 15C**).

Finally, we assessed HDR activity by measuring the frequency of gene targeting. To accomplish this, CRISPR was first utilized to disrupt the phosphatidylinositol glycan anchor biosynthesis class A (PIGA) gene in both WT and BRD3$^{-/-}$ cells by inserting a single nucleotide into exon 6 to disrupt its reading frame (**Figure 16A**). PIGA can serve as a screening marker because it is required for the biosynthesis of glycophosphatidylinositol (GPI) anchors and the inactivation of PIGA leads to the loss of GPI anchors. The absence of GPI anchors, in turn, can be quantitated using a specific stain (an Alexa-488 conjugated proaerolysin variant called FLAER) that normally binds to the anchors[169,170]. To correct the PIGA mutation, we induced a second CRISPR-mediated DSB into the intronic region 47 bp away from the insertion site during gene-editing and provided a plasmid-based donor DNA (**Figure 16A**) that should facilitate the conversion of PIGA-null (PIGA$^{o/-}$) cells back to PIGA-proficient (PIGA^{+}). Thus, the gene targeting efficiency can be calculated as the ratio of FLAER-positive (PIGA^{+}) cells to FLAER-negative (PIGA^{-})[169,170]. In the parental cells, correction could be achieved about 1% of the time. In two independent BRD3 cell lines, however, PIGA correction occurred at

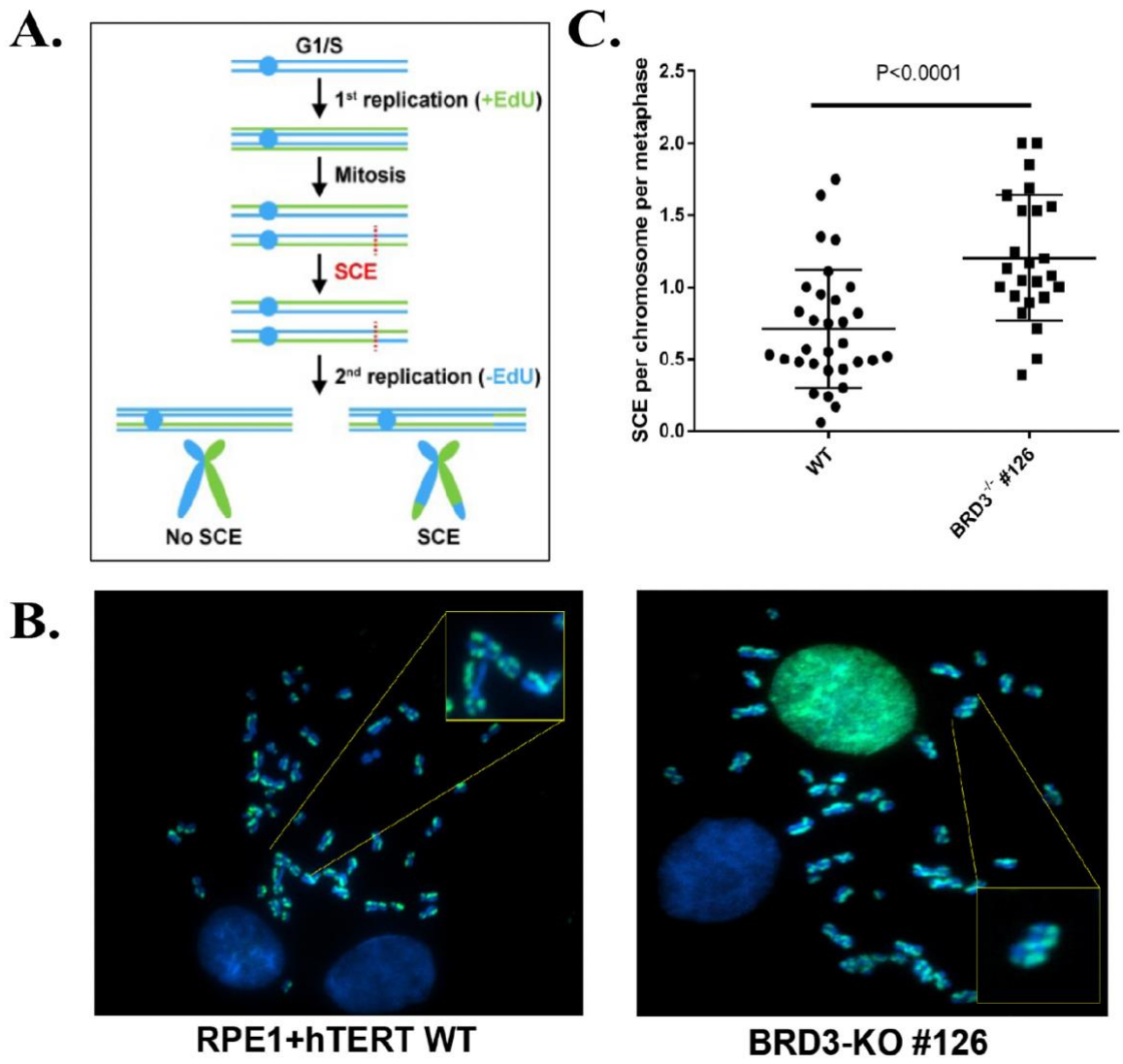

Figure 15. BRD3-null cells have elevated levels of SCEs

A. *A schematic of the EdU labeling protocol used for measuring SCEs.*
B. *A representative metaphase image for the parental RPE1+hTERT (left) or the BRD3-null #126 (right) cell lines are shown including an enlargement of metaphase chromosomes that have undergone SCEs*.
C. *Quantitation of the SCEs for the parental (WT) and the BRD3-null clone #126.*
The data represent three independent experiments and a double-blind method was used for quantification.

frequencies of ~3% and 4%, respectively (**Figure 16B**).

In summary, by 3 completely independent methodologies: 1) exogenous reporter assays, 2) SCEs and 3) gene targeting, BRD3-null cells were reproducibly hyper-recombinogenic.

4.4.5 Reconstitution of BRD3 expression rescues the hyper-recombination phenotype of BRD3$^{-/-}$ cells

Two endogenous BRD3 isoforms have been reported for human cells in the NCBI database (**Figure 17A**). Isoform 1 conforms to the expected wild type BRD3 protein. Isoform 2 is identical to isoform 1 except that it is missing a single amino acid (alanine 647) in its C-terminus. Although isoform 2 is likely just a cloning artefact, we nonetheless isolated sublclones of BRD3-null cells (clone #43) stably expressing either isoform 1 or isoform 2. Three subclones were selected for analysis. Subclones 1-2 and 2-6 (expressing isoforms 1 and 2, respectively) expressed supra levels of BRD3 whereas subclone 1-8 (expressing isoform 1) expressed approximately wild-type levels (**Figure 17B**). These cell lines were then tested for their ability to carry out HDR gene conversion (**Figure 17C**), the frequency at which they generated SCEs (**Figure 17D**) and the frequency at which they underwent gene targeting at the PIGA locus (**Figure 17E**). In all cases, regardless of whether isoform 1 or isoform 2 was expressed and regardless of the level of that expression, the restoration of

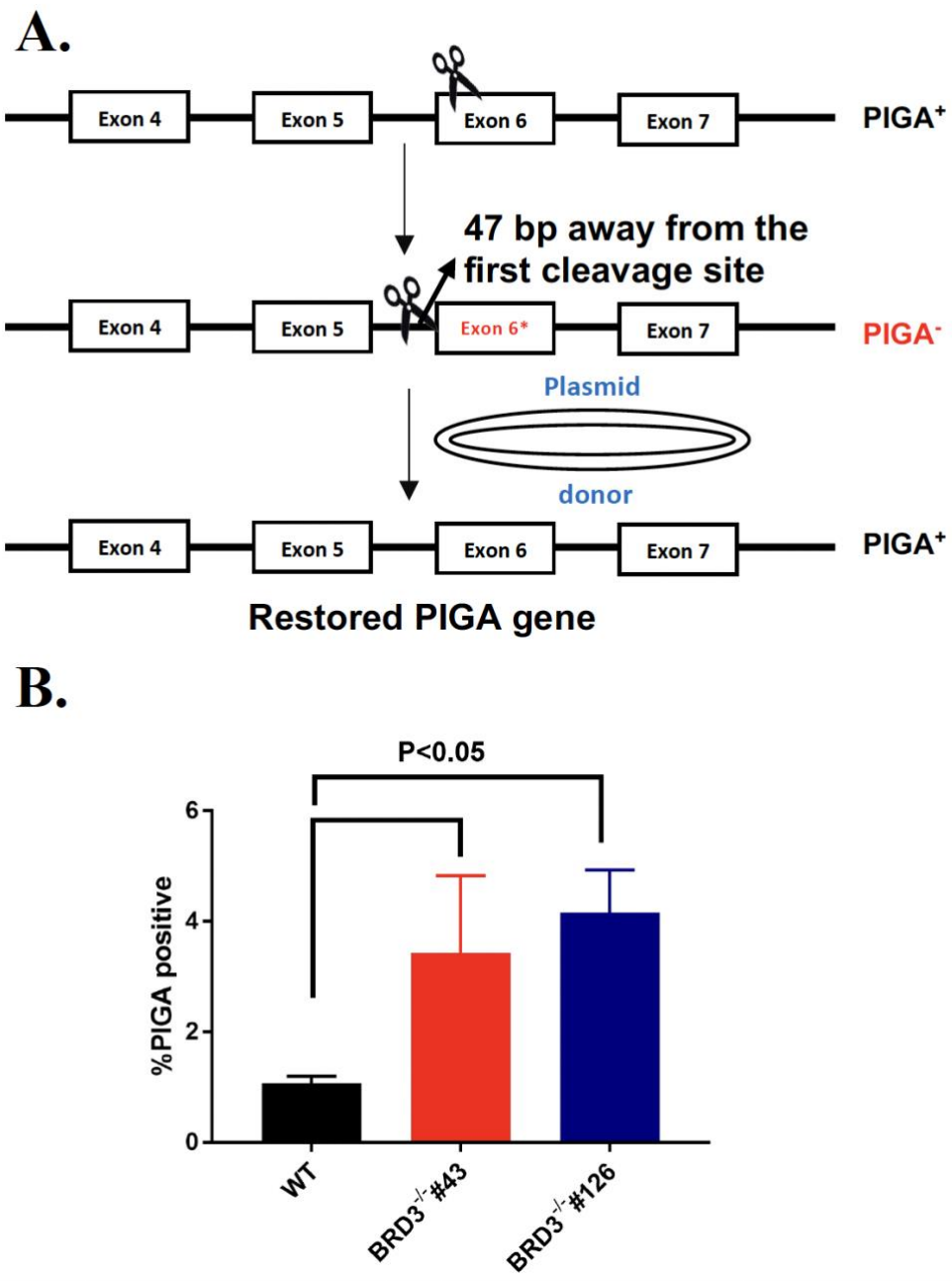

Figure 16. BRD3-null cells are hyper-recombinogenic for gene targeting

A. A schematic of the PIGA locus that was utilized for the gene editing experiments. In the first step, CRISPR/Cas9 was used to introduce a stop codon into exon 6 (scissors). In the second step, a second CRISPR/Cas9-mediated DSB was introduced 47 nt downstream of the stop mutation and then (step 3) a donor plasmid containing WT BRD3 exon 6 sequences was used to restore PIGA expression.

B. The percentage of PIGA-null cells that were converted to PIGA-positive for WT, and two independent BRD3-null clones (#43 and #126) are shown.
The data shown are derived from three independent experiments

BRD3 expression complemented the hyper-recombination phenotypes of the BRD3-null cells. From these experiments we concluded that one of the normal functions of endogenous BRD3 is to suppress hyper-recombination.

4.4.6 The depletion of BRD3 facilitates the formation of RAD51 filaments and impairs 53BP1 recruitment to DSB sites

To gain some mechanistic insight into the underlying role of BRD3 in hyper-recombination/DSB repair, we queried the status of RAD51, 53BP1 as well as g-H2AX as indicators of HDR, C-NHEJ and DSBs, respectively. Immunofluorescence staining was performed with both RAD51 and 53BP1 antibodies on IR-treated (2 Gy) or untreated WT, $BRD3^{-/-}$, and $BRD3^{-/-:+BRD3:cDNA\ \#1\text{-}8}$ cells at different time points (**Figure 19A**). There was no significant difference in the number of g-H2AX foci introduced by IR exposure into the cell lines nor in their temporal resolution (**Figure 19B**). These data suggested that the levels of initial DSB damage in the 3 cell lines was comparable and that in the short term (*i.e*., within 16 hr) there was no significant difference in the number of those DSBs resolved. BRD3-null cells did show a reduction in the formation of 53BP1 foci 2 hr after IR exposure (**Figure 19C**). However, since this phenotype was not rescued by the re-expression of BRD3 and there was no difference at any other time points the significance of this reduction at this single time point was unclear (**Figure 19C**). In contrast, the kinetics of RAD51

focus formation were clearly altered (**Figure 19D**). In BRD3-null cells, RAD51 foci accumulated at the earliest time point examined (2 hr) and then were rapidly resolved. The parental WT cells and the complemented cell line, on the other hand, showed an expected slower accumulation of RAD51 foci (peaking at 4 hr) as well as a slower resolution (**Figure 19D**). This alteration in RAD51 focus formation was observed in an independent experiment that was carried out for 18 hr, with the exception that the distinction between the nulls and the parental/complemented cell lines was even more extreme, principally because the parental/complemented cell lines did not show a peak of RAD51 accumulation until 8 hr (**Figure 18**). The slow [4 hr (**Figure 19D**) to 8 hr (**Figure 18**)] accumulation of RAD51 foci in the parental and complemented cell lines was consistent with the HDR repair kinetics observed in normal human cells[138] and contrasted sharply with the kinetics observed in BRD3-null cells (**Figure 19D and Figure 18**).

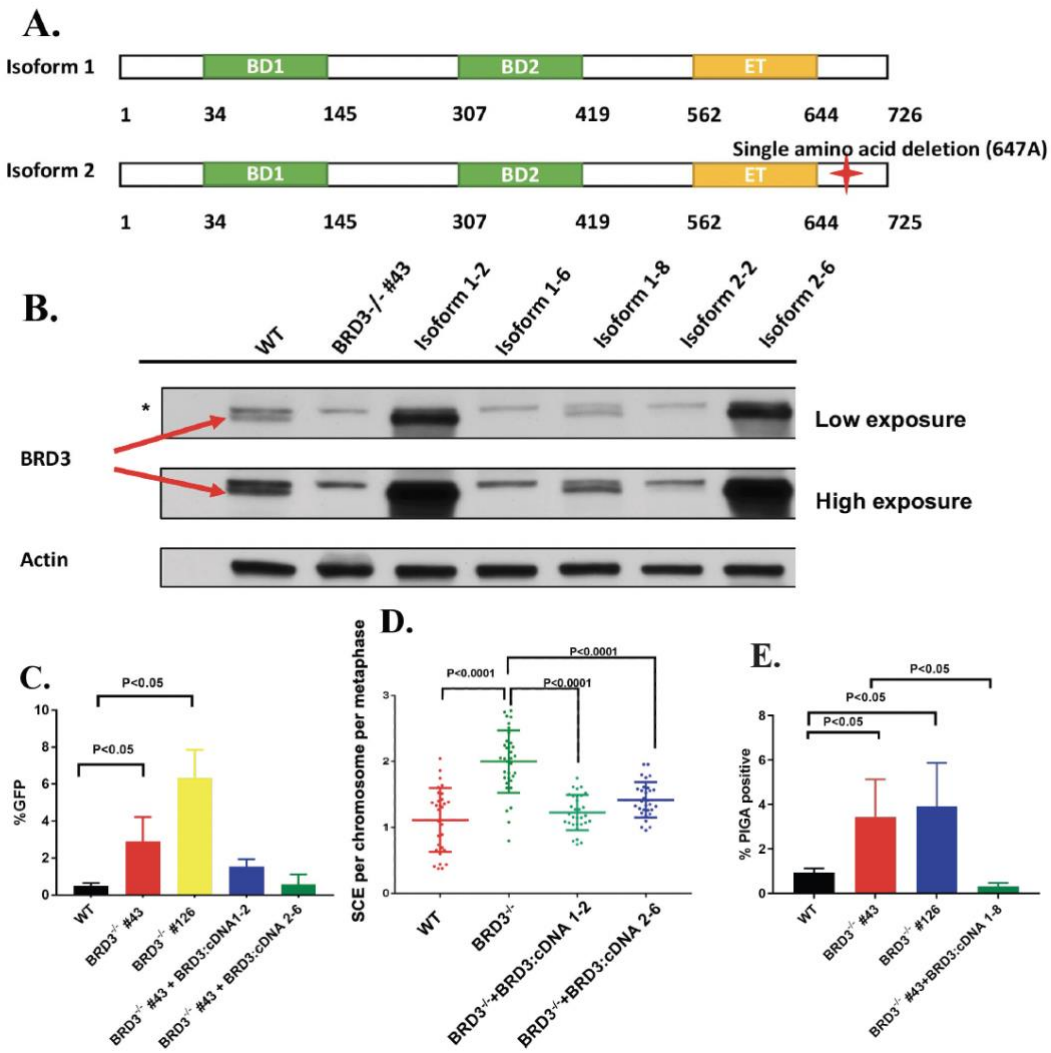

Figure 17. Expression of a wild type BRD3 cDNA rescues all of the hyper-recombination phenotypes of a BRD3-null cell.

A. *Schematics of two BRD3 wild-type cDNAs listed in the National Center for Biotechnology Information (NCBI) database. The cDNAs are identical except that isoform 2 lacks a single amino acid (647A) in the C-terminus.*

B. *BRD3-null subclones stably expressing either isoform 1 or isoform 2 were subjected to Western blot analysis to demonstrate the re-expression of BRD3. A higher non-specific band is seen in all the lanes probed with the anti-BRD3 antibody whereas the red arrow indicates the position of BRD3. Actin was used as a loading control. Three subclones (1-2, 1-6 and 1-8) expressing isoform 1 and two subclones (2-2 and 2-6) expressing isoform 2 are shown.*

C. *Complementation of the elevated HDR gene conversion activity in BRD3-null clone #43 by the re-expression of either isoform 1-2 or 2-6.*

D. *Complementation of the elevated SCE activity in BRD3-null clone #43 by the re-expression of either isoform 1-2 or 2-6.*

E. *Complementation of the elevated PIGA gene targeting activity in BRD3-null clone #43 by the re-expression of isoform 1-8.*

The data shown are derived from two or three independent experiments.

4.4.7 The BD and ET domains are important for BRD3 activity

BRD3 is a presumed chromatin remodeler. One of the reasons for believing this is that BRD3 contains two BD domains, which facilitate binding to acetylated lysines (a moiety often found on histones)[158]. To investigate if these domains played a role in BRD3's ability to suppress hyper-recombination, we generated stable cell lines containing cDNAs deleted for BD1, BD2 or the ET domain (**Figure 20A**). To facilitate identification of the BRD3 variants a FLAG epitope moiety was appended onto their C-termini. These variants were then stably introduced in BRD3-null cells and individual clones expressing the deletion variants were isolated (**Figure 20B**) although it should be noted that for the BD1Δ isoform our best clone contained only a low level of expression. Each of the cell lines was then assessed for the frequency of SCEs. The BRD3-null cells once again showed an increase in SCEs compared to the parental WT cell line (**Figure 20C**). Importantly, while the expression of a WT BRD3 cDNA completely rescued this hyper-SCE formation phenotype, BD1D-, BD2D- and ETD-expressing clones were just as hyper-recombinogenic as the null cells (**Figure 20D**). From these experiments we concluded that the 3 known functional domains of BRD3 were all required for BRD3's ability to suppress hyper-recombination.

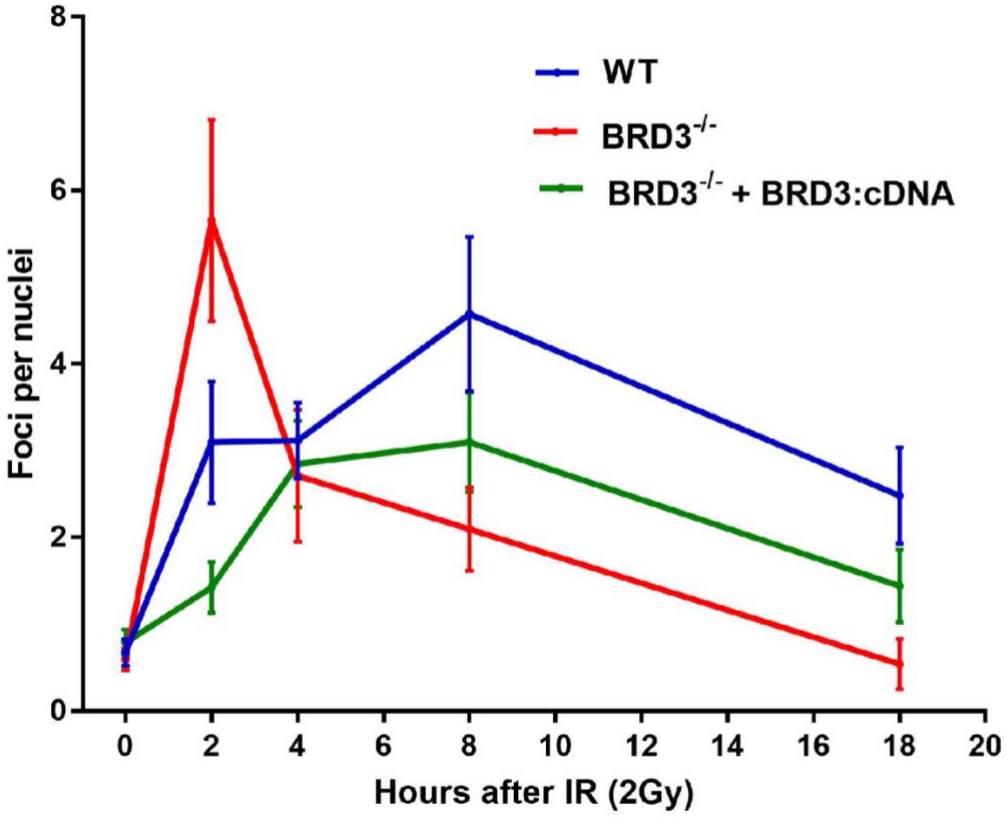

Figure 18. Confirmation that RAD51 foci formation kinetics are altered in BRD3-null cells

An independent experiment (from the one shown in Figure 19) quantitating the temporal appearance of RAD51 foci formation following 2 Gy of X-irradiation is shown for the 3 indicated cell lines. At least 50 independent images were scored for each data point.

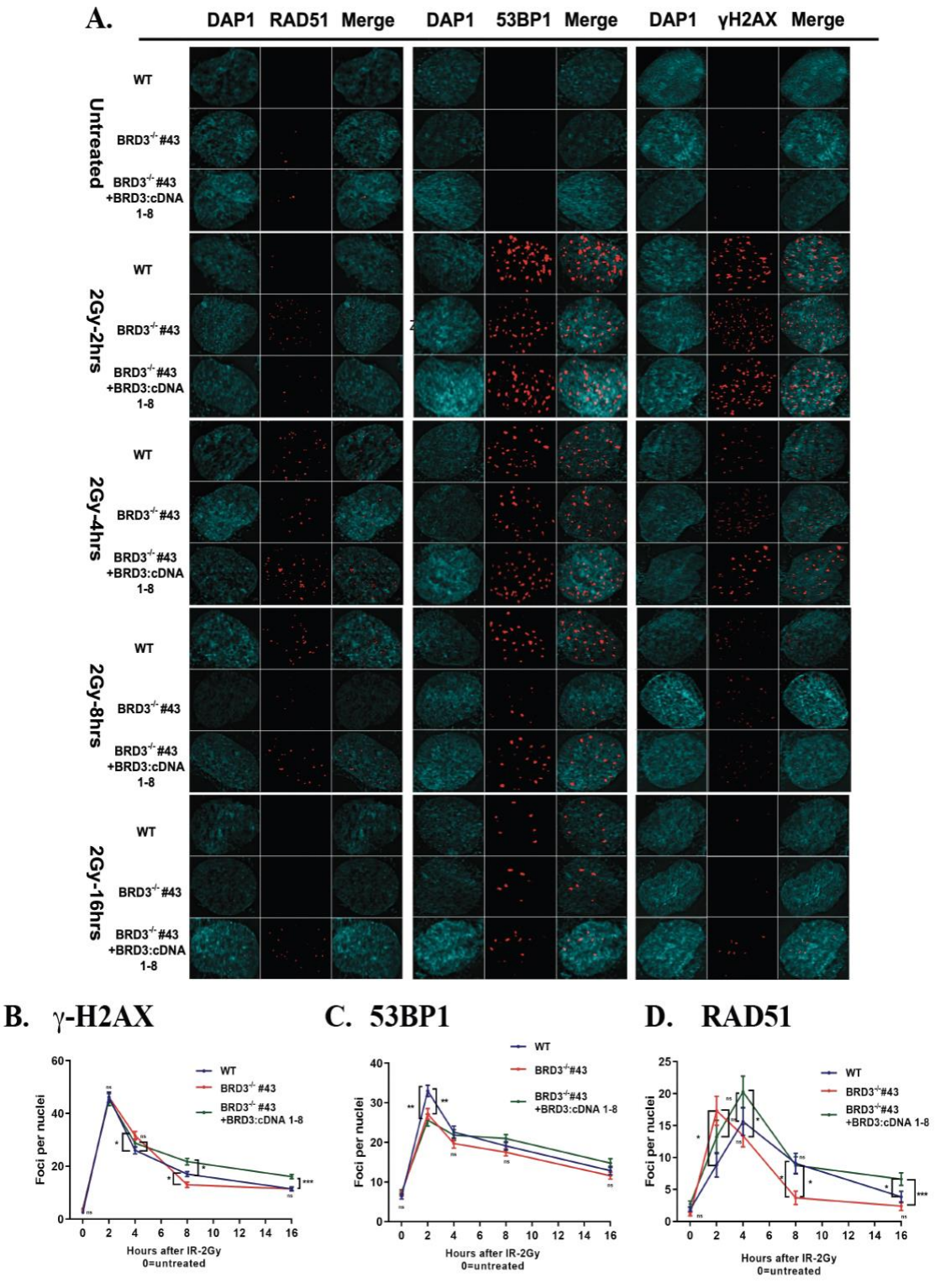
A.
DAP1 RAD51 Merge
DAP1 53BP1 Merge
DAP1 γH2AX Merge
Untreated
2Gy-2hrs
2Gy-4hrs
2Gy-8hrs
2Gy-16hrs
WT
BRD3-/- #43
BRD3-/- #43 +BRD3:cDNA 1-8
B. γ-H2AX
C. 53BP1
D. RAD51
Foci per nuclei
Hours after IR-2Gy
0=untreated

Figure 19. The kinetics of RAD51 foci formation are altered in BRD3-null cells

A. Representative images for immunofluorescent analyses of the parental cell line (WT), BRD3-null cells (clone #43) and BRD3-null cells complemented clone #1-8 at the indicated times following exposure to 2 Gy of X-irradiation. The images are arranged in sets of 3 with a DAPI image, the corresponding antibody-stained image (RAD51, 53BP1 or g-H2AX as indicated) and a merged image.

B. Quantification of γ-H2AX foci per nucleus, n>50.

C. Quantification of 53BP1 foci per nucleus, n>50.

D. Quantification of RAD51 foci per nucleus, n>50.

*The data shown are derived from two independent experiments. n.s. = not significant; * = p < 0.05; ** = p < 0.01; *** = p < 0.0001.*

4.4.8 ATAD5 is epistatic to BRD3

The inability of BD1D and BD2D BRD3 cDNAs to rescue the hyper-recombination activity of BRD3-null cells was somewhat expected as BD1 and BD2 are the domains through which BRD3 interacts with chromatin. We were, however, surprised that the ETΔ–expressing clone was equally as inactive. Very little is known about the biochemical activity of ET domains, other than that they appear to be protein:protein interaction modules[156,157]. One protein that the BRD3 ET domain is known to interact with is ATPase family AAA domain containing 5 (ATAD5). ATAD5, in turn, has been implicated in the chromatin unloading of proliferating cell nuclear antigen (PCNA)[160] and loading of RAD51[171], the latter protein being one whose recruitment kinetics are clearly altered in BRD3-null cells (**Figure 19D**). Thus, we inquired whether BRD3's anti-recombination activity required ATAD5 expression. To accomplish this, we utilized siRNA to knockdown the expression of ATAD5 (**Figure 21A**).

Importantly, the reduction in ATAD5 expression completely suppressed the hyper-recombination activity of BRD3-null cells using the DR-GFP assay (**Figure 21B**). As importantly, a reduction in ATAD5 expression also completely suppressed the aberrant RAD51 recruitment kinetics to DSBs in BRD3-null cells (**Figure 21C**). From these experiments, we conclude that ATAD5 is epistatic to BRD3 and this, in turn, is consistent with the requirement for the presence of the ET domain (*i.e*., the ATAD5 interaction domain) in BRD3(**Figure 20**).

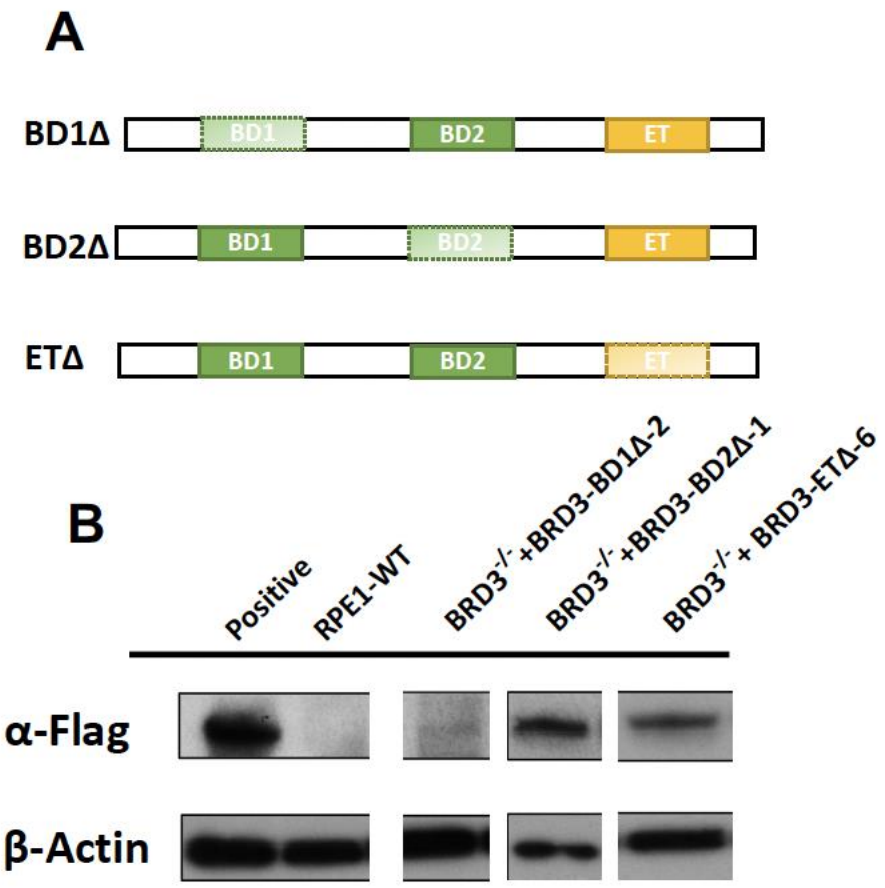
A
BD1Δ
BD1
BD2
ET
BD2Δ
BD1
BD2
ET
ETΔ
BD1
BD2
ET
B
Positive
RPE1-WT
BRD3-/- +BRD3-BD1Δ-2
BRD3-/- +BRD3-BD2Δ-1
BRD3-/- + BRD3-ETΔ-6
α-Flag
β-Actin
C
P<0.05
P<0.05
P<0.05
P<0.05
SCE per chromosome per metaphase
0
1
2
3
WT
BRD3-/- #43
BRD3-/- #43+ BRD3:BD1Δ-2
BRD3-/- #43+ BRD3:BD2Δ-1
BRD3-/- #43+ BRD3:ETΔ-6
BRD3-/- #43+ BRD3:cDNA 1-8

Figure 20. The BD and ET domains of BRD3 are required for significant complementation

A. *Representative cartoons of the 3 BRD3 cDNA constructs lacking either BD1, BD2 or the ET domain that were used in the complementation experiments.*
B. *Immunoblot analysis using an anti-FLAG antibody to demonstrate the expression of the indicated BRD3 derivative proteins in BRD3-null cells. b-actin was used as a loading control.*
C. *Inability of the BRD3 deletion constructs to rescue the SCE hyper-recombination phenotype of BRD3-null cells. SCEs were scored as described in the Material and Methods and in the legend to Figure 2. As a positive control, a clone expressing a full-length, wild-type BRD3 cDNA (#1-8) was assessed, and this clone showed full complementation.*

SCEs were scored as described in the Material and Methods and in the legend to Figure 2. As a positive control, a clone expressing a full-length, wild-type BRD3 cDNA (#1-8) was assessed, and this clone showed full complementation. The data are derived from two independent experiments. Each of the BD domain deletions reduces the wild-type protein size by ~10 kDa (95 AAs) whereas the ET deletion reduces the wild-type protein size by ~7 kDa (62 AAs). The actin band migrates around 40 kDa, whereas the wild-type BRD3 protein with a predicted MW of around 80 kDa and its deletion derivatives generally migrated higher in the gels around 110 kDa.

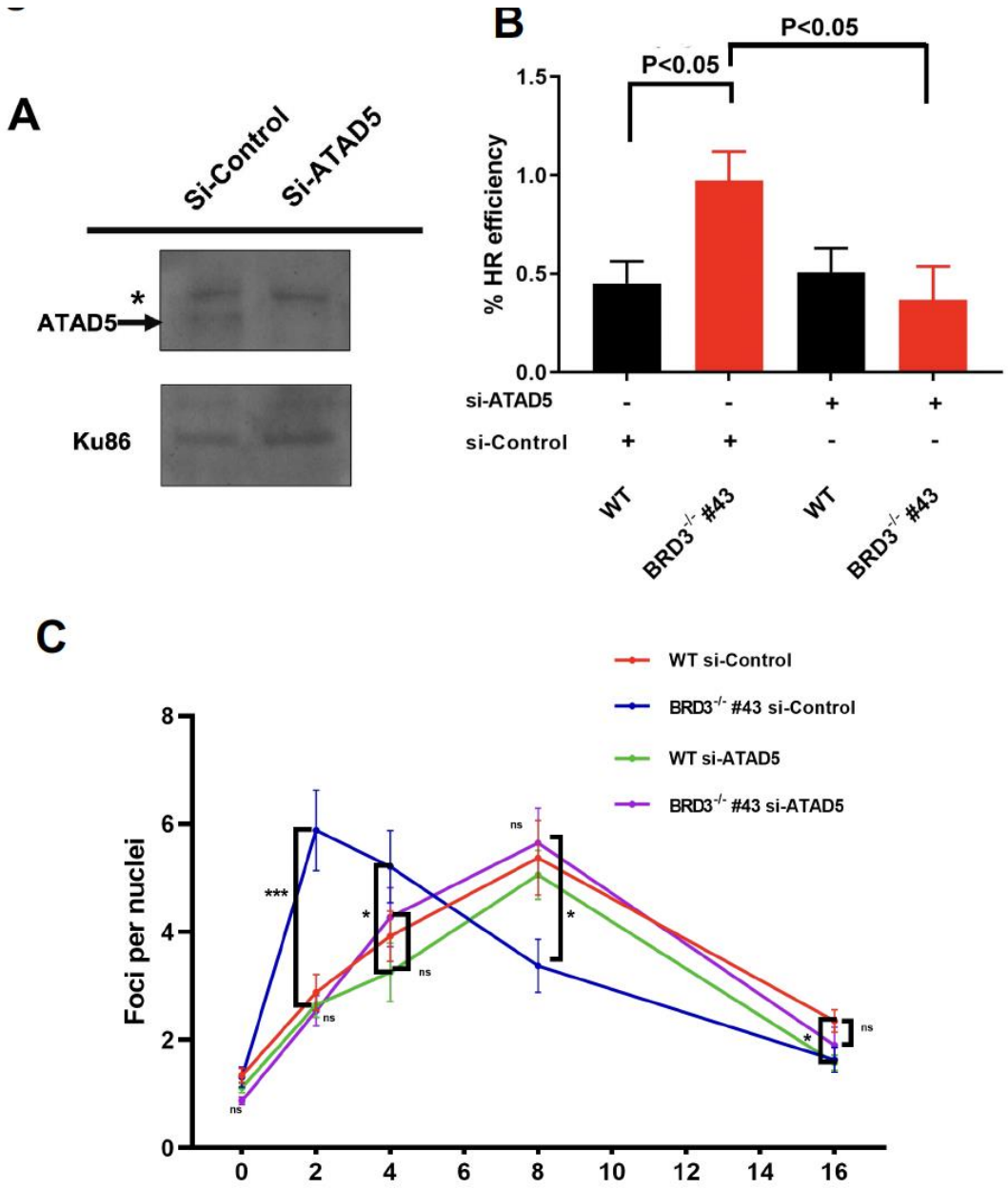

Figure 21. ATAD5 is epistatic to BRD3

A. An immunoblot analysis demonstrates significant knockdown of ATAD5 expression in BRD3-null cells. An irrelevant band is marked by the asterisk (*) and ATAD5 expression by the arrow. Ku86 was used as a loading control.

B. The knockdown of ATAD5 expression suppresses the hyper-recombination of BRD3-null cells. Either wild type (WT) or BRD3-null (clone #43) cells are shown treated either with a control siRNA or one specific for ATAD5. The HDR activity was assessed by a DR-GFP assay as described in the Material and Methods and in the legend to Figure 15.

C. The knockdown of ATAD5 expression suppresses the aberrant RAD51 recruitment kinetics in BRD3-null cells. Either wild type (WT) or BRD3-null (clone #43) cells exposed to 2 Gy of IR are shown treated either with a control siRNA or one specific for ATAD5.

*n.s. = not significant; * = $p < 0.05$; *** = $p < 0.0001$.*

4.5 Discussion

4.5.1 A kinome analysis approach to identifying novel regulators of DNA DSB repair

Although the regulation of DSB repair is complicated, this has not detracted a veritable bevy of researchers from trying to identify the genes involved in, and the mechanism(s) required for, this process[129,130]. Because much of the mammalian DDR is regulated by kinases and kinase cascades[144,146,147] a significant amount of effort (which has yielded a corresponding significant amount of success) has gone into identifying the immediate downstream substrates for the regulatory kinases[148]. Alternatively, in a more indirect manner, differences in gene expression (generally measured at the mRNA level) have been quantitated in cells that were either genetically modified and/or exposed to DNA damaging agents[149–151].

To augment these strategies, we have taken what we believe is a unique approach to identifying novel regulators of DSB repair. In a kinome analysis, the difference in ATP-binding protein expression between two cell lines is determined. While not all cellular signaling occurs via kinases and phosphorylation events, much of it is. This is especially true of DSB repair, which appears to be regulated predominately by 3 PI-like kinases: ATM, ATR and PRKDC. Consequently, we hypothesized that if we were to inactivate one

of these kinases (specifically PRKDC), we might be able to observe compensatory or rescuing alterations in other kinase cascades or kinase substrates and in so doing identified BRD3. This result demonstrates that the kinome approach can be added to the toolbox of approaches currently used to dissect signaling pathways. In addition, a kinome analysis offers the additional advantage of identifying proteins that are neither kinases nor kinase substrates, but which simply bind ATP. With all that said, it is nonetheless unclear why BRD3 was identified in this screen since 1) BRD3 is not a kinase, 2) BRD3 has never been reported to be a substrate for a kinase, 3) nor does BRD3 contain canonical ATP-binding motifs, such as Walker A/B boxes[172]. It should be noted, however, that BRD3 does contain a cluster of residues (AA69 to 78; NlpDYhKliK) that have been reported to be (at least theoretically) ATP-interacting[173]. Alternatively, if BRD3 does not directly interact with ATP, then it is also possible that it may have been identified because it was interacting with another protein that was binding to the ATP analogs on the MIBs [e.g., NuRD, BAF, ATAD5 or INO80 complexes[174]]. Regardless, and importantly, the identification of BRD3 — a gene that has never been directly implicated in regulating DSB repair — validates the utility of the kinome methodology.

4.5.2 The loss of BRD3 results in cells that are IR-sensitive

Cells defective in any of the C-NHEJ pathway components are uniformly IR-sensitive. While the BRD3 cells are not profoundly so, they are nonetheless IR-sensitive (**Figure 11**), which was surprising since we could not detect a defect in C-NHEJ activity (**Figure 13**). Importantly, there was no difference in DSB induction following IR exposure between the parental and BRD3-null cells and the frank resolution of those DSBs also appeared relatively unaltered (**Figure 13B**). Thus, we hypothesize that in a BRD3-null cell, the DSBs are kinetically resolved in a manner similar to wild type, but that a significant fraction of those repair events is faulty such that ultimately they result in the cell lethality that is observed in the clonogenic survival assays (**Figure 11**). Importantly, this faulty repair likely extends to other types of DSBs besides IR-induced lesions, as the knockdown of BRD3 also resulted in hypersensitivity to ATR inhibition as well hydroxyurea exposure[160].

HDR is often referred to as “error-free” repair and superficially one could envision that a hyper-recombination state might be hypomutable. This bias is, however, likely not accurate. Thus, even when the donor for a recombination reaction is the sister chromatid, serious aberrant products of recombination can result such as loss-of-heterozygosity. One of the most well-described hyper-recombination situations involves mutations to the Blooms Syndrome (BLM) gene. While BLM-null cells are not particularly IR-sensitive, they have significant genomic instability and the patients are quite cancer-prone[175]. Similarly, when the C-NHEJ factor Ku86 is depleted from human cells, HDR is

increased throughout the genome[165] but with unfortunate consequences such that inappropriate HDR occurs at chromosome ends, where it results in lethal telomeric recombination events[176,177]. Thus, in the cases of BLM and Ku86 deficiencies, too much HDR is unequivocally a pathological state. We believe that in the absence of BRD3, where a similar hyper-recombination atmosphere reigns that DSBs can be slowly (**Figure 13**), albeit properly, repaired, but that some fraction of them are also mis-repaired in a manner more deleterious than the indels associated with C-NHEJ processes and that this ultimately results in reduced viability (**Figure 11**).

Lastly, it is relevant to point out that other BR-containing proteins have been implicated in DNA repair. For example, Zinc Finger MYND-Type Containing 8 (ZMYND8) has been reported to recognize DNA damage in transcriptionally active chromosome region and interact with Chromodomain Helicase DNA binding Protein 4 (CHD4) to facilitate HDR[115,178]. Similarly, another BR-containing protein, BRD9, assists in the formation of a RAD51:RAD54 complex to promote HDR[128]. Finally, BRD4 has also been directly implicated in HDR-mediated DSB repair using an *in vitro Xenopus* extract system[87]. In addition to involvement in HDR, two BR-containing proteins, CREB Binding Protein (CBP) and p300, assist NHEJ by facilitating the localization of the Switch/Sucrose Non-Fermentable) SWI/SNF complex to DSBs[179]. More importantly, a recent BR-containing protein screening has identified more than one third of all BR-containing proteins are recruited to DSB sites[115]. To these studies we now

demonstrate that BRD3 appears to be a *bona fide* HDR inhibitor and its absence results in a hyper-recombination state. Illuminating the role of BR-containing proteins in DSBs repair is critical for understanding of the mechanism(s) of DSB repair and for fulfilling their potential clinical applications.

4.5.3 The loss of BRD3 results in cells that are hyper-recombinogenic by a mechanism that is ATAD5-dependent

Our data demonstrate that human somatic cells lacking BRD3 are hyper-recombinogenic for extrachromosomal HDR assays (**Figure 14**), sister chromatid exchanges (**Figure 15**) and chromosomal gene targeting (**Figure 16**). An unequivocal conclusion from these observations is that BRD3 is a *bona fide* inhibitor of HDR. The corollary of this conclusion is that inhibition of BRD3 could potentially be used to enhance HDR. The current commercially available inhibitors (*e.g.*, JQ1) of BRD3 are pan-inhibitors to the whole BET family[180]. This is clearly sub-optimal as, for example, BRD4 is involved in the DDR and in the prevention of R-loops accumulation and its depletion results in accumulated endogenous DNA damage[82–84]. From that perspective, the development of a BRD3-specific inhibitor to enhance, for example, gene editing experiments seems eminently worthwhile.

Insight into the mechanism of how the loss of BRD3 expression in human cells causes hyper-recombination came from a structure:function analysis of

the BRD3 protein. The absence of either BD (BD1 or BD2) resulted in the complete inability to rescue the hyper-recombination phenotypes (**Figure 20**). This observation was not unexpected as BD domains are used for interaction with acetylated histones in chromatin[118] and this interaction/activity is per force likely necessary for a chromatin binding protein. In contrast, the inability of BRD3 lacking the ET domain (a protein:protein interaction module) to complement the hyper-recombination phenotype (**Figure 20**) was unexpected. One of the few proteins described to interact with BRD3's ET domain is ATAD5. ATAD5 is a AAA domain ATPase and it has been implicated in regulating the loading (RAD51)[171] or unloading (PCNA)[160] of other proteins onto chromatin, although how it precisely does this is unknown. Importantly, however, subsequent experiments demonstrated that the hyper-recombination phenotype (**Figure 21B**) and the aberrant chromatin binding kinetics of RAD51 (**Figure 21C**) of BRD3-null cells were completely dependent upon the expression of ATAD5. Thus, our current model is that in BRD3-proficient cells that BRD3 is recruited to DSBs via nearby acetylated nucleosomes via its BD modules (**Figure 22**). BRD3, in turn, uses its ET domain to interact with ATAD5 and we postulate that this interaction hinders ATAD5's ability to load RAD51 onto DSBs (**Figure 22**). This permits predominately C-NHEJ-mediated repair of the DSB (**Figure 22**). In contrast, in BRD3-deficient cells, ATAD5 is now unrestricted and can (hyper)load RAD51 on the DSB and this facilitates proportionately more HDR, which, as discussed above, is generally associated

with ancillary genomic instability (**Figure 22**). In the case where BRD3 and ATAD5 are both deficient, the lack of ATAD5 to bolster RAD51 loading reverses the hyper-recombination phenotype and results in a scenario where C-NHEJ once again predominates (**Figure 21** and **Figure 22**). Lastly, this model predicts that BRD3-proficient, ATAD5-null cells should be HDR defective (due to the absence of ATAD5-mediated RAD51 loading; **Figure 22**). We are currently trying to test this prediction directly, but it should be noted that it was recently reported that ATAD5-reduced human A2780 cells were hypersensitive to poly(ADP)ribose polymerase inhibitors, a phenotype often associated with a HDR deficiency[181].

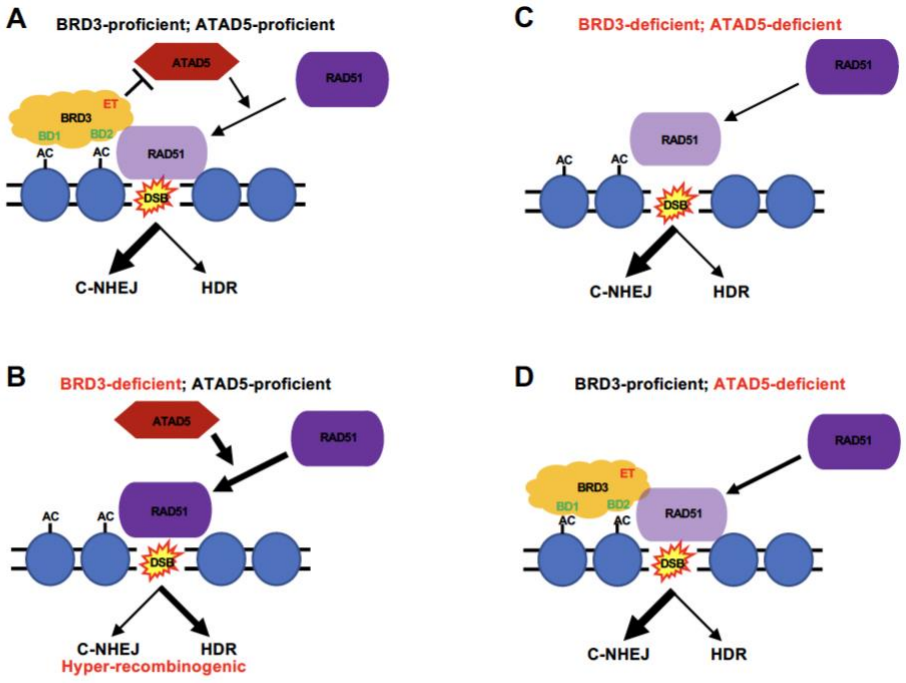

Figure 22. A schematic for the action of BRD3

A. *In BRD3-proficient, ATAD5-proficient cells BRD3 can be localized to chromatin near a DSB via its BD domains (BD1 and BD2) to acetylated (AC) histones in nucleosomes. BRD3, in turn, via its ET domain can interact with ATAD5. This interaction impedes ATAD5's activity (which is to load RAD51 on the DSB) thus encouraging C-NHEJ and limiting HDR.*
B. *In BRD3-deficient, ATAD5-proficient cells BRD3 cannot be localized to chromatin near a DSB and hence ATAD5 is unrestricted in its RAD51 loading activity. As a consequence, RAD51 encourages enhanced HDR at the expense of C-NHEJ and results in a hyper-recombinogenic phenotype.*
C. *In BRD3-deficient, ATAD5-deficient cells the absence of ATAD5 diminishes RAD51's ability to be loaded at a DSB and this suppresses the hyper-recombination phenotype of a BRD3-deficiency.*
D. *In BRD3-proficient, ATAD5-deficient cells the absence of ATAD5 again diminishes RAD51's ability to be loaded at a DSB and this should result in a HDR-deficient phenotype.*

Table 2. Nucleic acid sequences used in these studies

The cDNA sequence of BRD3 isoform X1 (the genetic code of BRD3 was optimized by IDT to generate a gblock):

ATGAGTACCGCTACGACTGTTGCCCCCGCCGGTATTCCAGCGACCCCTG
GCCCAGTAAATCCCCCGCCGCCCGAGGTGTCCAACCCATCAAAGCCTGG
CCGCAAGACCAACCAGCTGCAGTACATGCAGAATGTGGTGGTGAAGACG
CTCTGGAAACACCAGTTCGCCTGGCCCTTCTACCAGCCCGTGGACGCAA
TCAAATTGAACCTGCCGGATTATCATAAAATAATTAAAAACCCAATGGATAT
GGGGACTATTAAGAAGAGACTAGAAAATAATTATTATTGGAGTGCAAGCGA
ATGTATGCAGGACTTCAACACCATGTTTACAAATTGTTACATTTATAACAAG
CCCACAGATGACATAGTGCTAATGGCCCAAGCTTTAGAGAAAATTTTTCTA
CAAAAAGTGGCCCAGATGCCCCAAGAGGAAGTTGAATTATTACCCCCTGC
TCCAAAGGGCAAAGGTCGGAAGCCGGCTGCGGGAGCCCAGAGCGCAG
GTACACAGCAAGTGGCGGCCGTGTCCTCTGTCTCCCCAGCGACCCCCTT
TCAGAGCGTGCCCCCCACCGTCTCCCAGACGCCCGTCATCGCTGCCAC
CCCTGTACCAACCATCACTGCAAACGTCACGTCGGTCCCAGTCCCCCCA
GCTGCCGCCCCACCTCCTCCTGCCACACCCATCGTCCCCGTGGTCCCTC
CTACGCCGCCTGTCGTCAAGAAAAAGGGCGTGAAGCGGAAAGCAGACA
CAACCACTCCCACGACGTCGGCCATCACTGCCAGCCGGAGTGAGTCGC
CCCCGCCGTTGTCAGACCCCAAGCAGGCCAAAGTGGTGGCCCGGCGG
GAGAGTGGTGGCCGCCCCATCAAGCCTCCCAAGAAGGACCTGGAGGAC
GGCGAGGTGCCCCAGCACGCAGGCAAGAAGGGCAAGCTGTCGGAGCA
CCTACGCTACTGCGACAGCATCCTCAGGGAGATGCTATCCAAGAAGCAC
GCGGCCTACGCCTGGCCCTTCTACAAGCCAGTGGATGCCGAGGCCCTG
GAGCTGCACGACTACCACGACATCATCAAGCACCCGATGGACCTCAGCA
CCGTGAAAAGGAAGATGGATGGCCGAGAGTACCCAGACGCACAGGGCT
TTGCTGCTGATGTCCGGCTGATGTTCTCGAATTGCTACAAATACAATCCCC
CAGACCACGAGGTTGTGGCCATGGCCCGGAAGCTCCAGGACGTGTTTG
AGATGAGGTTTGCCAAGATGCCAGATGAGCCCGTGGAGGCACCGGCGC
TGCCTGCCCCCGCGGCCCCCATGGTGAGCAAGGGCGCTGAGAGCAGCC
GTAGCAGTGAGGAGAGCTCTTCGGACTCAGGCAGCTCGGACTCGGAGG
AGGAGCGGGCCACCAGGCTGGCGGAGCTGCAGGAGCAGCTGAAGGCC
GTGCACGAGCAGCTGGCCGCCCTGTCTCAGGCCCCAGTAAACAAACCAA
AGAAGAAAAAAGAGAAAAAAGAGAAAGAGAAGAAAAAGAAAGACAAAGA
GAAGGAGAAGGAGAAACATAAAGTGAAGGCCGAGGAAGAGAAGAAGGC
CAAGGTGGCTCCGCCTGCCAAGCAGGCTCAGCAGAAGAAGGCTCCTGC
CAAGAAGGCCAACAGCACGACCACGGCCGGCAGACAGCTGAAGAAAGG
CGGCAAGCAGGCATCTGCCTCCTACGACTCAGAGGAAGAGGAGGAGGG
CCTGCCCATGAGCTACGATGAAAAGCGCCAGCTTAGCCTGGACATCAAC
CGGCTGCCCGGGGAGAAGCTGGGCCGGGTAGTGCACATCATCCAATCT
CGGGAGCCCTCGCTCAGGGACTCCAACCCCGACGAGATAGAAATTGACT
TTGAGACTCTGAAACCCACCACTTTGCGGGAACTGGAGAGATATGTCAAG

TCTTGTTTACAGAAAAAGCAAAGGAAACCGTTCTCAGCAAGCGGGAAGAA
ACAGGCAGCCAAGTCGAAAGAGGAGCTAGCTCAGGAAAAGAAGAAGGA
GCTGGAAAAGCGTCTGCAGGATGTCAGCGGGCAGCTGAGCAGCAGCAA
GAAGCCCGCCCGGAAAGAGAAGCCCGGCTCAGCACCCTCAGGGGGCC
CGTCCAGGCTCAGCAGCAGCAGCTCCTCCGAGTCTGGGAGCAGCAGCT
CCAGCGGGTCCAGCTCTGACAGCAGTGACTCAGAATGA

The cDNA sequence of 3xFlag-BRD3-BD1 Δ:

ATGGATTATAAAGATGATGATGATAAAGATTATAAAGATGATGATGATAAAGA
TTATAAAGATGATGATGATAAAAGTACCGCTACGACTGTTGCCCCCGCCGG
TATTCCAGCGACCCCTGGCCCAGTAAATCCCCCGCCGCCCGAGGTGTCC
AACCCATCAAAGCCTGGCGAATTATTACCCCCTGCTCCAAAGGGCAAAGG
TCGGAAGCCGGCTGCGGGAGCCCAGAGCGCAGGTACACAGCAAGTGGC
GGCCGTGTCCTCTGTCTCCCCAGCGACCCCCTTTCAGAGCGTGCCCCC
CACCGTCTCCCAGACGCCCGTCATCGCTGCCACCCCTGTACCAACCATC
ACTGCAAACGTCACGTCGGTCCCAGTCCCCCCAGCTGCCGCCCCACCT
CCTCCTGCCACACCCATCGTCCCCGTGGTCCCTCCTACGCCGCCTGTCG
TCAAGAAAAAGGGCGTGAAGCGGAAAGCAGACACAACCACTCCCACGA
CGTCGGCCATCACTGCCAGCCGGAGTGAGTCGCCCCCGCCGTTGTCAG
ACCCCAAGCAGGCCAAAGTGGTGGCCCGGCGGGAGAGTGGTGGCCGC
CCCATCAAGCCTCCCAAGAAGGACCTGGAGGACGGCGAGGTGCCCCAG
CACGCAGGCAAGAAGGGCAAGCTGTCGGAGCACCTACGCTACTGCGAC
AGCATCCTCAGGGAGATGCTATCCAAGAAGCACGCGGCCTACGCCTGGC
CCTTCTACAAGCCAGTGGATGCCGAGGCCCTGGAGCTGCACGACTACCA
CGACATCATCAAGCACCCGATGGACCTCAGCACCGTGAAAAGGAAGATG
GATGGCCGAGAGTACCCAGACGCACAGGGCTTTGCTGCTGATGTCCGG
CTGATGTTCTCGAATTGCTACAAATACAATCCCCCAGACCACGAGGTTGT
GGCCATGGCCCGGAAGCTCCAGGACGTGTTTGAGATGAGGTTTGCCAAG
ATGCCAGATGAGCCCGTGGAGGCACCGGCGCTGCCTGCCCCCGCGGCC
CCCATGGTGAGCAAGGGCGCTGAGAGCAGCCGTAGCAGTGAGGAGAGC
TCTTCGGACTCAGGCAGCTCGGACTCGGAGGAGGAGCGGGCCACCAGG
CTGGCGGAGCTGCAGGAGCAGCTGAAGGCCGTGCACGAGCAGCTGGC
CGCCCTGTCTCAGGCCCCAGTAAACAAACCAAAGAAGAAAAAAGAGAAA
AAAGAGAAAGAGAAGAAAAAGAAAGACAAAGAGAAGGAGAAGGAGAAAC
ATAAAGTGAAGGCCGAGGAAGAGAAGAAGGCCAAGGTGGCTCCGCCTG
CCAAGCAGGCTCAGCAGAAGAAGGCTCCTGCCAAGAAGGCCAACAGCA
CGACCACGGCCGGCAGACAGCTGAAGAAAGGCGGCAAGCAGGCATCTG
CCTCCTACGACTCAGAGGAAGAGGAGGAGGGCCTGCCCATGAGCTACG
ATGAAAAGCGCCAGCTTAGCCTGGACATCAACCGGCTGCCCGGGGAGAA
GCTGGGCCGGGTAGTGCACATCATCCAATCTCGGGAGCCCTCGCTCAGG
GACTCCAACCCCGACGAGATAGAAATTGACTTTGAGACTCTGAAACCCAC
CACTTTGCGGGAACTGGAGAGATATGTCAAGTCTTGTTTACAGAAAAAGC
AAAGGAAACCGTTCTCAGCAAGCGGGAAGAAACAGGCAGCCAAGTCGA
AAGAGGAGCTAGCTCAGGAAAAGAAGAAGGAGCTGGAAAAGCGTCTGCA

GGATGTCAGCGGGCAGCTGAGCAGCAGCAAGAAGCCCGCCCGGAAAGA
GAAGCCCGGCTCAGCACCCTCAGGGGGCCCGTCCAGGCTCAGCAGCA
GCAGCTCCTCCGAGTCTGGGAGCAGCAGCTCCAGCGGGTCCAGCTCTG
ACAGCAGTGACTCAGAATGA

The cDNA sequence of 3xFlag-BRD3-BD2 Δ:

ATGGATTATAAAGATGATGATGATAAAGATTATAAAGATGATGATGATAAAGA
TTATAAAGATGATGATGATAAAAGTACCGCTACGACTGTTGCCCCCGCCGG
TATTCCAGCGACCCCTGGCCCAGTAAATCCCCCGCCGCCCGAGGTGTCC
AACCCATCAAAGCCTGGCCGCAAGACCAACCAGCTGCAGTACATGCAGA
ATGTGGTGGTGAAGACGCTCTGGAAACACCAGTTCGCCTGGCCCTTCTA
CCAGCCCGTGGACGCAATCAAATTGAACCTGCCGGATTATCATAAAATAAT
TAAAAACCCAATGGATATGGGGACTATTAAGAAGAGACTAGAAAATAATTAT
TATTGGAGTGCAAGCGAATGTATGCAGGACTTCAACACCATGTTTACAAAT
TGTTACATTTATAACAAGCCCACAGATGACATAGTGCTAATGGCCCAAGCT
TTAGAGAAAATTTTTCTACAAAAAGTGGCCCAGATGCCCCAAGAGGAAGT
TGAATTATTACCCCCTGCTCCAAAGGGCAAAGGTCGGAAGCCGGCTGCG
GGAGCCCAGAGCGCAGGTACACAGCAAGTGGCGGCCGTGTCCTCTGTC
TCCCCAGCGACCCCCTTTCAGAGCGTGCCCCCCACCGTCTCCCAGACG
CCCGTCATCGCTGCCACCCCTGTACCAACCATCACTGCAAACGTCACGT
CGGTCCCAGTCCCCCCAGCTGCCGCCCCACCTCCTCCTGCCACACCCAT
CGTCCCCGTGGTCCCTCCTACGCCGCCTGTCGTCAAGAAAAAGGGCGT
GAAGCGGAAAGCAGACACAACCACTCCCACGACGTCGGCCATCACTGC
CAGCCGGAGTGAGTCGCCCCCGCCGTTGTCAGACCCCAAGCAGGCCAA
AGTGGTGGCCCGGCGGGAGAGTGGTGGCCGCCCCATCAAGCCTCCCAA
GAAGGACCTGGAGGACGGCGAGGTGCCCCAGCACGCAGGCAAGAAGG
GCGTGGAGGCACCGGCGCTGCCTGCCCCCGCGGCCCCCATGGTGAGC
AAGGGCGCTGAGAGCAGCCGTAGCAGTGAGGAGAGCTCTTCGGACTCA
GGCAGCTCGGACTCGGAGGAGGAGCGGGCCACCAGGCTGGCGGAGCT
GCAGGAGCAGCTGAAGGCCGTGCACGAGCAGCTGGCCGCCCTGTCTCA
GGCCCCAGTAAACAAACCAAAGAAGAAAAAAGAGAAAAAAGAGAAAGAG
AAGAAAAAGAAAGACAAAGAGAAGGAGAAGGAGAAACATAAAGTGAAGG
CCGAGGAAGAGAAGAAGGCCAAGGTGGCTCCGCCTGCCAAGCAGGCTC
AGCAGAAGAAGGCTCCTGCCAAGAAGGCCAACAGCACGACCACGGCCG
GCAGACAGCTGAAGAAAGGCGGCAAGCAGGCATCTGCCTCCTACGACTC
AGAGGAAGAGGAGGAGGGCCTGCCCATGAGCTACGATGAAAAGCGCCA
GCTTAGCCTGGACATCAACCGGCTGCCCGGGGAGAAGCTGGGCCGGGT
AGTGCACATCATCCAATCTCGGGAGCCCTCGCTCAGGGACTCCAACCCC
GACGAGATAGAAATTGACTTTGAGACTCTGAAACCCACCACTTTGCGGGA
ACTGGAGAGATATGTCAAGTCTTGTTTACAGAAAAAGCAAAGGAAACCGT
TCTCAGCAAGCGGGAAGAAACAGGCAGCCAAGTCGAAAGAGGAGCTAG
CTCAGGAAAAGAAGAAGGAGCTGGAAAAGCGTCTGCAGGATGTCAGCG
GGCAGCTGAGCAGCAGCAAGAAGCCCGCCCGGAAAGAGAAGCCCGGC

TCAGCACCCTCAGGGGGCCCGTCCAGGCTCAGCAGCAGCAGCTCCTCC
GAGTCTGGGAGCAGCAGCTCCAGCGGGTCCAGCTCTGACAGCAGTGAC
TCAGAATGA

The cDNA sequence of 3xFlag-BRD3-ET Δ:

ATGGATTATAAAGATGATGATGATAAAGATTATAAAGATGATGATGATAAAGA
TTATAAAGATGATGATGATAAAAGTACCGCTACGACTGTTGCCCCCGCCGG
TATTCCAGCGACCCCTGGCCCAGTAAATCCCCCGCCGCCCGAGGTGTCC
AACCCATCAAAGCCTGGCAACTTCCTCTTGGGGCATCTGGGCCACTTTTT
GTAGAAAAATTTTCTCTAAAGCTTGGGCCATTAGCACTATGTCATCTGTGG
GCTTGTTATAAATGTAACAATTTGTAAACATGGTGTTGAAGTCCTGCATACA
TTCGCTTGCACTCCAATAATAATTATTTTCTAGTCTCTTCTTAATAGTCCCCA
TATCCATTGGGTTTTTAATTATTTTATGATAATCCGGCAGGTTCAATTTGATT
GCGTCCACGGGCTGGTAGAAGGGCCAGGCGAACTGGTGTTTCCAGAGC
GTCTTCACCACCACATTCTGCATGTACTGCAGCTGGTTGGTCTTGCGGAA
TTATTACCCCCTGCTCCAAAGGGCAAAGGTCGGAAGCCGGCTGCGGGAG
CCCAGAGCGCAGGTACACAGCAAGTGGCGGCCGTGTCCTCTGTCTCCC
CAGCGACCCCCTTTCAGAGCGTGCCCCCCACCGTCTCCCAGACGCCCG
TCATCGCTGCCACCCCTGTACCAACCATCACTGCAAACGTCACGTCGGT
CCCAGTCCCCCCAGCTGCCGCCCCACCTCCTCCTGCCACACCCATCGTC
CCCGTGGTCCCTCCTACGCCGCCTGTCGTCAAGAAAAAGGGCGTGAAG
CGGAAAGCAGACACAACCACTCCCACGACGTCGGCCATCACTGCCAGC
CGGAGTGAGTCGCCCCCGCCGTTGTCAGACCCCAAGCAGGCCAAAGTG
GTGGCCCGGCGGGAGAGTGGTGGCCGCCCCATCAAGCCTCCCAAGAAG
GACCTGGAGGACGGCGAGGTGCCCCAGCACGCAGGCAAGAAGGGCAA
GCTGTCGGAGCACCTACGCTACTGCGACAGCATCCTCAGGGAGATGCTA
TCCAAGAAGCACGCGGCCTACGCCTGGCCCTTCTACAAGCCAGTGGATG
CCGAGGCCCTGGAGCTGCACGACTACCACGACATCATCAAGCACCCGAT
GGACCTCAGCACCGTGAAAAGGAAGATGGATGGCCGAGAGTACCCAGA
CGCACAGGGCTTTGCTGCTGATGTCCGGCTGATGTTCTCGAATTGCTACA
AATACAATCCCCCAGACCACGAGGTTGTGGCCATGGCCCGGAAGCTCCA
GGACGTGTTTGAGATGAGGTTTGCCAAGATGCCAGATGAGCCCGTGGAG
GCACCGGCGCTGCCTGCCCCCGCGGCCCCCATGGTGAGCAAGGGCGC
TGAGAGCAGCCGTAGCAGTGAGGAGAGCTCAAGTGATTCTGGGAGTTCT
GATTCTGAAGAGGAGCGAGCGACTCGCCTTGCGGAACTGCAGGAGCAG
CTTAAAGCAGTACATGAACAGCTCGCCGCCCTTAGTCAGGCGCCCGTGA
ATAAACCCAAGAAAAAAAAAGAAAAAAAGGAAAAGGAAAAAAAGAAGAAA
GATAAAGAAAAGGAGAAAGAGAAGCACAAGGTGAAGGCCGAAGAAGAAA
AAAAGGCAAAGGTAGCTCCCCCGGCAAAGCAAGCGCAGCAAAAGAAAG
CGCCCGCTAAGAAGGCCAATAGTACGACGACTGCAGGGCGACAACTCAA
GAAGGGCGGTAAACAAGCGTCTGCATCATACCAGCGGAAACCGTTCTCA
GCAAGCGGGAAGAAACAGGCAGCCAAGTCGAAAGAGGAGCTAGCTCAG
GAAAAGAAGAAGGAGCTGGAAAAGCGTCTGCAGGATGTCAGCGGGCAG

CTGAGCAGCAGCAAGAAGCCCGCCCGGAAAGAGAAGCCCGGCTCAGCA CCCTCAGGGGGCCCGTCCAGGCTCAGCAGCAGCAGCTCCTCCGAGTCT GGGAGCAGCAGCTCCAGCGGGTCCAGCTCTGACAGCAGTGACTCAGAA TGA

The pDONOR201-3xFlag-BRD3-WT plasmid was constructed by Q5. Site-Directed Mutagenesis Kit (E0554) and the following oligonucleotides were obtained from IDT:

Forward:
gatgatgataaagattataaagatgatgatgataaaAGTACCGCTACGACTGTT

Reverse:
atctttataatctttatcatcatcatctttataatcCATTCATTCTGAGTCACTGC

The pDONOR201-3xFlag-BRD3-BD1Δ plasmid was constructed by Q5. Site-Directed Mutagenesis Kit (E0554) and the following oligonucleotides were obtained from IDT:

Forward:
GAATTATTACCCCCTGCTCC

Reverse:
GCCAGGCTTTGATGGGTT

The pDONOR201-3xFlag-BRD3-BD2Δ plasmid was constructed by Q5. Site-Directed Mutagenesis Kit (E0554) and the following oligonucleotides were obtained from IDT:

Forward:
GTGGAGGCACCGGCGCTG

Reverse:
GCCCTTCTTGCCTGCGTGC

The pDONOR201-3xFlag-BRD3-ETΔ plasmid was constructed by Q5. Site-Directed Mutagenesis Kit (E0554) and the following oligonucleotides were obtained from IDT:

Forward:
TGCCAAGCAGGCTCAGCA

Reverse:
AGAGCTCTCCTCACTGCTAC

Acknowledgements

Dr. Anja-Katrin Bielinsky provided helpful discussions for the manuscript for publication. Fluorescence microscopy was performed at the UMN Imaging Center (UIC). Flow cytometry was performed at the UMN Flow Cytometry Resource (UFCR). The authors disclosed receipt of the following financial support for the research, authorship, and /or publication of this article: This work was supported by the National Institutes of General Medicine [GM088351] and the National Cancer Institute [CA154461].

Declaration of Conflicting Interests

E.A.H sits on the Scientific Advisory Boards of Horizon Discovery, Ltd. And Intellia Therapeutics.

Chapter 5: Summary and future directions

Our studies of the kinome changes of PRKDC-KD cells identified multiple kinases or proteins with ATP binding ability that are *bona fide* effectors or regulators of DDR and DSB repair pathways. Thus, at least in the HCT116 genetic background, the expression of a dominant negative DNA-PK$_{cs}$ significantly altered how mammalian cells cope with DSBs. Interestingly, our study also identified BRD3, a BET family member, as being misregulated. Perhaps due to the circular logic of it being the most well-characterized BET family and due to its previously implied involvement in DNA repair, BRD4 was the mostly likely BET family member that we expected to identify. Instead, we have now demonstrated a unique function of BRD3 in regulating HR pathways via the modulation of the RAD51 loading activity of ATAD5 (a putative PCNA unloader). Although we believe that we have unequivocally documented a role for BRD3 in the HR pathway, some interesting questions still need to be answered.

5.1 The relationship between BRD3, DNA-PK$_{cs}$ and the NHEJ pathway

It may seem ironic that we utilized a NHEJ-defective cell line (PRKDC-KD) to identify HDR regulator (BRD3). In retrospect, however, given that BRD3 can physically interacts with DNA-PK$_{cs}$ via its ET domain[174] , we should perhaps not be so surprised. We have discussed above the disparate results that are

observed for BRD3 regulation in a human cell line completely lacking DNA-PKcs protein. These data strongly imply that the kinase activity of DNA-PK$_{cs}$ is important for regulating the level or activity of BRD3, but this is a feature that has yet to be directly tested.

Since DNA-PK$_{cs}$ is essential for NHEJ, the relationship between BRD3 and NHEJ also needs to be answered. Despite the results of the pEGFP-Pem1-AD2 extrachromosomal repair assay that we performed in this study (**Error! Reference source not found.**), the observation that the formation of 53BP1 foci is suppressed in BRD3-KO cell lines, suggests that the impact of BRD3 on the NHEJ pathway could be at the chromosome level. In our kinome analysis, we also queried kinase changes following IR (30 min and 8 hr) in WT cells (data not shown). BRD3 levels in the HCT116 WT cell line were significantly decreased following IR treatment, suggesting that BRD3 is responsive to DSB formation albeit BRD3 does not relocalize to the damaged sites[115]. The global presence of BRD3 may also explain why we did not find a change in NHEJ efficiency via the plasmid-based assay.

5.2 The interactomes of BRD3

In 2018, Wai *et al*., described that the ET domain of BRD3 can recognize a specific short peptide motif[174]. Through that motif, BRD3 interacts with multiple proteins, including ZMYND8[115,175], BRD9[128], SMARCA4 and SMARCA5 that regulate DDR and HR pathways. Consequently, it will also be worthwhile to test

if the interaction between BRD3 and those proteins plays a role in regulating HDR.

5.3 The binding of BRD3 to histone

BRD3, as a member of the BET family, can bind to acetylated histones via its two tandem BDs. H3K14ac, H3K18ac, and H4K5/8/12/16/20ac are reported to be recognized and bound by BRD3[182]. Investigating the exact binding site of BRD3 should help us understand the role of BRD3 and histone acetylation in DSB repair and the DDR pathway.

References

1. Dahm, R. Friedrich Miescher and the discovery of DNA. *Developmental Biology* vol. 278 274–288 Preprint at https://doi.org/10.1016/j.ydbio.2004.11.028 (2005).
2. Avery, O. T., Macleod, C. M. & Mccarty, M. Studies on the chemical nature of the substance inducing transformation of pneumococcal types: Induction of transformation by a deoxyribonucleic acid fraction isolated from pneumococcus type III. *J Exp Med.* **79**, 137–158 (1944).
3. Chargaff, E., Lipshitz, R. & Green, C. *COMPOSITION OF THE DESOXYPENTOSE NUCLEIC ACIDS OF FOUR GENERA OF SEA-URCHIN**.
4. Watson, J. D. & Crick, F. H. C. *Molecular structure of nucleic acids: a structure for deoxyribose nucleic acid.* (1953).
5. Sirbu, B. M. & Cortez, D. DNA damage response: Three levels of DNA repair regulation. *Cold Spring Harb Perspect Biol* **5**, (2013).
6. Lee, J.-H. & Paull, T. T. *ATM Activation by DNA Double-Strand Breaks Through the Mre11-Rad50-Nbs1 Complex*. *SCIENCE* vol. 308 www.sciencemag.org (2005).
7. Wu, X., Shell, S. M. & Zou, Y. Interaction and colocalization of Rad9/Rad1/Hus1 checkpoint complex with replication protein A in human cells. *Oncogene* **24**, 4728–4735 (2005).
8. Delacroix, S., Wagner, J. M., Kobayashi, M., Yamamoto, K. I. & Karnitz, L. M. The Rad9-Hus1-Rad1 (9-1-1) clamp activates checkpoint signaling via TopBP1. *Genes Dev* **21**, 1472–1477 (2007).
9. Choi, J.-H. *et al.* Reconstitution of RPA-covered single-stranded DNA-activated ATR-Chk1 signaling. doi:10.1073/pnas.1007856107/-/DCSupplemental.
10. Ward, I. M. & Chen, J. Histone H2AX Is Phosphorylated in an ATR-dependent Manner in Response to Replicational Stress. *Journal of Biological Chemistry* **276**, 47759–47762 (2001).
11. Burma, S., Chen, B. P., Murphy, M., Kurimasa, A. & Chen, D. J. ATM Phosphorylates Histone H2AX in Response to DNA Double-strand Breaks. *Journal of Biological Chemistry* **276**, 42462–42467 (2001).
12. Lou, Z. *et al.* MDC1 maintains genomic stability by participating in the amplification of ATM-dependent DNA damage signals. *Mol Cell* **21**, 187–200 (2006).
13. Cortez, D., Wang, Y., Qin, J. & Elledge, S. science.286.5442.1162. *Science (1979)* **286**, 1162–1166 (1999).
14. Tibbetts, R. S. *et al.* Functional interactions between BRCA1 and the checkpoint kinase ATR during genotoxic stress. *Genes Dev* **14**, 2989–3002 (2000).
15. Guo, Z., Kumagai, A., Wang, S. X. & Dunphy, W. G. Requirement for Atr in phosphorylation of Chk1 and cell cycle regulation in response to DNA replication blocks and UV-damaged DNA in Xenopus egg extracts. *Genes Dev* **14**, 2745–2756 (2000).
16. Matsuoka, S. *et al. Ataxia telangiectasia-mutated phosphorylates Chk2 in vivo and in vitro*.

www.pnas.orgcgidoi10.1073pnas.190030497 (2000).

17. Falck, J., Mailand, N., Syljuasen, R., Bartek, J. & Lukas Jiri. The ATM-Chk2-Cdc25A checkpoint pathway guards against radioresistant DNA synthesis. *Nature* **410**, 842–847 (2001).
18. Cao, L. *et al.* ATM-Chk2-p53 activation prevents tumorigenesis at an expense of organ homeostasis upon Brca1 deficiency. *EMBO Journal* **25**, 2167–2177 (2006).
19. Uto, K., Inoue, D., Shimuta, K., Nakajo, N. & Sagata, N. Chk1, but not Chk2, inhibits Cdc25 phosphatases by a novel common mechanism. *EMBO Journal* **23**, 3386–3396 (2004).
20. Lees-Miller, S. P. & Meek, K. Repair of DNA double strand breaks by non-homologous end joining. *Biochimie* vol. 85 1161–1173 Preprint at https://doi.org/10.1016/j.biochi.2003.10.011 (2003).
21. Yaneva, M. *et al. Interaction of DNA-dependent protein kinase with DNA and with Ku: biochemical and atomic-force microscopy studies*. *The EMBO Journal* vol. 16 (1997).
22. Lieber, M. R., Grawunder, U., Wu, X. & Yaneva, M. *Tying loose ends: roles of Ku and DNA-dependent protein kinase in the repair of double-strand breaks*. (1997).
23. Moshous, D. *et al. Artemis, a Novel DNA Double-Strand Break Repair/V(D)J Recombination Protein, Is Mutated in Human Severe Combined Immune Deficiency*. *Cell* vol. 105 (2001).
24. Iles, N., Rulten, S., El-Khamisy, S. F. & Caldecott, K. W. APLF (C2orf13) Is a Novel Human Protein Involved in the Cellular Response to Chromosomal DNA Strand Breaks. *Mol Cell Biol* **27**, 3793–3803 (2007).
25. Chappell, C., Hanakahi, L. A., Karimi-Busheri, F., Weinfeld, M. & West, S. C. Involvement of human polynucleotide kinase in double-strand break repair by non-homologous end joining. *EMBO J* **21**, 2827–2832 (2002).
26. Yamtich, J. & Sweasy, J. B. DNA polymerase Family X: Function, structure, and cellular roles. *Biochimica et Biophysica Acta - Proteins and Proteomics* vol. 1804 1136–1150 Preprint at https://doi.org/10.1016/j.bbapap.2009.07.008 (2010).
27. Wilson, T. E., Grawunder, U. & Lieber, M. R. Yeast DNA ligase IV mediates non-homologous DNA end joining. *Nature* **388**, 495–498 (1997).
28. Ahnesorg, P., Smith, P. & Jackson, S. P. XLF interacts with the XRCC4-DNA Ligase IV complex to promote DNA nonhomologous end-joining. *Cell* **124**, 301–313 (2006).
29. Ackerson, S. M., Romney, C., Schuck, P. L. & Stewart, J. A. To Join or Not to Join: Decision Points Along the Pathway to Double-Strand Break Repair vs. Chromosome End Protection. *Frontiers in Cell and Developmental Biology* vol. 9 Preprint at https://doi.org/10.3389/fcell.2021.708763 (2021).
30. Paull, T. T. & Gellert, M. *The 3 to 5 Exonuclease Activity of Mre11 Facilitates Repair of DNA Double-Strand Breaks Other genetic clues to the identity of DNA repair fac-tors have come from yeast, which primarily utilizes ho-mologous recombination to repair its chromosomal*. *Molecular Cell* vol. 1 (1998).
31. Sartori, A. A. *et al.* Human CtIP promotes DNA end resection. *Nature* **450**, 509–514 (2007).
32. Mimitou, E. P. & Symington, L. S. Sae2, Exo1 and Sgs1 collaborate in DNA double-strand break processing. *Nature* **455**, 770–774 (2008).
33. Wang, W. *et al.* A DNA nick at Ku-blocked double-strand break ends serves as an entry site for exonuclease 1 (Exo1) or Sgs1–Dna2 in long-range DNA end resection. *Journal of Biological Chemistry* **293**, 17061–17069 (2018).
34. Gravel, S., Chapman, J. R., Magill, C. & Jackson, S. P. DNA helicases Sgs1 and BLM promote

DNA double-strand break resection. *Genes Dev* **22**, 2767–2772 (2008).

35. Stark, J. M. *et al.* ATP hydrolysis by mammalian RAD51 has a key role during homology-directed DNA repair. *Journal of Biological Chemistry* **277**, 20185–20194 (2002).
36. Prakash, R., Zhang, Y., Feng, W. & Jasin, M. Homologous recombination and human health: The roles of BRCA1, BRCA2, and associated proteins. *Cold Spring Harb Perspect Biol* **7**, (2015).
37. Orthwein, A. *et al.* A mechanism for the suppression of homologous recombination in G1 cells. *Nature* **528**, 422–426 (2015).
38. Yun, M. H. & Hiom, K. CtIP-BRCA1 modulates the choice of DNA double-strand-break repair pathway throughout the cell cycle. *Nature* **459**, 460–463 (2009).
39. Sharma, S. *et al.* Homology and enzymatic requirements of microhomology-dependent alternative end joining. *Cell Death Dis* **6**, e1697 (2015).
40. Mortense, U. H., Bendixen, C., Sunjevaric, I. & Rothstein, R. DNA strand annealing is promoted by the yeast Rad52 protein. *Proc. Natl. Acad. Sci. USA* **93**, 10729–10734 (1996).
41. Al-minawi, A. Z., Saleh-gohari, N. & Helleday, T. The ERCC1/XPF endonuclease is required for efficient single-strand annealing and gene conversion in mammalian cells. *Nucleic Acids Res* **36**, 1–9 (2008).
42. Truong, L. N. *et al.* Microhomology-mediated End Joining and Homologous Recombination share the initial end resection step to repair DNA double-strand breaks in mammalian cells. *Proc Natl Acad Sci U S A* **110**, 7720–7725 (2013).
43. Yun, M. H. & Hiom, K. CtIP-BRCA1 modulates the choice of DNA double-strand-break repair pathway throughout the cell cycle. *Nature* **459**, 460–463 (2009).
44. Samuels, D. C., Schon, E. A. & Chinnery, P. F. Two direct repeats cause most human mtDNA deletions. *Trends Genet* **20**, 393–398 (2004).
45. Schon, E. A. *et al. A Direct Repeat is a Hotspot for Large-Scale Deletion of Human Mitochondrial DNA*. *New Series* vol. 244 (1989).
46. Mimori, T. & Hardin, J. A. Mechanism of interaction between Ku protein and DNA. *Journal of Biological Chemistry* **261**, 10375–10379 (1986).
47. Scully, R., Panday, A., Elango, R. & Willis, N. A. DNA double-strand break repair-pathway choice in somatic mammalian cells. *Nature Reviews Molecular Cell Biology* vol. 20 698–714 Preprint at https://doi.org/10.1038/s41580-019-0152-0 (2019).
48. Ali, K. *et al.* DNA end resection, homologous recombination and DNA damage checkpoint activation require CDK1. *Nature* **431**, 1007–1011 (2004).
49. Huertas, P., Cortés-Ledesma, F., Sartori, A. A., Aguilera, A. & Jackson, S. P. CDK targets Sae2 to control DNA-end resection and homologous recombination. *Nature* **455**, 689–692 (2008).
50. Yu, X. & Chen, J. DNA Damage-Induced Cell Cycle Checkpoint Control Requires CtIP, a Phosphorylation-Dependent Binding Partner of BRCA1 C-Terminal Domains. *Mol Cell Biol* **24**, 9478–9486 (2004).
51. Tkáč, J. *et al.* HELB Is a Feedback Inhibitor of DNA End Resection. *Mol Cell* **61**, 405–418 (2016).
52. Fujisawa, T. & Filippakopoulos, P. Functions of bromodomain-containing proteins and their roles in homeostasis and cancer. *Nature Reviews Molecular Cell Biology* vol. 18 246–262 Preprint at https://doi.org/10.1038/nrm.2016.143 (2017).
53. Bannister, A. J. & Kouzarides, T. Regulation of chromatin by histone modifications. *Cell*

Research vol. 21 381–395 Preprint at https://doi.org/10.1038/cr.2011.22 (2011).

54. Mujtaba, S., Zeng, L. & Zhou, M. M. Structure and acetyl-lysine recognition of the bromodomain. *Oncogene* vol. 26 5521–5527 Preprint at https://doi.org/10.1038/sj.onc.1210618 (2007).
55. Tamkun, J. W. *et al. brahma: A Regulator of Drosophila Homeotic Genes Structurally Related to the Yeast Transcriptional Activator SNF2BWl2*. *Cell* vol. 66 (1992).
56. Choudhary, C. *et al.* Lysine Acetylation Targets Protein Complexes and Co-Regulates Major Cellular Functions. *Science (1979)* **325**, 834–840 (2009).
57. Sanchez, R. & Zhou, M.-M. The role of human bromodomains in chromatin biology and gene transcription. *Curr Opin Drug Discov Devel* 695–665 (2009).
58. Paillisson, A. *et al.* Bromodomain testis-specific protein is expressed in mouse oocyte and evolves faster than its ubiquitously expressed paralogs BRD2, -3, and -4. *Genomics* **89**, 215–223 (2007).
59. Rahman, S. *et al.* The Brd4 Extraterminal Domain Confers Transcription Activation Independent of pTEFb by Recruiting Multiple Proteins, Including NSD3. *Mol Cell Biol* **31**, 2641–2652 (2011).
60. Wai, D. C. C. *et al.* The BRD3 ET domain recognizes a short peptide motif through a mechanism that is conserved across chromatin remodelers and transcriptional regulators. *Journal of Biological Chemistry* **293**, 7160–7175 (2018).
61. Dey, A., Chitsaz, F., Abbasi, A., Misteli, T. & Ozato, K. *The double bromodomain protein Brd4 binds to acetylated chromatin during interphase and mitosis*. *National Institutes of Health* vol. 100 www.pnas.orgcgidoi10.1073pnas.1433065100 (2003).
62. Dey, A., Chitsaz, F., Abbasi, A., Misteli, T. & Ozato, K. *The double bromodomain protein Brd4 binds to acetylated chromatin during interphase and mitosis*. *National Institutes of Health* vol. 100 www.pnas.orgcgidoi10.1073pnas.1433065100 (2003).
63. Devaiah, B. N. & Singer, D. S. Two faces of BRD4: Mitotic bookmark and transcriptional lynchpin. *Transcription* **4**, 13–17 (2013).
64. Zhao, R., Nakamura, T., Fu, Y., Lazar, Z. & Spector, D. L. Gene bookmarking accelerates the kinetics of post-mitotic transcriptional re-activation. *Nat Cell Biol* **13**, 1295–1304 (2011).
65. Donati, B., Lorenzini, E. & Ciarrocchi, A. BRD4 and Cancer: Going beyond transcriptional regulation. *Molecular Cancer* vol. 17 Preprint at https://doi.org/10.1186/s12943-018-0915-9 (2018).
66. Dey, A. *et al. A Bromodomain Protein, MCAP, Associates with Mitotic Chromosomes and Affects G 2-to-M Transition*. *MOLECULAR AND CELLULAR BIOLOGY* vol. 20 https://journals.asm.org/journal/mcb (2000).
67. Yang, Z., He, N. & Zhou, Q. Brd4 Recruits P-TEFb to Chromosomes at Late Mitosis To Promote G 1 Gene Expression and Cell Cycle Progression . *Mol Cell Biol* **28**, 967–976 (2008).
68. Mochizuki, K. *et al.* The bromodomain protein Brd4 stimulates g1 gene transcription and promotes progression to S phase. *Journal of Biological Chemistry* **283**, 9040–9048 (2008).
69. Dey, A., Nishiyama, A., Karpova, T., Mcnally, J. & Ozato, K. Brd4 Marks Select Genes on Mitotic Chromatin and Directs Postmitotic Transcription. *Mol Biol Cell* **20**, 4899–4909 (2009).
70. Wu, T., Pinto, H. B., Kamikawa, Y. F. & Donohoe, M. E. The BET family member BRD4 interacts with OCT4 and regulates pluripotency gene expression. *Stem Cell Reports* **4**, 390–403

(2015).
71. di Micco, R. *et al.* Control of embryonic stem cell identity by brd4-dependent transcriptional elongation of super-enhancer-associated pluripotency genes. *Cell Rep* **9**, 234–247 (2014).
72. Liu, W. *et al.* BRD4 regulates Nanog expression in mouse embryonic stem cells and preimplantation embryos. *Cell Death Differ* **21**, 1950–1960 (2014).
73. Houzelstein, D. *et al.* Growth and Early Postimplantation Defects in Mice Deficient for the Bromodomain-Containing Protein Brd4. *Mol Cell Biol* **22**, 3794–3802 (2002).
74. Puissant, A. *et al.* Targeting MYCN in neuroblastoma by BET bromodomain inhibition. *Cancer Discov* **3**, 309–323 (2013).
75. Dawson, M. A. *et al.* Inhibition of BET recruitment to chromatin as an effective treatment for MLL-fusion leukaemia. *Nature* **478**, 529–533 (2011).
76. Asangani, I. A. *et al.* Therapeutic targeting of BET bromodomain proteins in castration-resistant prostate cancer. *Nature* **510**, 278–282 (2014).
77. Mertz, J. A. *et al.* Targeting MYC dependence in cancer by inhibiting BET bromodomains. *Proc Natl Acad Sci U S A* **108**, 16669–16674 (2011).
78. Delmore, J. E. *et al.* BET bromodomain inhibition as a therapeutic strategy to target c-Myc. *Cell* **146**, 904–917 (2011).
79. Liu, W. *et al.* Brd4 and JMJD6-associated anti-pause enhancers in regulation of transcriptional pause release. *Cell* **155**, 1581–1595 (2013).
80. Devaiah, B. N. & Singer, D. S. Cross-talk among RNA polymerase II kinases modulates C-terminal domain phosphorylation. *Journal of Biological Chemistry* **287**, 38755–38766 (2012).
81. Yang, Z., He, N. & Zhou, Q. Brd4 Recruits P-TEFb to Chromosomes at Late Mitosis To Promote G 1 Gene Expression and Cell Cycle Progression . *Mol Cell Biol* **28**, 967–976 (2008).
82. Floyd, S. R. *et al.* The bromodomain protein Brd4 insulates chromatin from DNA damage signalling. *Nature* **498**, 246–250 (2013).
83. Lam, F. C. *et al.* BRD4 prevents the accumulation of R-loops and protects against transcription–replication collision events and DNA damage. *Nat Commun* **11**, (2020).
84. Edwards, D. S. *et al.* BRD4 Prevents R-Loop Formation and Transcription-Replication Conflicts by Ensuring Efficient Transcription Elongation. *Cell Rep* **32**, (2020).
85. Li, X. *et al.* BRD4 Promotes DNA Repair and Mediates the Formation of TMPRSS2-ERG Gene Rearrangements in Prostate Cancer. *Cell Rep* **22**, 796–808 (2018).
86. Stanlie, A., Yousif, A. S., Akiyama, H., Honjo, T. & Begum, N. A. Chromatin reader Brd4 functions in Ig class switching as a repair complex adaptor of nonhomologous end-joining. *Mol Cell* **55**, 97–110 (2014).
87. Barrows, J. K. *et al.* BRD4 promotes resection and homology-directed repair of DNA double-strand breaks. *Nat Commun* **13**, (2022).
88. LeRoy, G., Rickards, B. & Flint, S. J. The Double Bromodomain Proteins Brd2 and Brd3 Couple Histone Acetylation to Transcription. *Mol Cell* **30**, 51–60 (2008).
89. Xu, L. *et al.* Targetable BET proteins- and E2F1-dependent transcriptional program maintains the malignancy of glioblastoma. *Proc Natl Acad Sci U S A* **115**, E5086–E5095 (2018).
90. Peng, J. *et al.* Brd2 is a TBP-associated protein and recruits TBP into E2F-1 transcriptional complex in response to serum stimulation. *Mol Cell Biochem* **294**, 45–54 (2007).

91. Tsume, M. *et al.* Brd2 is required for cell cycle exit and neuronal differentiation through the E2F1 pathway in mouse neuroepithelial cells. *Biochem Biophys Res Commun* **425**, 762–768 (2012).
92. Wang, C. Y. & Filippakopoulos, P. Beating the odds: BETs in disease. *Trends in Biochemical Sciences* vol. 40 468–479 Preprint at https://doi.org/10.1016/j.tibs.2015.06.002 (2015).
93. Shang, E., Wang, X., Wen, D., Greenberg, D. A. & Wolgemuth, D. J. Double bromodomain-containing gene Brd2 is essential for embryonic development in Mouse. *Developmental Dynamics* **238**, 908–917 (2009).
94. Wisniewski, A. & Georg, G. I. BET proteins: Investigating BRDT as a potential target for male contraception. *Bioorganic and Medicinal Chemistry Letters* vol. 30 Preprint at https://doi.org/10.1016/j.bmcl.2020.126958 (2020).
95. Berkovits, B. D. & Wolgemuth, D. J. The first bromodomain of the testis-specific double bromodomain protein Brdt is required for chromocenter organization that is modulated by genetic background. *Dev Biol* **360**, 358–368 (2011).
96. Gaucher, J. *et al.* Bromodomain-dependent stage-specific male genome programming by Brdt. *EMBO Journal* **31**, 3809–3820 (2012).
97. Bisgrove, D. A., Mahmoudi, T., Henklein, P. & Verdin, E. Conserved P-TEFb-interacting domain of BRD4 inhibits HIV transcription. *Proc Natl Acad Sci U S A* **104**, 13690–13695 (2007).
98. Bourova-Flin, E., Chuffart, F., Rousseaux, S. & Khochbin, S. The role of bromodomain testis-specific factor, brdt, in cancer: A biomarker and a possible therapeutic target. *Cell J* **19**, 1–8 (2017).
99. Chen, L. *et al.* BRDT promotes ovarian cancer cell growth. *Cell Death Dis* **11**, (2020).
100. Wan, P. *et al.* BRDT is a novel regulator of eIF4EBP1 in renal cell carcinoma. *Oncol Rep* **44**, 2475–2486 (2020).
101. Gong, F. & Miller, K. M. Mammalian DNA repair: HATs and HDACs make their mark through histone acetylation. *Mutation Research - Fundamental and Molecular Mechanisms of Mutagenesis* vol. 750 23–30 Preprint at https://doi.org/10.1016/j.mrfmmm.2013.07.002 (2013).
102. Jacquet, K. *et al.* The TIP60 Complex Regulates Bivalent Chromatin Recognition by 53BP1 through Direct H4K20me Binding and H2AK15 Acetylation. *Mol Cell* **62**, 409–421 (2016).
103. Ikura, M. *et al.* Acetylation of Histone H2AX at Lys 5 by the TIP60 Histone Acetyltransferase Complex Is Essential for the Dynamic Binding of NBS1 to Damaged Chromatin. *Mol Cell Biol* **35**, 4147–4157 (2015).
104. Ikura, T. *et al.* DNA Damage-Dependent Acetylation and Ubiquitination of H2AX Enhances Chromatin Dynamics. *Mol Cell Biol* **27**, 7028–7040 (2007).
105. Xie, A., Odate, S., Chandramouly, G. & Scully, R. H2AX post-translational modifications in the ionizing radiation response and homologous recombination. *Cell Cycle* **9**, 3602–3610 (2010).
106. Kim, Y. C. *et al.* Activation of ATM depends on chromatin interactions occurring before induction of DNA damage. *Nat Cell Biol* **11**, 92–96 (2009).
107. Miller, K. M. *et al.* Human HDAC1 and HDAC2 function in the DNA-damage response to promote DNA nonhomologous end-joining. *Nat Struct Mol Biol* **17**, 1144–1151 (2010).
108. Das, C., Lucia, M. S., Hansen, K. C. & Tyler, J. K. CBP/p300-mediated acetylation of histone

H3 on lysine 56. *Nature* **459**, 113–117 (2009).

109. Vempati, R. K. *et al.* p300-mediated acetylation of histone H3 lysine 56 functions in DNA damage response in mammals. *Journal of Biological Chemistry* **285**, 28553–28564 (2010).
110. Toiber, D. *et al.* SIRT6 recruits SNF2H to DNA break sites, preventing genomic instability through chromatin remodeling. *Mol Cell* **51**, 454–468 (2013).
111. Murr, R. *et al.* Histone acetylation by Trrap-Tip60 modulates loading of repair proteins and repair of DNA double-strand breaks. *Nat Cell Biol* **8**, 91–99 (2006).
112. Ogiwara, H. *et al.* Histone acetylation by CBP and p300 at double-strand break sites facilitates SWI/SNF chromatin remodeling and the recruitment of non-homologous end joining factors. *Oncogene* **30**, 2135–2146 (2011).
113. Kim, J. J., Lee, S. Y. & Miller, K. M. Preserving genome integrity and function: the DNA damage response and histone modifications. *Critical Reviews in Biochemistry and Molecular Biology* vol. 54 208–241 Preprint at https://doi.org/10.1080/10409238.2019.1620676 (2019).
114. Gong, F. & Miller, K. M. Mammalian DNA repair: HATs and HDACs make their mark through histone acetylation. *Mutation Research - Fundamental and Molecular Mechanisms of Mutagenesis* vol. 750 23–30 Preprint at https://doi.org/10.1016/j.mrfmmm.2013.07.002 (2013).
115. Gong, F. *et al.* Screen identifies bromodomain protein ZMYND8 in chromatin recognition of transcription-associated DNA damage that promotes homologous recombination. *Genes Dev* **29**, 197–211 (2015).
116. Zhao, M. *et al.* PCAF/GCN5-Mediated Acetylation of RPA1 Promotes Nucleotide Excision Repair. *Cell Rep* **20**, 1997–2009 (2017).
117. Guo, R., Chen, J., Mitchell, D. L. & Johnson, D. G. GCN5 and E2F1 stimulate nucleotide excision repair by promoting H3K9 acetylation at sites of damage. *Nucleic Acids Res* **39**, 1390–1397 (2011).
118. Chiu, L. Y., Gong, F. & Miller, K. M. Bromodomain proteins: Repairing DNA damage within chromatin. *Philosophical Transactions of the Royal Society B: Biological Sciences* vol. 372 Preprint at https://doi.org/10.1098/rstb.2016.0286 (2017).
119. Oppikofer, M. *et al.* Non-canonical reader modules of BAZ1A promote recovery from DNA damage. *Nat Commun* **8**, (2017).
120. Lan, L. *et al.* The ACF1 Complex Is Required for DNA Double-Strand Break Repair in Human Cells. *Mol Cell* **40**, 976–987 (2010).
121. Kakarougkas, A. *et al.* Requirement for PBAF in Transcriptional Repression and Repair at DNA Breaks in Actively Transcribed Regions of Chromatin. *Mol Cell* **55**, 723–732 (2014).
122. Hu, K. *et al.* ATM-Dependent Recruitment of BRD7 is required for Transcriptional Repression and DNA Repair at DNA Breaks Flanking Transcriptional Active Regions. *Advanced Science* **7**, (2020).
123. Wang, H. *et al.* BRCA1/FANCD2/BRG1-Driven DNA Repair Stabilizes the Differentiation State of Human Mammary Epithelial Cells. *Mol Cell* **63**, 277–292 (2016).
124. Hays, E. *et al.* The SWI/SNF ATPase BRG1 stimulates DNA end resection and homologous recombination by reducing nucleosome density at DNA double strand breaks and by promoting the recruitment of the CtIP nuclease. *Cell Cycle* **19**, 3096–3114 (2020).
125. Chen, Y. *et al.* A PARP1-BRG1-SIRT1 axis promotes HR repair by reducing nucleosome

density at DNA damage sites. *Nucleic Acids Res* **47**, 8563–8580 (2019).

126. Qi, W. *et al.* BRG1 Promotes chromatin remodeling around DNA damage sites. *Anim Cells Syst (Seoul)* **22**, 360–367 (2018).
127. Qi, W. *et al.* BRG1 promotes the repair of DNA double-strand breaks by facilitating the replacement of RPA with RAD51. *J Cell Sci* **128**, 317–330 (2015).
128. Zhou, Q. *et al.* The bromodomain containing protein BRD-9 orchestrates RAD51–RAD54 complex formation and regulates homologous recombination-mediated repair. *Nat Commun* **11**, (2020).
129. Verma, P. & Greenberg, R. A. Noncanonical views of homology-directed DNA repair. (2016) doi:10.1101/gad.280545.
130. Chen, C. C., Feng, W., Lim, P. X., Kass, E. M. & Jasin, M. Homology-Directed Repair and the Role of BRCA1, BRCA2, and Related Proteins in Genome Integrity and Cancer. *Annual Review of Cancer Biology* vol. 2 313–336 Preprint at https://doi.org/10.1146/annurev-cancerbio-030617-050502 (2018).
131. Rickman, K. & Smogorzewska, A. Advances in understanding DNA processing and protection at stalled replication forks. *Journal of Cell Biology* vol. 218 1096–1107 Preprint at https://doi.org/10.1083/jcb.201809012 (2019).
132. Goodarzi, A. A. & Jeggo, P. A. The Repair and Signaling Responses to DNA Double-Strand Breaks. in *Advances in Genetics* vol. 82 1–45 (Academic Press Inc., 2013).
133. Jackson, S. P. & Bartek, J. The DNA-damage response in human biology and disease. *Nature* vol. 461 1071–1078 Preprint at https://doi.org/10.1038/nature08467 (2009).
134. Bonilla, B., Hengel, S. R., Grundy, M. K. & Bernstein, K. A. Annual Review of Genetics RAD51 Gene Family Structure and Function. (2020) doi:10.1146/annurev-genet-021920.
135. Bétermier, M., Bertrand, P. & Lopez, B. S. Is Non-Homologous End-Joining Really an Inherently Error-Prone Process? *PLoS Genetics* vol. 10 Preprint at https://doi.org/10.1371/journal.pgen.1004086 (2014).
136. Frock, R. L., Sadeghi, C., Meng, J. & Wang, J. L. Dna end joining: G0-ing to the core. *Biomolecules* vol. 11 Preprint at https://doi.org/10.3390/biom11101487 (2021).
137. Nickoloff, J. A. *et al.* Roles of homologous recombination in response to ionizing radiation-induced DNA damage. *Int J Radiat Biol* (2021) doi:10.1080/09553002.2021.1956001.
138. Wang, H. *et al. E□cient rejoining of radiation-induced DNA double-strand breaks in vertebrate cells de®cient in genes of the RAD52 epistasis group*. www.nature.com/onc.
139. Chen, S., Lees-Miller, J. P., He, Y. & Lees-Miller, S. P. Structural insights into the role of DNA-PK as a master regulator in NHEJ. *Genome Instab Dis* **2**, 195–210 (2021).
140. Matsumoto, Y., Asa, A. D. D. C., Modak, C. & Shimada, M. Dna-dependent protein kinase catalytic subunit: The sensor for dna double-strand breaks structurally and functionally related to ataxia telangiectasia mutated. *Genes* vol. 12 Preprint at https://doi.org/10.3390/genes12081143 (2021).
141. Woodbine, L. *et al.* PRKDC mutations in a SCID patient with profound neurological abnormalities. *Journal of Clinical Investigation* **123**, 2969–2980 (2013).
142. Chen, Y. *et al.* Role of PRKDC in cancer initiation, progression, and treatment. *Cancer Cell International* vol. 21 Preprint at https://doi.org/10.1186/s12935-021-02229-8 (2021).
143. Esenboga, S. *et al.* Two siblings with PRKDC defect who presented with cutaneous granulomas and review of the literature. *Clinical Immunology* **197**, 1–5 (2018).

144. Ackerson, S. M., Romney, C., Schuck, P. L. & Stewart, J. A. To Join or Not to Join: Decision Points Along the Pathway to Double-Strand Break Repair vs. Chromosome End Protection. *Frontiers in Cell and Developmental Biology* vol. 9 Preprint at https://doi.org/10.3389/fcell.2021.708763 (2021).
145. Becker, J. R. *et al.* BARD1 reads H2A lysine 15 ubiquitination to direct homologous recombination. *Nature* **596**, 433–437 (2021).
146. Blackford, A. N. & Jackson, S. P. ATM, ATR, and DNA-PK: The Trinity at the Heart of the DNA Damage Response. *Molecular Cell* vol. 66 801–817 Preprint at https://doi.org/10.1016/j.molcel.2017.05.015 (2017).
147. Neal, J. A., Dunger, K., Geith, K. & Meek, K. Deciphering the role of distinct DNA-PK phosphorylations at collapsed replication forks. *DNA Repair (Amst)* **94**, (2020).
148. Dylgjeri, E. & Knudsen, K. E. DNA-PKcs: A Targetable Protumorigenic Protein Kinase. *Cancer Research* vol. 82 523–533 Preprint at https://doi.org/10.1158/0008-5472.CAN-21-1756 (2022).
149. Adamson, B., Smogorzewska, A., Sigoillot, F. D., King, R. W. & Elledge, S. J. A genome-wide homologous recombination screen identifies the RNA-binding protein RBMX as a component of the DNA-damage response. *Nat Cell Biol* **14**, 318–328 (2012).
150. Bouwman, P. *et al.* 53BP1 loss rescues BRCA1 deficiency and is associated with triple-negative and BRCA-mutated breast cancers. *Nat Struct Mol Biol* **17**, 688–695 (2010).
151. Balmus, G. *et al.* ATM orchestrates the DNA-damage response to counter toxic non-homologous end-joining at broken replication forks. *Nat Commun* **10**, (2019).
152. Ruis, B. L., Fattah, K. R. & Hendrickson, E. A. The Catalytic Subunit of DNA-Dependent Protein Kinase Regulates Proliferation, Telomere Length, and Genomic Stability in Human Somatic Cells. *Mol Cell Biol* **28**, 6182–6195 (2008).
153. Lu, H., Saha, J., Beckmann, P. J., Hendrickson, E. A. & Davis, A. J. DNA-PKcs promotes chromatin decondensation to facilitate initiation of the DNA damage response. *Nucleic Acids Res* **47**, 9467–9479 (2019).
154. Duncan, J. S. *et al.* Dynamic reprogramming of the kinome in response to targeted MEK inhibition in triple-negative breast cancer. *Cell* **149**, 307–321 (2012).
155. Hsu, S. C. & Blobel, G. A. The Role of Bromodomain and Extraterminal Motif (BET) Proteins in Chromatin Structure. *Cold Spring Harb Symp Quant Biol* **82**, 37–43 (2017).
156. Stathis, A. & Bertoni, F. BET proteins as targets for anticancer treatment. *Cancer Discovery* vol. 8 24–36 Preprint at https://doi.org/10.1158/2159-8290.CD-17-0605 (2018).
157. Taniguchi, Y. The bromodomain and extra-terminal domain (BET) family: Functional anatomy of BET paralogous proteins. *International Journal of Molecular Sciences* vol. 17 Preprint at https://doi.org/10.3390/ijms17111849 (2016).
158. Gokani, S. & Bhatt, L. K. Bromodomains: A novel target for the anticancer therapy. *European Journal of Pharmacology* vol. 911 Preprint at https://doi.org/10.1016/j.ejphar.2021.174523 (2021).
159. Hajmirza, A. *et al.* BET family protein BRD4: An emerging actor in NFκB signaling in inflammation and cance. *Biomedicines* vol. 6 Preprint at https://doi.org/10.3390/biomedicines6010016 (2018).
160. Wessel, S. R., Mohni, K. N., Luzwick, J. W., Dungrawala, H. & Cortez, D. Functional Analysis of the Replication Fork Proteome Identifies BET Proteins as PCNA Regulators. *Cell Rep* **28**,

3497-3509.e4 (2019).
161. Jinek, M. *et al.* RNA-programmed genome editing in human cells. *Elife* **2013**, (2013).
162. Cong, L. *et al.* Multiplex genome engineering using CRISPR/Cas systems. *Science (1979)* **339**, 819–823 (2013).
163. Kim, S. *et al.* Multiplex genome engineering using CRISPR/Cas systems. *Science (1979)* **339**, 816–819 (2013).
164. Stroik, S., Kurtz, K. & Hendrickson, E. A. CtIP is essential for telomere replication. *Nucleic Acids Res* **47**, 8927–8940 (2019).
165. Fattaha, F. *et al.* Ku regulates the non-homologous end joining pathway choice of DNA double-strand break repair in human somatic cells. *PLoS Genet* **6**, (2010).
166. Chaplin, A. K. *et al.* Cryo-EM of NHEJ supercomplexes provides insights into DNA repair. *Mol Cell* **81**, 3400-3409.e3 (2021).
167. Seluanov, A. *et al. DNA end joining becomes less efficient and more error-prone during cellular senescence*. www.pnas.orgcgidoi10.1073pnas.0400726101 (2004).
168. Pierce, A. J., Johnson, R. D., Thompson, L. H. & Jasin, M. *XRCC3 promotes homology-directed repair of DNA damage in mammalian cells*. www.genesdev.org (1999).
169. Kan, Y., Batada, N. N. & Hendrickson, E. A. Human somatic cells deficient for RAD52 are impaired for viral integration and compromised for most aspects of homology-directed repair. *DNA Repair (Amst)* **55**, 64–75 (2017).
170. Karnan, S. *et al.* Simple Monitoring of Gene Targeting Efficiency in Human Somatic Cell Lines Using the PIGA Gene. *PLoS One* **7**, (2012).
171. Park, S. H. *et al.* ATAD5 promotes replication restart by regulating RAD51 and PCNA in response to replication stress. *Nat Commun* **10**, (2019).
172. Walker, J. E., Saraste, M., Runswick, M. J. & Gay, N. J. Distantly related sequences in the alpha- and beta-subunits of ATP synthase, myosin, kinases and other ATP-requiring enzymes and a common nucleotide binding fold. *EMBO J* **1**, 945–951 (1982).
173. Chauhan, J. S., Mishra, N. K. & Raghava, G. P. S. Identification of ATP binding residues of a protein from its primary sequence. *BMC Bioinformatics* **10**, 434 (2009).
174. Wai, D. C. C. *et al.* The BRD3 ET domain recognizes a short peptide motif through a mechanism that is conserved across chromatin remodelers and transcriptional regulators. *Journal of Biological Chemistry* **293**, 7160–7175 (2018).
175. Kaur, E., Agrawal, R. & Sengupta, S. Functions of BLM Helicase in Cells: Is It Acting Like a Double-Edged Sword? *Frontiers in Genetics* vol. 12 Preprint at https://doi.org/10.3389/fgene.2021.634789 (2021).
176. Wang, Y., Ghosh, G. & Hendrickson, E. A. *Ku86 represses lethal telomere deletion events in human somatic cells*. www.pnas.orgcgidoi10.1073pnas.0903362106.
177. Indiviglio, S. M. & Bertuch, A. A. *Ku's essential role in keeping telomeres intact*. www.pnas.orgcgidoi10.1073pnas.0906427106.
178. Gong, F., Clouaire, T., Aguirrebengoa, M., Legube, G. & Miller, K. M. Histone demethylase KDM5A regulates the ZMY ND8-NuRD chromatin remodeler to promote DNA repair. *Journal of Cell Biology* **216**, 1959–1974 (2017).
179. Ogiwara, H. *et al.* Histone acetylation by CBP and p300 at double-strand break sites facilitates SWI/SNF chromatin remodeling and the recruitment of non-homologous end joining factors. *Oncogene* **30**, 2135–2146 (2011).

180. Schwalm, M. P. & Knapp, S. BET bromodomain inhibitors. *Current Opinion in Chemical Biology* vol. 68 Preprint at https://doi.org/10.1016/j.cbpa.2022.102148 (2022).
181. Giovannini, S. *et al.* ATAD5 deficiency alters DNA damage metabolism and sensitizes cells to PARP inhibition. *Nucleic Acids Res* **48**, 4928–4939 (2020).
182. Filippakopoulos, P. & Knapp, S. The bromodomain interaction module. *FEBS Letters* vol. 586 2692–2704 Preprint at https://doi.org/10.1016/j.febslet.2012.04.045 (2012).
183. Sulli, G., di Micco, R. & di Fagagna, F. D. A. Crosstalk between chromatin state and DNA damage response in cellular senescence and cancer. *Nature Reviews Cancer* vol. 12 709–720 Preprint at https://doi.org/10.1038/nrc3344 (2012).
184. Ciccia, A. & Elledge, S. J. The DNA Damage Response: Making It Safe to Play with Knives. *Molecular Cell* vol. 40 179–204 Preprint at https://doi.org/10.1016/j.molcel.2010.09.019 (2010).
185. Dhalluin, C. *et al.* Structure and ligand of a histone acetyltransferase bromodomain. *Nature* **399**, 491–496 (1999).
186. Filippakopoulos, P. *et al.* Histone recognition and large-scale structural analysis of the human bromodomain family. *Cell* **149**, 214–231 (2012).
187. Alqahtani, A. *et al.* Bromodomain and extra-terminal motif inhibitors: A review of preclinical and clinical advances in cancer therapy. *Future Science OA* vol. 5 Preprint at https://doi.org/10.4155/fsoa-2018-0115 (2019).